A study on individual behavior of e-scooter and e-bike users during overtaking

by

Wenyi Zhang

Student number: 5702615

Thesis committee:

Dr. ir. W. Daamen,	TU Delft, Chair
Dr. ir. Y. Yuan,	TU Delft,Daily supervisor
Dr. ir. J. K. Moore,	TU Delft,Supervisor

TU Delft

Preface

Reflecting on the past two years, it seems that nothing has unfolded according to plan, including my decision to study in the Netherlands. I have never been one to create detailed plans, nor do I particularly enjoy doing so. However, this journey has allowed me to learn and grow immensely—not only academically but also in building meaningful friendships. I have cherished every moment spent with my friends.

Completing this thesis marks a significant accomplishment for me. Although the delay in finishing my thesis meant that I could not take up a position at my favorite brewery, I believe that fortune and misfortune often go hand in hand; perhaps it was simply not meant for me, and something better may be waiting just around the corner. Besides, I now have plenty of time to enjoy myself.

I am deeply grateful to my esteemed supervisors. Yufei Yuan, my daily supervisor, provided unwavering guidance and support throughout this process. Winnie Daamen, as chair, offered invaluable insights and that helped steer my research in meaningful directions. Jason Moore, my other supervisor, contributed his expertise and mentorship, which greatly enhanced my work.

Additionally, I want to extend my heartfelt thanks to the students and teachers from Beijing Jiaotong University and Cangzhou Institute of Water Conservancy. Your significant assistance in implementing the experiments was crucial, and this work would not have been possible without your contributions.

Lastly, I want to express my deepest gratitude to my family and friends. Your unwavering love and support have meant the world to me, instilling in me the courage and confidence to embrace whatever the future holds.

Additionally, thanks for the AI tools like ChatGPT and Claude to help me refine my language and debug my coding.

It is an immense honor to have completed my master's degree, and I look forward to the adventures that lie ahead.

Wenyi Zhang
Delft, October 2024

Summary

With the rapid rise of micromobility vehicles such as e-bikes and e-scooters, concerns about the safety of shared cycling spaces have increased significantly. These vehicles, owing to their higher speeds and motorized assistance, are now more frequently sharing infrastructure with conventional bicycles, which introduces new challenges for road safety. As e-bikes and e-scooters typically operate at higher speeds than traditional bicycles, the likelihood of accidents rises, especially during interactions between different types of micromobility and conventional bikes. These interactions are complex, especially in scenarios involving overtaking, where riders must adjust their behavior to safely navigate shared spaces. This study aims to provide a detailed examination on the behavior of e-scooter and e-bike riders during overtaking maneuvers. By analyzing such interactions, this research offers insights that are critical for informing future traffic management strategies, enhancing safety measures, and guiding infrastructure development.

The research methodology involved a controlled experiment in which detailed data were collected on the behavior of micromobility riders during overtaking scenarios. Cameras were strategically placed to track the trajectories of the vehicles, while inertial measurement units (IMUs) were used to capture roll rate and roll angle. After the data collection, significant processing was undertaken to ensure the accuracy and reliability of the dataset. The raw trajectories obtained from each camera were corrected to eliminate detection errors, and multiple cameras were timely synchronized. Following the correction of trajectories, the data from various cameras were merged to form a unified set of trajectory information. Additionally, the IMU data were synchronized with the trajectory data to ensure that roll-related metrics such as roll angle and roll rate were precisely aligned with the positional information of the vehicles. This comprehensive dataset enabled a detailed analysis of rider behavior, particularly in relation to the overtaking phase.

The analysis yielded several important findings. One of the key observations was that when e-bikes overtook e-scooters, the riders typically initiated the maneuver from a greater distance than e-bike overtaking e-bike, while maintaining smaller lateral distances during the overtaking process. Conversely, when e-bikes overtook other e-bikes, the overtaking maneuver was initiated from a shorter distance, but the lateral distances were larger, suggesting that riders were more cautious when overtaking the same type of vehicle. Speed dynamics also played a crucial role in the overtaking behavior, with lateral position differences showing a stronger correlation with speed difference than longitudinal position differences. Moreover, the study found that the highest roll rates and roll angles occurred during the overtaking phase, which was particularly evident in scenarios where e-bikes were overtaking e-scooters. However, prior to the overtaking phase, higher roll rates and roll angles were observed in cases where e-bikes overtook other e-bikes, indicating greater control adjustments were made in anticipation of overtaking vehicles of the same type.

Gender differences were not evident in overtaking.But in non-interactive scenario, particularly in the case of e-scooter riders. Male e-scooter riders were found to travel at significantly higher speeds than their female counterparts. In contrast, no significant gender-based differences were observed among e-bike riders.

Overall, the results of this study provide valuable insights into the complex interactions between different types of micromobility vehicles during overtaking maneuvers. By highlighting the influence of vehicle type and gender, the findings underscore the need for targeted safety interventions and infrastructure improvements that can mitigate the risks associated with shared cycling spaces. By analyzing overtaking behavior in such detail, this study not only enhances our understanding of micromobility interactions but also provides actionable insights that can be used to design safer, more efficient cycling infrastructures, ensuring that both micromobility users and conventional cyclists can coexist in urban spaces with minimal risk.

Keywords: overtaking; micromobility rider; e-bike; e-scooter; video data; roll angle; roll rate

Contents

1 Introduction

Firstly, the Section1.1 provides an overview and introduction to the study's background information. The global expansion of e-scooters and e-bikes has been accompanied by a significant rise in the number of incidents and more severe injury risks and outcomes for both riders in comparison to traditional bicycles. The e-bikes and e-scooters are distinct from bicycles, which may contribute to a greater number and severity of accidents. In a vast majority of countries today, they are required to share space with bicycles in bike lanes and are subject to nearly identical regulations. The safety of all users on bike paths is reliant upon an investigation and understanding of the microscopic behavior of e-bike and e-scooter riders when interacting between them and conventional bicycles. Then, Section1.2 specifies the research focus of this study, which is overtaking, and explains the decision. Section1.3 gives the research objective and questions of this thesis.Section1.4 shows an outline of this thesis report.

1.1. Background

Travel patterns and lifestyles in cities around the world have been undergoing significant transformations recently, primarily due to the explosive growth of various modes of transportation collectively termed micro-mobility. These vehicles, which facilitate personal mobility and augment the capabilities of pedestrians, encompass a broad spectrum of designs and functionalities, ranging from lightweight rollers and skis to more substantial options like two-wheeled self-balancing personal transporters[1]. Notably, both motorized and non-motorized varieties of these vehicles exist, offering flexible choices for individual users, whether owned privately or accessed through shared services.

Among the most popular types of micro-mobility vehicles are e-scooters and e-bikes. Their popularity has surged remarkably over the last few years. This surge can be attributed to several factors: the decreasing costs of purchasing these vehicles, improvements in the efficiency of their motors, and innovations leading to more lightweight and manageable designs. Furthermore, there is an increasing global emphasis on sustainability, which has propelled the adoption of these environmentally friendly transportation alternatives[2]. The integration of these vehicles into urban transport ecosystems represents a pivotal shift towards more sustainable urban mobility, promoting reduced reliance on traditional fuel-based vehicles and encouraging a more active, health-conscious urban populace. These trends are reshaping urban environments, making them more navigable and less congested, thus significantly enhancing the quality of urban life.

The notable rise in the number of micro-mobility vehicles, particularly e-bikes and scooters, is evidenced by the significant increases in both private ownership and participation in shared mobility programs. This trend also manifests in the broader metrics of transportation such as the increase in the total distance traveled and the number of trips undertaken by users. Specifically, the market for e-bikes has seen an exponential growth in recent years. For instance, electric bicycle sales in the European Union surged to approximately 5.3 million units in 2022, a stark contrast to the 854,000 units recorded in 2012[3]. This surge is not uniformly distributed across Europe; Germany stands out as a particularly strong market, with over 2.2 million e-bikes sold in 2022 alone[4], making it the largest e-bike market

in Europe for that year. Moreover, the expansion of e-scooter services further illustrates the growing appeal of micromobility. VOI, a leading e-scooter service provider that started its operations in Sweden in 2018, exemplifies this growth. Within just a year, VOI expanded its operations to 10 countries. By 2020, they recorded nearly 16 million rides[5], highlighting not only the rapid adoption of e-scooters as a viable mode of urban transport but also reflecting a broader shift in urban mobility preferences. This shift suggests a significant change in how people choose to navigate city environments, increasingly favoring smaller, more efficient forms of transportation that align with growing environmental consciousness and urban planning aimed at reducing traffic congestion and pollution.

With the significant rise in both the number and use of e-bikes, there has been a corresponding increase in traffic accidents involving these vehicles. For instance, in Germany, which boasts the largest e-bike market in the European Union, there has been a notable increase in traffic crash injuries among e-bike riders. Statistics from 2019 to 2022 show a worrying trend: in 2022, approximately 22,500 e-bike riders were injured in traffic crashes, a sharp rise from 10,505 in 2019[6]. Research indicates that the frequency and severity of accidents involving e-bikes are considerably higher than those involving traditional bicycles. A study from Denmark highlights that e-bike users are more likely to experience an accident compared to traditional bicycle riders[7]. Additionally, it has been found that e-bike users suffer more frequent thoracic trauma and soft-tissue injuries than those riding conventional bicycles[8]. The heightened risk associated with e-bikes can be attributed to several factors. E-bikes typically achieve higher speeds due to their motorized assistance, often reaching the maximum allowable speed of 25 km/h under EU standards, which is considerably faster than the average speed of conventional bicycles[9]. Studies indicate that on average, e-bikes are ridden 2–9 km/h faster than regular bicycles, whether on urban roads, rural areas, or dedicated bike paths[9, 10, 11]. This increased speed reduces the rider's response time, making it more challenging to react promptly to prevent accidents or lessen their severity[12].

Moreover, the similarity in appearance between traditional bicycles and e-bikes can create difficulties in distinguishing between them from a distance, potentially leading to misunderstandings and accidents on the road[13]. The added weight of the battery, which enhances pedal force, also contributes to the increased mass of e-bikes compared to traditional bicycles. This additional mass not only impacts the handling and dynamics of e-bikes but also increases the likelihood of more severe injuries during accidents[13].

Similarly to e-bikes, e-scooters have also seen a surge in popularity, which has been accompanied by an increase in accident rates. However, the data on e-scooter crashes is less comprehensive, as many city agencies do not specifically categorize e-scooter crashes[14]. In Germany, where e-scooter accidents have been recorded separately from other motorized two-wheelers since 2021, there has been a notable increase in the number of injuries. In 2022, approximately 7,400 e-scooter riders were injured in traffic crashes, a significant rise from the 4,800 incidents reported in 2021[6]. The outcomes and nature of injuries from e-scooter accidents have been the subject of various studies, often using data from hospitals and emergency centers. These studies have yielded mixed results regarding the severity and types of injuries compared to those sustained in bicycle accidents. For example, one study found that e-scooter accident victims had injury profiles similar to those of cyclists but with a higher incidence of severe traumatic brain injuries[15]. Conversely, another study highlighted that injured bicycle riders were more likely to require immediate medical care compared to their e-scooter counterparts (7% vs 1%)[16].

Research indicates that both e-scooters and e-bikes typically reach higher peak speeds than traditional bicycles, necessitating quicker reactions when interacting with other road users[17, 18]. E-scooters, in particular, face additional challenges due to their smaller wheels and stand-up riding posture, which can lead to more severe vibrations on uneven road surfaces. This, coupled with their rapid acceleration, can complicate speed management for riders. Consequently, e-scooters are often more prone to accidents than bicycles, especially in environments where they must navigate close to other vehicles and stationary objects[19]. This heightened risk underscores the need for more targeted safety regulations and better infrastructure to accommodate the growing number of e-scooter users in urban areas.

The motorized features of e-bikes and e-scooters place them in a unique position within urban traffic dynamics. On one hand, their motorized features, such as better acceleration capability and higher top speeds than traditional bicycles, make them vulnerable to serious injuries in accidents. On the

other hand, these same features pose a risk to other vulnerable road users, including pedestrians and traditional cyclists, due to the potential for causing collisions.

Despite the distinct differences in speed, power assistance, and weight between traditional bikes, e-bikes, and e-scooters, the regulatory framework often treats e-bikes and e-scooters similarly to conventional bicycles. For example, in many European countries, both e-bikes and e-scooters are legally required to use bike lanes or paths, just like traditional bicycles[20, 21, 22]. However, these paths were originally designed for non-motorized bicycles, and the presence of faster, motorized vehicles like e-scooters and e-bikes can lead to increased disturbances and safety risks for all users[14, 23]. The safety of these pathways, and by extension, the safety of all road users on these pathways, hinges on the individual behaviors of e-bike and e-scooter riders, particularly during their interactions with each other and with traditional cyclists. This behavior operates on two levels: operational mental layer and operational physical layer. The mental layer involves decisions about path choice, while the physical layer involves the actual controls exercised by the rider, such as steering, pedaling, and in the case of motorized vehicles, managing acceleration[24, 25]. Unique to e-bikes and e-scooters are the motorized controls, such as the acceleration grip, which necessitate different handling techniques compared to traditional bicycles. Furthermore, body gestures play a crucial role in maintaining control and stability while riding. Research focusing on the riding behavior of e-scooter users has highlighted body gestures as a critical element of safe vehicle operation[26]. Stability, therefore, is not just about maintaining physical balance but also involves a range of corrective actions including steering adjustments and body positioning, crucial for avoiding accidents and ensuring the safety of all road users[27, 28, 26].

To ensure the effective integration of e-bikes and e-scooters into urban environments, understanding and adapting to the behavioral nuances of micro-mobility users, especially on shared paths, is crucial. By addressing these behavioral patterns, there is a potential to significantly reduce the incidence of accidents and enhance safety for all road users. This approach necessitates the incorporation of such insights into safety regulations and urban infrastructure planning. Effective management and design of urban spaces must account for the growing prevalence of e-bikes and e-scooters to create a safe and inclusive environment for all forms of mobility.

1.2. Focus on overtaking

The specific focus of this study would be the overtaking maneuver of micro-mobility users. The focus stems from several critical considerations. Firstly, unlike motor vehicles, micro-mobility vehicles such as e-bikes and e-scooters have lower visibility in vehicle-following scenarios, making overtaking a pivotal aspect of their interaction within mixed traffic flows[29]. This behavior is not only frequent but also a significant safety concern, as overtaking maneuvers often lead to conflicts that can disrupt the regular movement of both the overtaking vehicle and others in the vicinity. Such incidents directly compromise the safety of traffic movements in bike lanes, making them a primary focus of safety assessments in practical engineering applications[30]. Moreover, with the widespread adoption of these vehicles, the risk of collisions during overtaking maneuvers is increasingly prevalent in lanes designated for non-motorized vehicles[31].

Investigating the microscopic behavior of these users during overtaking is essential for several reasons. It aids in determining the appropriate width of bicycle tracks and influences the estimation of bicycle level of service (BLOS). Moreover, it supports the development of micro-simulation models. These models are invaluable tools for enhancing the planning of bicycle tracks, improving traffic modeling, and conducting thorough safety assessments. Additionally, they contribute to broader objectives such as energy conservation, public health enhancement, and informed policy-making[14].

1.3. Research objective and questions

Thus, this thesis aims to investigate the individual behavior of micromobility users (including e-bike and e-scooter users) during their interaction with regular bikes, and within themselves. Particularly, this thesis focuses on looking into the impact of types/modes ridden by participants (e-bike, e-scooter), the modes they overtake (bike, e-bike, e-scooter), and individual factors on the individual behavior during the interaction of overtaking. So the main question is formulated as follows:

"How do different combinations of ridden types of micro-mobility vehicles and overtaken types of micro-mobility vehicles and individual characteristics of the rider affect individual behavior during overtaking?".

The sub-questions are designed to dissect how rider characteristics and micromobility types influence overtaking behavior, particularly focusing on the strategic decisions made by the rider. These decisions include selecting the overtaking path, adjusting speed, and determining the extent of body gestures. However, these decision-making processes are not directly observable. Instead, they manifest as physical control actions taken by the rider after the decision is made. The outcomes of these control actions can be observed and reflected in various traffic data and information.

Therefore, the core of this research involves collecting and analyzing traffic information to investigate how various factors influence these observable parameters. By extension, this approach allows us to infer the impact of these factors on riders' decision-making processes.

Then the following 4 sub-questions are formulated:

1. **What data and information need to be collected to analyze overtaking behavior between micromobility vehicles?**
2. **What are the appropriate data collection methods and equipment for analyzing overtaking behavior?**
3. **Based on the collected data, what is the conceptual model of overtaking behavior that includes influencing factors, decision-making, and control actions?**
4. **What is the influence of different combinations of micromobility vehicles and rider characteristics on decision-making and control actions in the conceptual model?**

The first sub-question will be addressed through a literature review to identify the types of data needed to analyze micromobility overtaking behaviors. The second sub-question will also be informed by a literature review, drawing on previous studies' experience, as well as adapting the methods to the specific practical conditions of this study. The third sub-question will involve developing a conceptual model that integrates the identified influencing factors, decision-making, and control actions.The fourth sub-question will be addressed by using common statistical analysis techniques to examine the relationships outlined in the conceptual framework.

1.4. Outline

- Chapter1 introduces the background of the research, the focus of the study, the research objectives and questions, and the outline of the report.
- Chapter2 conducts the literature review to find answers for the subquestions 1 and 2 constructs a conceptual framework (subquestion 3) based on the literature review.
- Chapter3 explains the data collection methodology adopted in the research, including the data requirement and the methodology to collect the data.
- Chapter4 describes the data processing methodology and the data analysis methodology, which are used to process and analyse the data collected.
- Chapter5 explains the detailed implementation of the data collection methodology of Chapter3.
- Chapter6 explains the detailed implementation of the data processing methodology of Chapter4.
- Chapter7 implemented the data analysis methodology and presents the findings.
- Chapter8 presents the conclusion of the research and reflects to limitations.

2

Literature review

The literature review serves two primary objectives within the context of this research. As this study aims to investigate the effect of individual factors and microbility types on the behavior of riders during overtaking, First the literature review summarized the current research, in order to understand what kind of individual factors would have any effect on their behavior, and during this process, some other influences were found which were summarized in section2.1. Then based on these factors, section2.2 built a rough conceptual model to help us understand what data needed to be collected. Then, this literature answers the first two sub-questions. Through the literature, we can identify the types of information and data that can be effectively collected to study overtaking behavior in micromobility scenarios and explore various methodologies and techniques for collecting these data and information. These two sections are corresponding in section2.3 and section2.4.

After deciding on the information and data needed, and taking into account the main research questions of this study, section2.5 developed a complete conceptual model representing the relationships between factors and microvariables. These possible relationships need to be analyzed using statistical methods, and section2.6 summarizes the methods of analysis.

For this literature review, a systematic approach to identifying relevant sources was employed. The primary search engines utilized were Scopus and Google Scholar, chosen for their comprehensive coverage of academic publications across various disciplines. The search strategy primarily relied on a keyword-based method. Key search terms included ”micromobility,” ”e-bike,” ”e-scooter,” ”overtaking,” ”interaction,” and ”behavior.” These terms were used both individually and in combination to ensure a thorough exploration of the research landscape. In addition to the keyword search, a snowballing technique was implemented. This involved examining the reference lists of particularly relevant articles identified through the initial search. This method, also known as citation chaining or reference mining, allowed for the discovery of additional pertinent studies that may not have been captured by the keyword search alone.

2.1. Factoring influencing riding behavior

First, section 2.1.1 and section 2.1.2 summarize the two main factors of greatest interest in this study: one is the individual factor, and the other is the current state of research on micromobility type.

2.1.1. Micro-mobility type

Studies have assessed the safety, stability, maneuverability, and comfort of micromobility vehicles. A study revealed that although e-bikes and e-scooters offer superior rider comfort and stability, e-scooters tend to fall short in terms of safety due to inadequate braking performance [27]. Additionally, when compared to bicycles, both e-scooters and other similar micro-mobility devices like Segways also demonstrate inferior braking capabilities, where bicycles are considered to be more stable and safer [32].

Regarding speed, e-bikes and e-scooters generally achieve higher maximum and average speeds than traditional bikes, particularly in conditions that allow the right of way or involve inclines. This

capability enhances their overtaking potential but also increases the risks associated with high-speed travel. Studies in different urban settings have shown that while e-scooters often match or slightly exceed the average travel speeds of bicycles, their ability to accelerate more quickly necessitates shorter response times to avoid hazards [33, 9, 18, 34, 35].

Moreover, e-bikes tend to have more conflicts with motorized vehicles than conventional bikes due to their higher speeds and different interaction dynamics with other road users. The design, weight, and acceleration capabilities of e-bikes and e-scooters not only influence their overtaking behavior but also impact how pedestrians and other cyclists perceive and react to these vehicles. For instance, e-bike riders are more likely to undertake overtaking maneuvers, followed by riders of human-powered tricycles and traditional bicycles [12, 31].

Overview:
Overall, the literature supports that different micromobility types significantly impact rider behavior, particularly regarding safety, stability, and speed. Specifically, studies such as [27, 32] support the idea that while e-bikes and e-scooters are generally more stable, they exhibit poorer braking performance compared to bicycles. Additionally, six studies [33, 9, 18, 34, 35, 12] confirm that higher speeds, especially for e-bikes and e-scooters, enhance overtaking potential but also increase risks.

2.1.2. Demographic and experience

Various demographic factors, such as gender, age, and riding experience, influence the riding behavior of cyclists beyond just safety and violations. Gender, for instance, plays a significant role in shaping cyclists' behavior, with male riders exhibiting not only on increased violation rates but also higher speeds, more aggressive maneuvers compared to their female counterparts [33, 36, 31]. Men also tend to overtake more frequently, which impacts interactions with other cyclists and motorized vehicles.

Age is another important factor; younger riders are more likely to overtake frequently and ride at higher speeds. In contrast, older riders, particularly those over 60, tend to be more cautious due to balance issues and reduced physical agility, which is especially evident when handling heavier e-bikes [36, 37]. This age-related caution affects their overtaking frequency and distance maintained during overtaking.

Riding experience also has a notable impact. While one study found that cyclists with longer riding experience exhibit fewer violations [36], another study observed that frequent e-scooter users are more likely to develop risky behaviors [38]. Experienced riders tend to have better control over their vehicles, making them more comfortable in overtaking scenarios, whereas less experienced riders may be more hesitant and conservative in their behavior.

Overview:
The literature consistently highlights the influence of demographic factors on riding behavior, beyond safety and violations. Three studies [33, 36, 31] support that male riders engage in more aggressive behaviors compared to females. Two studies [36, 37] agree that younger riders are more prone to frequent overtaking, while older riders are more cautious. However, there are contrasting findings regarding riding experience—[36] suggests that more experience reduces violations, while [38] indicates that experienced e-scooter users might develop risky behaviors.

The following section summarizes other factors that were found during the literature search.

2.1.3. Infrastructure factors

Several studies consistently indicate that lane width affects the likelihood of overtaking maneuvers and meeting clearance. Wider lanes facilitate overtaking, while narrower lanes reduce lateral space and lead to more cautious riding behavior [31, 39].

The influence of obstacles and boundaries on cyclist behavior consistently shows that the presence of obstacles leads to more cautious riding behaviors.For example, obstacles positioned along the lane edges prompt cyclists to maintain lower clearances from these obstacles [14, 39]. Additionally, obstacles at handlebar height specifically have been found to increase braking behaviors, as riders become more cautious to avoid potential balance issues [39]. Thus, while different studies emphasize different cautious behaviors—either reducing clearance or increasing braking—the general trend remains that obstacles cause more cautious maneuvering.

Meeting and overtaking maneuvers are among the most common interactions on bicycle lanes. Many current studies, such as study [14, 39], choose to focus on the impact of bicycle lane characteristics on meeting maneuvers, as they are easier to collect during natural data collection compared to overtaking maneuvers. However, considering that both meeting and overtaking maneuvers require riders to pass side-by-side on the lateral horizontal plane, the factors that influence meeting behavior, such as lane width, boundary conditions, and obstacles, are likely to also impact overtaking behavior. Consequently, this study hypothesizes that lane width, topology, and boundaries will have a significant effect on riders' overtaking behavior, just as they do on meeting behavior.

Overview:
The influence of infrastructure on riding behavior is well-documented, especially regarding lane width and the presence of obstacles. Two studies [31, 39] support that wider lanes facilitate overtaking by increasing available lateral space, while obstacles along the lane edges prompt riders to reduce clearance and ride more cautiously. Studies [14, 39] agree that obstacles, particularly at handlebar height, significantly reduce clearance and lead to increased braking behaviors.

2.1.4. Traffic conditions

Lin et al. [40] provided insights into how traffic density affects overtaking dynamics on shared lanes. In scenarios of low traffic density, overtaking maneuvers such as moped-passing-bicycle are observed to be more stable and less likely to encounter disturbances, allowing vehicles to return smoothly to their original lanes post-overtaking. Conversely, in conditions of high traffic density, overtaking becomes more complex and often results in incomplete maneuvers, where vehicles fail to return to their lanes promptly. This variation in traffic dynamics can lead to increased interactions and potential conflicts among road users.

Speed plays a critical role in influencing the interactions of cyclists with other transportation modes and is a significant contributor to traffic accidents. Studies have consistently shown that traveling greater distances at higher speeds increases the likelihood of encountering dangerous situations, with cyclists traveling at speeds above 25km/h facing a significantly higher risk of accidents compared to those traveling at 15-25km/h [12, 41]. This heightened risk is not limited to potential accidents but extends to actual crash occurrences and the severity of resulting injuries.E-scooter riders, for example, are about twice as likely to sustain severe injuries on roads where travel speeds are typically higher, compared to injuries sustained in more controlled environments like bike lanes or sidewalks [42]. This trend is echoed in studies of bicycle safety, where high speed is a frequent contributor to single-bicycle crashes, significantly impairing the cyclist's ability to effectively respond to unexpected obstacles or sudden environmental changes [43]. Moreover, the speed of the bicycle being overtaken also plays a crucial roles in the dynamics of overtaking maneuvers on dedicated bike lanes, with higher speeds complicating these maneuvers and increasing the risk of close passes or collisions [29]. Collectively, these studies underscore the importance of managing cyclist speeds to enhance safety.

Overview:
The role of traffic conditions in overtaking behavior is consistently addressed in the literature. The study by [40] indicates that low traffic density contributes to more stable overtaking, while high traffic density complicates overtaking dynamics, increasing risks of incomplete maneuvers. Additionally, multiple studies [12, 41, 43, 42] emphasize that higher speeds, which are often influenced by traffic conditions, correlate with a higher risk of accidents and conflicts.

2.2. Overview and Rough Conceptual Model

Before discussing the required data and information, it is important to provide a comprehensive overview of the influencing factors previously discussed, leading to the formation of a conceptual model.

The core of this conceptual framework in Figure2.1 revolves around a cyclical interaction between the decision-making(mental) layer and the action (physical) layer. This cycle captures the dynamic nature of the overtaking process for micromobility users.

1. Decision-Making Layer: Riders first make decisions at a mental level, where they assess the need for speed adjustments, path selection, and body action adjustment to ensure a safe overtaking maneuver.

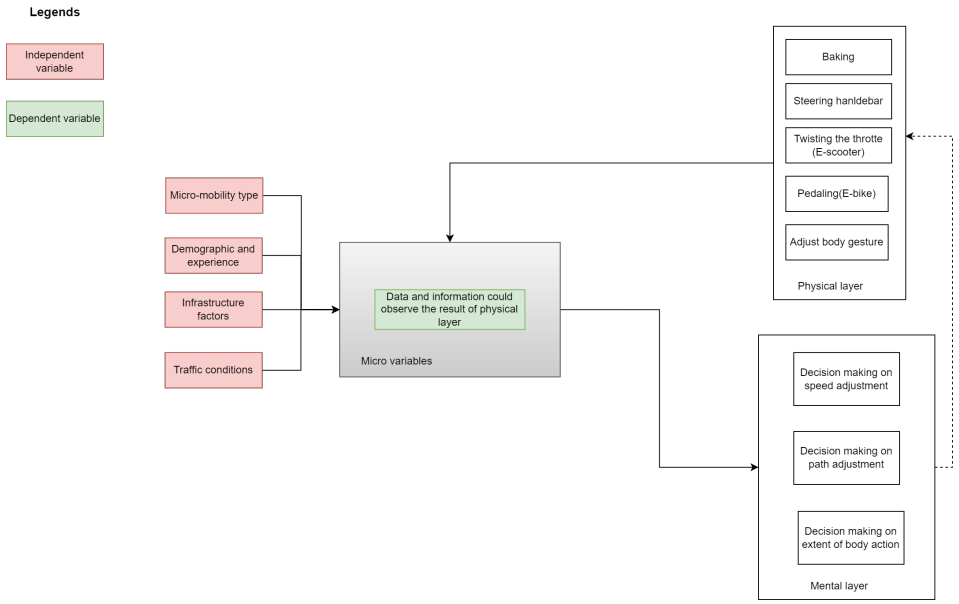

Figure 2.1: conceptual framework

2. Control Actions: These decisions are then executed physically through actions at the physical layer. These include actions like steering adjustments, acceleration, or even posture shifts, which directly affect the micromobility rider's position and movement in space.
3. Micro-Level Variables as Feedback: The result of these control actions is reflected in observable micro-level variables such as speed difference, lateral and longitudinal position differences, roll rate, and roll angle. These variables provide feedback on the success or necessity of further adjustments to the initial decisions.
4. Feedback to Decision-Making: This feedback loop enables the decision-making layer to constantly refine its strategies. The micro-level variables reflect the real-time state of the system, allowing for adjustments to be made, further feeding into control actions in a continuous loop.

In this model, the decision-making process informs actions, which are in turn reflected by micro-variables. These micro-variables provide feedback, creating a continuous cycle that ensures optimal and safe overtaking behavior. This cyclical interaction is fundamental to understanding how micromobility users navigate shared spaces during overtaking maneuvers.

To operationalize this model, it is crucial to identify the specific data and information(the micro-variables) that can effectively reflect the outcomes of physical actions and, by extension, the riders' decisions. To address this need, the following section synthesizes the micro-variables employed in existing research on bicycle overtaking behavior. This comprehensive review of current literature aims to elucidate the key parameters that have proven effective in capturing the nuances of overtaking decisions and actions in micromobility scenarios.

2.3. Required data and information

Previous studies on bicycle overtaking behavior have primarily focused on collecting and analyzing trajectory data, which includes the position information of each bicycle in time and space. Utilizing this fundamental trajectory information, researchers have further calculated more complex measurement indicators such as speed, lateral distance, longitudinal distance and speed difference to gain deeper insights into the behavioral patterns in environments like dedicated bicycle lanes [29, 40, 44, 45].

In addition to trajectory data, some studies employed roll rate and roll angle to compare the stability of different vehicle types in relatively simple task scenarios. The studies compared the absolute mean values of these parameters and the relationship between roll rate and steer rate[27, 28]. Another study Kovacsova et al. [46] utilized these indicators to compare the differences between elderly and young

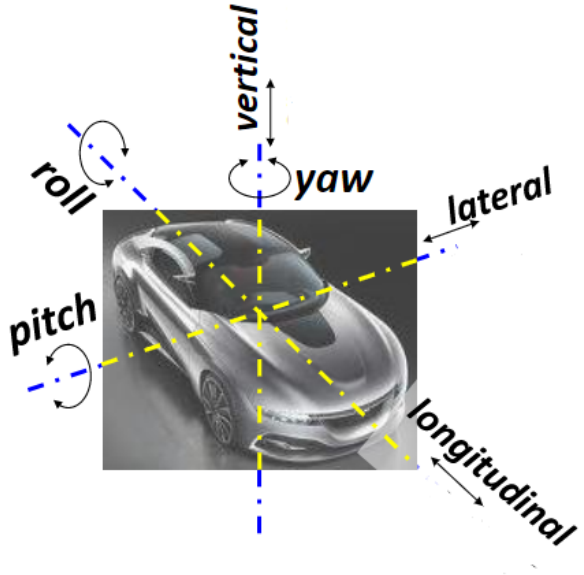

Figure 2.2: Reference system for the vehicles and directions names

riders. Roll angle refers to the rotational angle of an object along its longitudinal axis, as illustrated in the figure2.2 taken from Violin [28].

All of the aforementioned indicators are directly relevant to understanding micromobility overtaking behavior, particularly within the context of the decision-making(mental) layer and control action (physical) layer. The decision-making layer involves assessing and determining optimal speed, path selection, and maneuvering strategies to ensure a safe and effective overtaking process. Indicators like speed, speed difference, longitudinal distance, and lateral distance provide critical insights into these mental-level decisions. For instance, overtaking length and longitudinal distance are crucial for understanding path selection, while speed and speed difference reflect the strategies used for adjusting speed—key aspects of decision-making to ensure a safe overtaking maneuver. Lateral distance indicates the rider's avoidance behavior, reflecting safety considerations and decisions regarding adequate clearance from the overtaken vehicle. Roll rate and roll angle are also connected to the mental layer, as they reflect the rider's decisions regarding the extent of body posture adjustments.

Together, these indicators provide a comprehensive understanding of the interaction between the decision-making and control action layers. They demonstrate how decisions at the mental level are translated into physical actions and how these actions influence the dynamics of overtaking. This interaction is crucial for understanding the feedback loop between decision-making and physical control, which is at the core of the conceptual model for micromobility overtaking behavior

2.4. Data collection approaches

2.4.1. General data collection approaches

Recent advances in data collection methodologies have significantly enhanced the study of micromobility user behavior. The approaches used can be broadly categorized into real-world observations and controlled experiments, each with its own strengths and limitations. Following this, we delve into the specific techniques used to collect trajectory data and roll angle and roll rate data.

Real-World Observations

Some studies use real-world observation methods, such as the study byWang et al. [31], Gulino et al. [33], Lin et al. [40], Garcia et al. [39]. Real-world observational methods involve collecting data on micromobility users in natural traffic environments without any intervention that might alter their behavior. The key strength of this approach is its ability to capture genuine rider behavior, providing high ecological validity. Real-world settings allow for studying micromobility dynamics in varied and unpredictable conditions and enable the collection of data from multiple users simultaneously, offering

a broader context of interactions.

However, the main limitations include the presence of numerous uncontrollable factors that make it challenging to isolate the influence of specific variables, and the susceptibility of data to environmental factors, such as occlusions, which can lead to incomplete data collection.

Controlled experiments
Some studies have used controlled experiments, such as the study byGavriilidou et al. [25], Garman et al. [26], Billstein and Svernlöv [27], Violin [28], Yuan et al. [47]

Controlled experiments involve simulating specific riding scenarios in a structured environment where relevant variables can be controlled and manipulated. The main advantage of this approach is the precise manipulation of environmental factors, allowing researchers to study specific aspects of micromobility behavior under repeatable conditions. Controlled settings provide high-quality data with minimal noise from external sources, making it easier to analyze the effects of particular variables on rider behavior. However, controlled experiments have limited generalizability because the artificial environment may not fully replicate the complexities of real-world conditions. Additionally, riders may alter their behavior because they are aware of being observed, which could introduce bias.

2.4.2. Data collection techniques

Trajectory data collection techniques
Trajectory data, which includes information related to longitudinal and lateral positions, and then further processed to get speed, lateral and longitudinal distances, and speed differences, can be collected using a variety of techniques.

Video extraction techniques have been used to collect detailed trajectory data in both naturalistic and controlled settings[25, 31, 47]. The key advantage of this technique is its ability to provide a wide field of view, allowing the simultaneous tracking of multiple road users without interfering with their natural behavior. However, this approach is limited by occlusions, which can result in gaps in the data, especially in crowded environments.

Another approach involves using GPS and laser technologies to increase the precision of trajectory data collection. Garcia et al. [39], Lin et al. [40] utilized these technologies on instrumented bikes to accurately capture longitudinal and lateral positions, speed, and distances between users in different traffic densities. This method offers high accuracy but requires a complex setup and calibration, making it more resource-intensive.

Comprehensive sensor setups have also been employed to study micromobility behaviors.[12, 44] used video cameras and GPS on e-bikes to collect trajectory data in urban environments like the Brooklyn Bridge. This method allows for a rich understanding of rider trajectories, although it involves the challenge of integrating data from multiple sensors and potential issues with GPS signal loss in urban settings.

Roll angle and roll rate collection techniques

IMU(Inertial measurement unit)s have been widely used in different contexts to collect roll dynamic data, including roll angle and roll rate, providing high-resolution measurements of rider dynamics.

Gulino et al. [33] used IMUs to collect precise measurements of roll dynamics during road tests. Dozza, Piccinini, and Werneke [12] combined IMUs with GPS and video cameras to assess rider stability in urban environments. Violin [28] used IMUs in controlled experimental settings to capture stability metrics for e-scooters and e-bikes.

Overall, the use of IMUs across various studies has provided highly accurate roll dynamic data, with the main challenges being the synchronization with other data sources and potential differences in IMU models.

2.4.3. Assessment of Data Collection Approaches

Overall, each data collection approach has distinct advantages and limitations:

Real-World Observations offers high ecological validity by capturing rider behavior in authentic traffic

environments, which is valuable for understanding natural decision-making processes. However, the presence of uncontrollable environmental factors can compromise data completeness, especially with issues like occlusions. Collecting comprehensive data in real-world settings can also be challenging due to the lack of control over specific vehicle characteristics, potentially extending study durations and complicating analysis.

Controlled settings allow precise manipulation of variables, resulting in high-quality, low-noise data, which is ideal for repeatable observations. Nevertheless, the artificial nature of these environments may reduce generalizability, as participants might not behave as they would in real-world scenarios. To mitigate learning effects and fatigue, it's essential to design experiments with adequate rest periods and task variety.

Techniques like video extraction, GPS, and laser technologies are effective for capturing natural movement patterns with high precision. Video extraction allows simultaneous tracking of multiple users but is susceptible to occlusions. GPS and laser technologies offer high accuracy but are resource-intensive, requiring complex setups and calibration. Comprehensive sensor setups (e.g., GPS with video) provide valuable contextual information but require careful integration and can suffer from signal issues in urban areas.

IMUs are widely used for capturing roll dynamics such as roll angle and roll rate, offering high-resolution data suitable for detailed stability assessments. When combined with GPS and video cameras, they yield a comprehensive dataset, although sensor synchronization can be challenging. IMUs perform well in controlled environments, though differences between IMU models can affect consistency. Despite these challenges, IMUs are essential for analyzing micromobility user control actions.

2.5. Full conceptual framework

In section2.3, we specify the micro variables. And since the main research question of this study is to explore the influence of individual factors(Demographic and experience) and the overtaken vehicle, the conceptual framework in Figure2.1 can be further refined into the conceptual framework in Figure2.3.

Based on the literature, these factors can influence these micro variables, which in turn affects decision-making at the mental layer during overtaking maneuvers.

Gender has been shown to impact bike cycling speeds in non-interactive scenarios[33]. Younger riders are shown more likely to ride at higher speeds[36]. It is reasonable to postulate that gender, age and experience level may similarly influence the riding speeds of e-bikes and e-scooters.

The E-bike and E-scooter shows higer speed than bike due to their power assistance[33, 9]. Given the design differences between e-bikes and e-scooters, it is plausible that speed variations exist between these two modes as well.

In overtaking scenarios specifically, Wang et al. [31] found that both gender and micromobility type influence overtaking willingness and the aggressiveness.Pazzini et al. [48] showed the micromobility type could affect the lateral distance required for a safe overtaking maneuver. This suggests that the gender and micromobility types may also affect lateral distance and starting moment of overtaking.

Furthermore, studies have indicated that different micromobility devices exhibit varying roll rates and roll angles in simple maneuvering scenarios[27, 28]. This study hypothesizes that these differences may also manifest in overtaking scenarios, potentially influencing the roll rate and roll angle during the maneuver.

There may also be interrelationships among the micro-level variables themselves. For instance, previous research has shown a positive correlation between lateral distance and speed difference when motorized vehicles overtake bicycles [49]. Therefore, in this study, we hypothesize that lateral distance and speed difference also have a similar relationship during micromobility overtaking.

Additionally, speed of the overtkaing rider is influenced by the type of micromobility vehicle as earlier mentioned. At the same time, longitudinal distance difference might also play a role in influencing the rider's speed choices during overtaking. These will also reflect on the speed difference between ovetaking and overtaken micromobility. Therefore, this study hypothesizes that speed difference is influenced

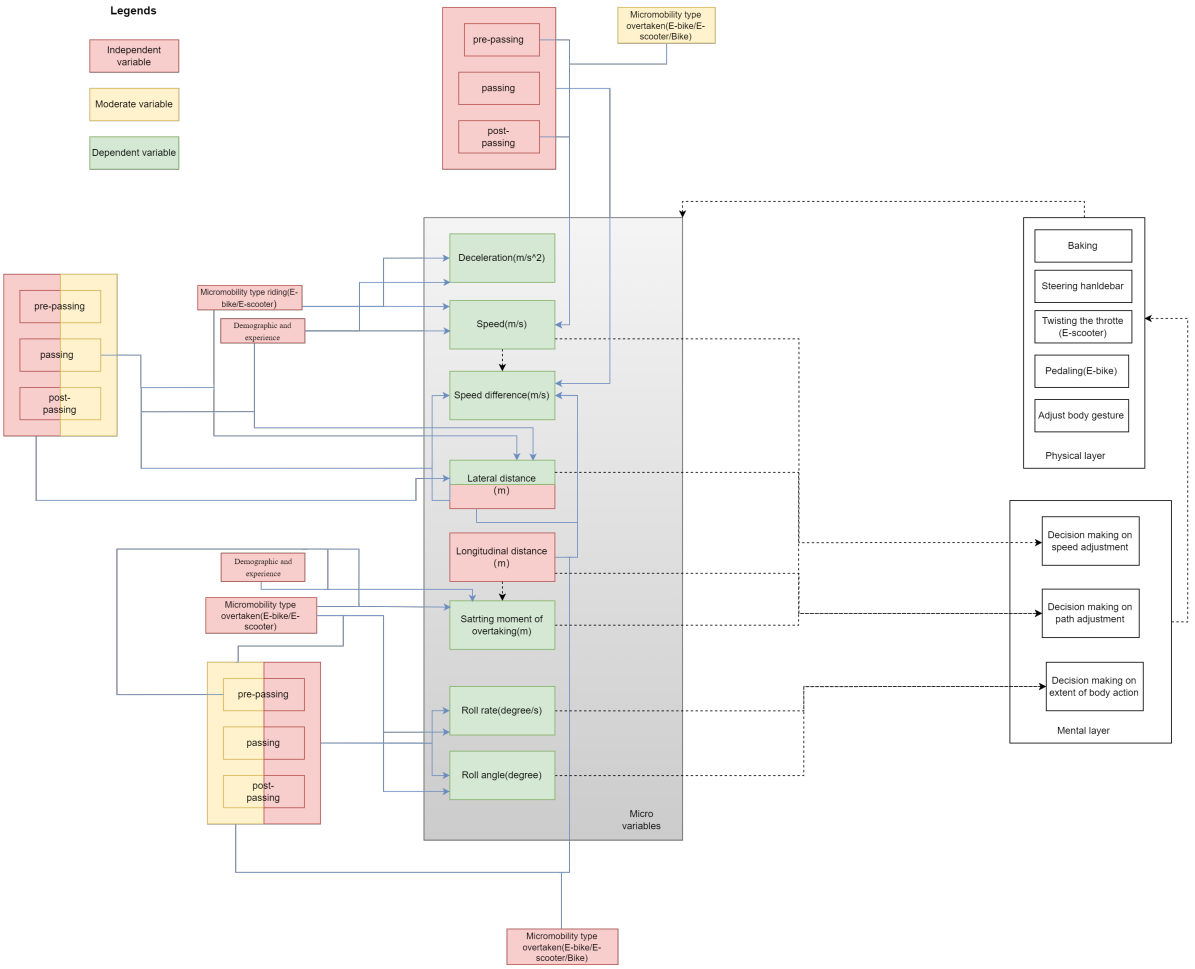

Figure 2.3: Detail conceptual framework for this study

not only by lateral distance but also by micromobility type and longitudinal distance difference.

Previous study have already segmented bicycle overtaking behavior into three distinct phases, including pre-passing, passing, and post-passing[29]. These phase concept has been adopted in the present study as moderating variables. The adoption is based on the following assumption: during different phases of overtaking, the influence of various attributes on micro variables may exhibit subtle yet significant differences. Of course, these three phases can also be used directly as an influencing attributes, for example, the difference in speed maintained between riders and the roll angle and roll rate due to different extent of control action may also be different in these three phases.

These relationships between attributes (gender and micromobility vehicle type) and micro-variables (speed, speed difference, lateral distance, longitudinal distance, roll rate, and roll angle), as well as the potential relationships among the micro-variables themselves, require further test through rigorous statistical methods

2.6. Data analysis approaches

To test the relationships of the conceptual framework, a thorough analysis of the collected data will be required. This section reviews existing methodologies for analyzing micromobility data to inform the approach.

Various studies on micromobility behavior have employed a range of statistical and modeling techniques, which inform the approach for this study. For instance, Wang et al. [31] applied a binary logit regression model to examine overtaking behaviors by incorporating independent variables such as gender, enabling the prediction of behavioral choices. Additionally, Gulino et al. [33] used ANOVA to assess the influence of factors like time to reach maximum speed, while employing linear regression to explore the relationships between gender and performance outcomes, evaluating model fit through R^2 values. In a related context, Useche et al. [36] applied independent sample t-tests to compare behavioral differences across age and gender groups, revealing specific influences of demographic factors on riding behavior.

Machine learning techniques have also been used in micromobility studies. For example, Haustein and Møller [37] implemented Random Forest models to rank variable importance, while using fixed and random parameter logit models to analyze risk-taking behaviors. Their work also included a structural equation model to examine the dynamics of risk acceptance among micromobility users. In other cases, regression models like ordered probit and bilinear regression have proven effective. Garcia et al. [39] used ordered probit and linear regression to study the effects of track characteristics on cyclist positioning and maneuver dynamics, whereas Lin et al. [40] demonstrated that a bilinear regression model better captured the relationship between lateral spacing and time compared to a parabolic model.

Furthermore, Khan and Raksuntorn [29] conducted moment-to-moment analyses of speed dynamics and lateral positioning during bicycle passing and meeting maneuvers, utilizing linear regression and paired t-tests to evaluate speed differences. To classify overtaking interactions, Mohammed, Bigazzi, and Sayed [44] applied a Gaussian Finite Mixture Model (GFMM), clustering data based on variables like longitudinal distance, lateral distance, and speed difference, thus identifying distinct interaction patterns.

These diverse methods provide a robust framework for analyzing micromobility interactions. T-tests can be employed to compare the influence of gender and riding experience on riding behavior. ANOVA analysis is suitable for comparing the effects of different overtaking combinations on behavior. Both T-tests and ANOVA analyses can be conducted using the indicators mentioned in section2.3. Regression analysis can be used to study the relationships between these indicators. By leveraging these techniques, this study aims to identify key determinants of overtaking decisions among e-bike, e-scooter, and conventional bicycle users, offering valuable insights into the various factors that influence rider behavior under different conditions.

3

Data collection Methodology

This section outlines the methodology to collect the required data. Initially, Section 3.1 details the necessary direct measurements for studying microscopic behaviors, including trajectory, steering angle/rate, and roll angle/rate. The subsequent Section 3.2 discusses the controlled experiment method chosen for this study, explaining the reasons for its selection and outlining its advantages and disadvantages. In Section 3.3, the selection of the experimental data acquisition equipment, specifically cameras, and IMUs, is described. This selection is closely tied to the required data identified earlier.

The following Sections delve into the experimental design. This includes track design in Section3.4. Section 3.5 then presents the tasks assigned to experimental participants. Section 3.6 elaborates on the vehicle selection and the experimental recruitment plan for participants. Section 3.7 estimates the duration of each scenario based on the number of samples to be collected and the dimensions of the track design.

3.1. Data requirements

The purpose of this study is to investigate the influence of individual factors and the different combinations of overtaking and overtaken types of vehicles on the microscopic behavior of the rider during overtaking. These microscopic behaviors can be observed through a number of microscopic measurements presented in Figure2.3.

First, trajectory data is the most necessary data used to study individual behavior. The trajectory data, which captures the position of the vehicle on a two-dimensional plane at specific times, could be used further to derive microscopic measurements reflecting the behavior. In section2.3, a comprehensive summary of the measurement variables pertinent to analyzing microscopic behaviors during overtaking maneuvers is provided. Key variables include speed, the speed difference, and longitudinal and lateral distance differences between overtaking and overtaken vehicles. The accuracy of these variables is heavily dependent on the precision of the trajectory data. For meaningful analysis, the trajectory's accuracy should ideally be around a 10cm range[25].

In addition, measurements including roll angle and their rate offer valuable insights into the rider's control action during the overtaking process. The angles mentioned here are important indicators of the control actions needed by the rider including steering the handlebar and adjusting their body posture. The extent of these control actions have been used in many studies[27, 28, 26].

Furthermore, since this study involves different types of micromobility combinations, it is necessary to ensure the controllability of the vehicle combinations and to make sure that the targeted interaction movement takes place.

3.2. Data collection approach

As in section2.4, the ability of isolating specific behaviors or conditions of laboratory settings allows for the replication of specific traffic scenarios, including various combinations of overtaking maneuvers

between e-bikes, e-scooters, and conventional bicycles. This control is particularly beneficial when studying interactions that are less common or require specific conditions for their occurrence. Given the wide range of possible vehicle combinations and interactions, it is challenging to gather comprehensive and valid data through real-world observations. These environments do not allow for the control of individual characteristics of each vehicle combination, potentially extending the duration of the study significantly and complicating the analysis. Therefore, a controlled experiment is determined to gather the data on the rider's behavior during overtaking.

One of the drawbacks of using a controlled experiment, however, is that as the experiment progresses and the participants become more familiar with the tasks they are performing, as well as possibly with physical and psychological fatigue, the behaviors they exhibit in the experiment may change from what they were at the beginning of the experiment. although physical fatigue is less likely to be an issue for powered vehicles. This disadvantage is referred to as the learning effect. To mitigate the learning effect, it is crucial to minimize riding time, provide adequate rest periods, and ensure that participants engage in a variety of tasks throughout the experiment.

3.3. Data Collection equipment selection

3.3.1. Cameras

In this study, video extraction technique is used to extract the user's trajectory data. Based on the trajectory data, other measurement variables can be further extrapolated. There are several reasons for choosing cameras to collect data. First, as specified in the section 3.1, we need to achieve trajectory data with an accuracy of approximately 10 cm. In the section2.4, the two most common methods for collecting trajectory data are video extraction and GPS as show in section2.4. To achieve this level of accuracy with GPS, high-precision GPS systems, typically classified as Real-Time Kinematic (RTK) GPS, are required. RTK GPS systems enhance the precision of position data using a combination of fixed base stations and mobile receivers[50]. These systems are not only more sophisticated but also significantly more expensive. Secondly, during the research process, there are often multiple vehicles on the track simultaneously, and to accurately capture the trajectory of each vehicle, multiple high-precision GPS devices are needed. In contrast, cameras can provide high-accuracy trajectory data at a lower cost, making them a more economical and practical choice.

Part of the reason for choosing video equipment is that the supervisor, Yufei has used video extraction in his previous project experience. Regarding the specific model selection, based on his previous project experience, he gave the camera parameters that have been used before. However, the specific equipment search and selection is done by the author.

3.3.2. Inertial Measurement Unit

In this experiment, the Inertial Measurement Unit (IMU) was employed to measure the roll angle and roll rate of e-bikes and e-scooters. Research by Violin [28], Billstein and Svernlöv [27] used roll angle and roll rate. The roll angle and roll rate were effectively captured using an IMU. The IMU's high integration and ease of installation, requiring only tie-wraps without further modifications and directly outputting data, made it the preferred choice for this study.

The reason for choosing IMU was that it is indeed an excellent choice for measuring roll angle and roll rate. Another reason was that the team from China could directly provide IMU. After communicating with them, the author confirmed the availability of this option.

3.4. Track design

In designing the track for this experiment, several critical factors were considered to ensure the successful completion of overtaking maneuvers. The track needed to be sufficiently long to accommodate the overtaking process. Assuming the speed of the overtaken mode at a higher bound of 4 m/s and the speed of the overtaking mode at a lower bound of 5 m/s, and considering 5 m safe distance before and after the overtaking process, the minimal track length should be 50 meters, based on the basic physical law (speed × distance / speed difference = $5 \times 10/(5 - 4)$ m). Consequently, a main track measuring 60 meters in length is designed to provide extra space to accommodate interactions occurring.

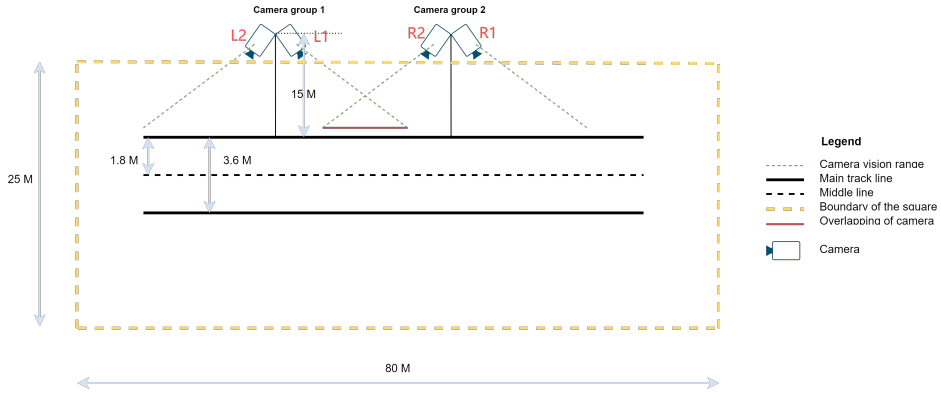

Figure 3.1: Track design

The order of the camera from right to left is R1-R2-L1-L2

This track includes two-way bike lanes, each lane being 1.8 meters wide (totaling 3.6 meters), with a buffer distance of ten meters on both the left and right sides. This buffer is intended to accommodate any necessary acceleration or deceleration. The layout is detailed in figure3.1. The main reference for the 1.8m width of the lanes is based on a study of field measurements of two-way bicycle lanes in the Netherlands[51] of field measurements of two-way bicycle lanes in the Netherlands, which is approximately 370 cm, including the width of the markings in the middle of the road, and therefore selected as 180 cm in this study.

During the track design process, the track length and track width design were all completed by the author, and the author's supervisor gave suggestions on the approximate positions of the two sets of cameras. However, on the day of the experiment, the specific positions were adjusted on site by the author and supervisor based on the actual situation.

3.5. Task design

3.5.1. Task design and general instructions

The main task for participants is to perform the overtaking maneuvers. The overtaking maneuver, consisted of two types of riders, in which some participants would ride at low speeds on the designed bike lanes as overtaken riders,and the other part of participants would overtake the low-speed vehicles from the left side in a safe manner as overtaking riders.

For the e-scooter, e-bikes and bikes, their speeds were not strictly when they act as the overtaken mode. The riders were instructed to ride at a low speed that does not interfere with their control of balance (e.g., requiring additional control maneuvers such as a large wiggle of the steering grip or adjustment of body position). Overtaking riders were merely asked to follow their habits and methods when overtaking low-speed vehicles without colliding.

The maneuver is summarized in Figure 3.2.

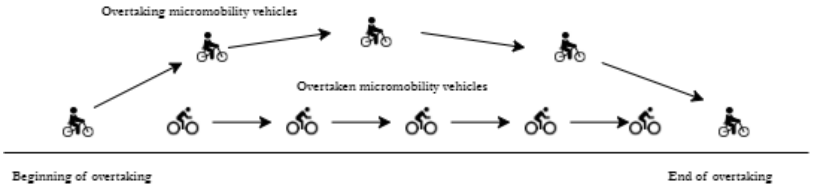

Figure 3.2: Overtaking maneuver

It is worth noting that since we want the experimental participants to be able to make overtaking behaviors continuously under normal driving speed. It is very important to ensure the continuity of the

participant's riding, in order to ensure this continuity, we chose to adopt the practice of letting the experimental participant run laps along a fixed line in the field, for overtaking, the participant's riding path is shown in Figure 3.3.

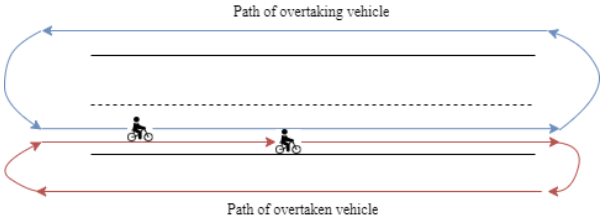

Figure 3.3: Path of overtaking

The experimental design incorporates specific measures to facilitate and control overtaking behavior within the designated main track area. Participants are instructed to follow either the red or blue lines according to their assigned roles. The layout of these routes is strategically designed to ensure that overtaking maneuvers can only occur within the main track zone. To increase the probability of overtaking interactions, multiple vehicles are simultaneously present on each route rather than just one. This approach significantly enhances the likelihood of overtaking and being overtaken within the main track area. Furthermore, the experiment supervisors have the ability to judiciously control the timing of vehicles re-entering the main track after completing a full circuit. For instance, they can allow vehicles on the slower path to enter first, followed by vehicles on the faster path entering the main track. This sequencing strategy maximizes the occurrence of overtaking events within the main track. The inclusion of buffer zones in the track design serves a crucial purpose. These areas ensure that participants have reached a steady-state riding condition before entering the main track, even if they have momentarily stopped and restarted. This design element contributes to the consistency and reliability of the observed overtaking behaviors by eliminating potential variability associated with the initial acceleration phase. This carefully structured experimental setup allows for the systematic observation and analysis of overtaking behaviors under controlled conditions, while still maintaining a degree of naturalistic riding scenarios. This part was completed independently by the author.

3.6. Vehicles selection and number of participants

The first step of the experiment design was to select the specific models of e-scooter and e-bikes that to be investigated in this study. In selecting the e-scooter and e-bike, the following three factors are taken into consideration:

- Popularity in the market.
- Easiness of learning to use these vehicles; the need to avoid vehicles that the participants of the experiment could not learn to ride in a short period of time.
- The maximum speed of the vehicle should not be too high; too high may cause safety problems during the experiment.

To address the heterogeneity among participants and ensure statistical significance, the experimental design incorporates a carefully considered sampling strategy. The ideal scenario would include at least 30 unique combinations, with each combination representing a rider proficient in the designated mode performing the requested maneuver. The least sample size of 30 is supported by statistical theory, specifically by the Central Limit Theorem (CLT). According to the CLT, with a sample size of around 30 or more, the sampling distribution of the mean is approximately normal, regardless of the population distribution. This allows researchers to apply parametric tests like t-tests and ANOVA even if the original data are not perfectly normally distributed[52].

This approach would ideally capture a diverse range of ages and genders within the rider population, providing a comprehensive representation of micromobility users. However, practical constraints related to time, financial resources, and overall feasibility necessitated an adjustment to this ideal scenario. After careful consideration, 12 combinations were ultimately selected as the optimal balance

between representativeness and practicality. This decision resulted in the recruitment of 12 riders per mode, ensuring a sufficiently diverse sample while remaining within the bounds of the study's resources. To compensate for the reduced number of combinations and to enhance the statistical robustness of the results, each combination of participants performs 4 repetitions or runs. This approach yields a total of 48 runs per scenario, which significantly bolsters the statistical power of the study. The repetition of runs allows for the assessment of within-subject variability and increases the reliability of the observed behaviors. This part was completed independently by the author of this thesis.

3.7. Scenario, duration and schedule design

This study design incorporates a range of intra-modal and intermodal interactions to comprehensively capture the dynamics of overtaking behavior across different micromobility modes.The planned scenario runs and their specific properties are summarized in TableA.1. This table provides a detailed overview of each overtaking combination, the modes involved, and the number of repetitions, offering a clear structure for the experimental design.

The scenario design of the experiment was designed by the author, but the duration and schedule design of each scenario of the experiment was completed with the help of the supervisor. This part is mainly through consultation with the supervisor and rough calculation to ensure when designing the experiment from the beginning, it will not end up with a scenario taking too much time. The specific process is placed in AppendixA.

Sce No.	**Sce Name**	**Participating mode**			**Exp. duration (min)**
		ES	EB	B	
1	Overtaking-intra1	✓	-	-	12 x 4
2	Overtaking-intra2	-	✓	-	12 x 4
3	Overtaking-inter1	✓	✓	-	12 x 4
4	Overtaking-inter2	✓	✓	-	12 x 4
5	Overtaking-bike1	✓	-	✓	12 x 4
6	Overtaking-bike2	-	✓	✓	12 x 4

Table 3.1: Table of Overtaking Scenarios and Experimental Details

3.8. Clarify on contribution

For the focus on behavior during overtaking in this thesis, the author proposed the necessary data requirements, designed the track, tasks, overtaking scenarios, and designed the number of experimental participants and vehicle selection.

With the help of the author's supervisor, Yufei, the author chose the video data collection method and selected a specific camera based on the infrared parameters given by my supervisor. The author of the thesis made the decision on the use of IMU, but received support from the Chinese team.

However, this research on overtaking is part of a large research project. This large research project also involves other interactive behaviors, including merging, meeting, crossing, etc. The entire larger project was also designed using the same data collection methods and equipment. In other scenarios, track design, task design, and schedule design are all joint work between the author and the supervisor. The workflow is in the following way: The author proposes a preliminary design, the supervisor modifies it, and the author further improved it.

4

Data processing and analysis methodology

This section describes the data processing methods in section4.1, and the data analysis methods in section4.2, which are used to analyse the data collected.

Before introducing the data processing process of this study, it should be clarified that the video data processing process used in this study mainly refers to the processes of two studies, namely Yuan et al. [47] and Gavriilidou et al. [25]. The steps 'pixel trajectory extraction', 'image correction', and 'height projection' of the data flow used in the study are derived from study[47] and use the same tool and algorithm.

In the next steps, 'combine video files from the same camera' and 'jump point fix' are inspired by study [25], but the specific algorithms used are different. As for the subsequent 'time synchronization' and 'merging of multiple camera trajectories', we learned from study [25] that these are necessary process, but the specific principles and algorithms are different from that study. This is mainly because the data collection method of study[25] is not consistent with this thesis, and the method used cannot be applied to this study. The other steps are targeted at the specific problems of this study and are methods proposed by the author of this thesis.

4.1. Data processing methodology

The video processing procedure consists of 10 steps.

Initially, the process focuses on handling individual camera feeds.

- 1. Video format conversion: This step addresses the issue of original video data being incompatible with many computers for direct parsing and processing.
- 2. Pixel trajectory extraction: This step extracts the trajectories of riders from the transformed video, which can be converted to real-world trajectories measured in meters after a series of transformations. These real trajectories reflect riders' behavior during overtaking[53].
- 3. Image Correction: This step corrects distortions in the video image, partly due to the camera angle not being directly downward, and partly due to wide-angle effects causing shape distortions at the edges. It corrects for camera angle distortion but not barrel distortion due to data limitations. This step also converts trajectory units from pixels to meters[54].
- 4. Height projection: This step further corrects the meter-converted trajectories to ensure they accurately reflect real movement states. It accounts for the height of the riders' hats (detection points) and projects these coordinates onto the ground plane using trigonometric transformations[55].

The first four steps used tools and algorithms developed by others.

After steps 2-4, we can extract riders' real-world coordinate trajectories from the original video. However, the results still contain many erroneous detections, including non-experimental objects, trajectory breaks due to shadows, and mismatched trajectory segments. The followings steps are the contribution of this study.

- 5. Combine video files from the same camera: Before addressing these errors, data from each camera is combined into a whole file to facilitate comprehensive error correction in the next step.
- 6. Fixes for trajectory errors: This step resolves detection issues, ensuring the remaining data consists only of meaningful, correct trajectories of experimental subjects.

After converting data from each camera from raw video to real-world trajectories in meters and correcting trajectory errors, the next steps involve combining trajectories from multiple cameras. The reason why the combination of trajectories from multiple cameras is needed is that the whole process of overtaking behaviour is relatively long and a single camera cannot cover the whole process.

- 7. Time synchronization: Before combining, the timestamps of all cameras are aligned with the R1 camera as a reference. This step is necessary because each camera's recording and storage was controlled by a separate computer, resulting in a few seconds of time discrepancies despite synchronized system times. This step also aligns IMU data timestamps with video data.
- 8. Multi-camera trajectory combination: After time correction, data from multiple cameras can be combined. Despite the challenges posed by uncorrected barrel distortion and shifting camera positions, the merging process relies primarily on the corrected timestamps. This approach is effective because, as long as there is an overlap in the cameras' coverage areas, the end point of one camera's trajectory can always be found in the next camera's data, given that the timestamps are correctly aligned. Even if there are discrepancies in the spatial coordinates between cameras, these can be reconciled through coordinate transformation techniques. This allows for a seamless connection of trajectory segments across different camera feeds, creating a continuous trajectory that spans the entire overtaking process. The time-based merging strategy, combined with coordinate transformations where necessary, ensures that the resulting merged trajectory accurately represents the subjects' movements across the full experimental area, despite the technical limitations of individual camera setups.
- 9. Freezing point handle: This step addresses issues where video frames freeze, causing consecutive data points to have identical positions. Smoothing corrects these anomalies to prevent significant speed calculation errors.
- 10. Accuracy verification and IMU data integration: After merging multi-camera trajectories and handle the freezing point, the resulting data is verified for accuracy using standard floor tiles at the experimental site. Once verified as sufficiently accurate for behavior analysis, IMU data is combined with trajectory data based on the corrected timeline for ease of analysis.
- 11.Trajectory labelling: Each extracted trajectory is labeled with its attributes, including gender, vehicle type and whether it carries an IMU.

4.1.1. Video format conversion

The video processing workflow begins with addressing compatibility issues between the original video files and the analysis tools used.

Initially, the videos are in HEVC format, a standard digital container used for transmission and storage of audio, video, and related data[56]. This encoding presents challenges for analysis in the researcher's laptops and the workstation of TU Delft. To overcome this limitation, the solution is to convert the video to MPEG-4 format encoded in AVC. MPEG-4 is a versatile digital multimedia container format that is used primarily to store video and audio content[57]. It offers a wide compatibility.

4.1.2. Pixel trajectory extraction

For trajectory extraction, the Moving Object Detection and Tracking (MODT) tool developed by Duives, Daamen, and Hoogendoorn [53] is employed.

Furthermore, the MODT tool has been improved and extended to include a new feature that calculates the precise Beijing time corresponding to each frame image in the video. Beijing time was chosen as

the reference because all computers used in the experiment were set to the Beijing time zone.

To implement this feature, the first step is to determine the precise start time of each video, accurate to the millisecond level. The calculation method is as follows: Assuming the start time of the video is known to be *A* seconds, after *X* frames, the video time changes from *A* seconds to *B* seconds. Using the frame rate information of the video, the time interval between adjacent frames can be calculated. Since the *B* moment starts from the whole second, which means the exact time of B starts at (xx:xx:xx.000), the millisecond-precise value of the *A* moment can be deduced through the formula:

$$A = B - (1000\text{ms/Framerate}) \cdot (X - 1) \tag{4.1}$$

The MODT tool, when processing the video frame by frame, also reads the relative time corresponding to each frame. This relative time ranges from 0 seconds at the beginning of the video to the current frame and continues until the end of the video. For example, for a video with a duration of 20 minutes, this relative time ranges from 0 seconds to 1200 seconds.

By adding the precise start time of the video to the relative time of each frame, the precise Beijing time in the format of hours, minutes, seconds, and milliseconds corresponding to that frame can be obtained.

This establishes a precise mapping relationship between video frames and real-world time. This precise mapping between video frames and real-world time is crucial for subsequent data processing in the research project, specifically on trajectory merging and IMU data synchronization.

4.1.3. Image Correction

Image distortion correction is a vital step in the data processing workflow to ensure accurate spatial analysis of video footage. The primary objective of this correction is to transform the camera's perspective from a side view to a bird's-eye view—perpendicular to the center of the image from above. This transformation allows for precise measurements and analysis of movements within the video frames.For this purpose, this study employed a tool called ImageTracker developed by Knoppers, van Lint, and Hoogendoorn [54]. The fundamental principle is shown in AppendixB.1

4.1.4. Height Projection

The forth step involves height projection. The reason for performing height projection is that when a camera captures images from an elevated position, objects in the image appear closer to the camera than their actual positions. Correction is necessary to obtain the true positions of the objects. The height projection method employed in this study is based on the approach developed by Knoop and Wierbos [55]. The principle is shown in AppendixB.2

4.1.5. Combine video files from the same camera

After performing height projection, the next step is to combine the trajectory files extracted from each video captured by the same camera. The purpose of this merging process is to facilitate the division of different scenarios, as most scenarios span across multiple videos. During the combining process, a challenge arises when a single trajectory is split by two consecutive videos. In such cases, the same trajectory may be assigned different IDs in each video, leading to inconsistencies in the combined data. To address this issue, algorithm1 in appendixB.2.1 was designed in this study to identify and reconcile the split trajectories. The algorithm aims to merge trajectory data from two videos by comparing the spatial distance and temporal difference between trajectory points to determine whether they can be connected. When the distance between the end of a trajectory from the first video and the start of a trajectory from the second video is less than or equal to a specified distance threshold D and the time difference is within an allowable range T, the algorithm generates intermediate frames through linear interpolation and connects the preceding and succeeding trajectories along with the intermediate frames into a complete trajectory.

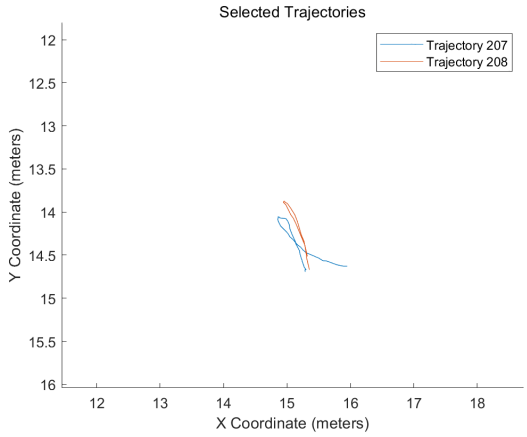

Figure 4.1: Trajectories deviated significantly from the expected path in R1 camera

4.1.6. Fixes for trajectory errors

Trajectory Filtering and U-turn Handling

The first step in the process involved removing incorrectly detected trajectories. These trajectories were caused by various reasons, such as participants not following instructions correctly and exiting the experiment prematurely, or the presence of static objects with similar colors. To aid in identifying these erroneous trajectories, animation playback was used to observe the overall trends and patterns of each detected trajectory. This visual inspection method allowed for a straightforward identification of two main types of errors:

1. Stationary Points: Some trajectories exhibited points that remained stationary, likely due to the system detecting static objects or participants remaining in place for extended periods.
2. Premature Exits: In other cases, participants exited the experiment area prematurely, resulting in trajectories that deviated significantly from the expected path. Such deviations were characterized by movement directions that did not align with the experimental design.

Figure4.1 shows the trajectories that deviated significantly from the expected path in R1 camera. For the R1 camera, the RGB value searching area of MODT tool was set larger than the coverage area of the bicycle lane during the first step of trajectory extraction to preserve as many trajectories as possible. Consequently, this approach captured not only the valid trajectories but also some that included U-turn behaviors. Figure 4.2 illustrates an example of a U-turn trajectory detected by Camera 1. These clearly unreasonable trajectories were either removed by manually deleting specific trajectory IDs or corrected by truncating the U-turn portion of the trajectory, ensuring that only data reflective of the intended experiment was retained.

Handle split trajectory

After removing erroneous trajectories, the second step of the processing pipeline involves handling trajectories fragmented due to shadow interference. Shadows cast by the aerial work platform used to mount the cameras move gradually into the center of the bicycle lane, reducing RGB values in the shadowed areas. For riders wearing red caps, this reduction often results in undetected segments as they pass through these shadowed areas, fragmenting their trajectories.

In this study, however, lowering RGB thresholds to enhance detection within shadowed areas proved challenging. Some vehicles, like bicycles, have orange bodies, and further reducing RGB values would increase false detections for these colors. Consequently, this limitation leads to trajectories being interrupted by shadows.

To address this, algorithm 2 in AppendixB.2.1 was developed to detect and merge adjacent trajectory segments that likely belong to the same vehicle. The algorithm enhances vehicle trajectory data by identifying and merging adjacent trajectory segments that likely belong to the same vehicle. It analyzes the spatial and temporal continuity between endpoint of trajectory *i* and start point of trajectory

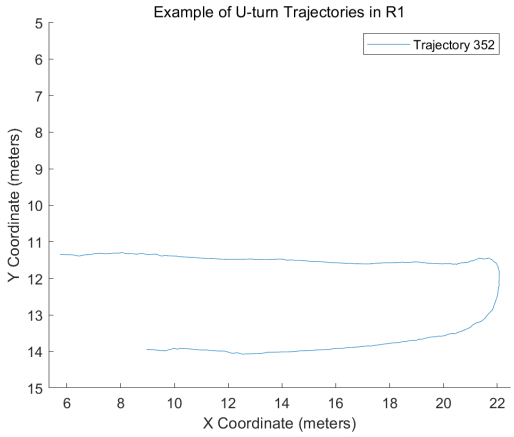

Figure 4.2: Example of U-turn trajectory in R1

j where j=i+1, applying predefined thresholds for both distance and time gaps. When two segments meet these criteria, the algorithm employs linear interpolation to fill the gap between them, assuming linear motion over short intervals. The algorithm then integrates the interpolated points into the existing data, removes any duplicate timestamps, and reassigns trajectory IDs for consistency. Instead of interpolating directly from the last point of one segment to the first of the next, the algorithm interpolates from the second-to-last point of the previous segment to the second point of the following segment. This adjustment helps reduce inaccuracies that can arise when part of the cap is in shadow while the rest remains visible.

Figure4.3(a) and Figure4.3(b) demonstrate the fragmented trajectories in the dataset and the reason behind the fragmentation, respectively.

((a)) Splitted Trajectory by Shallow

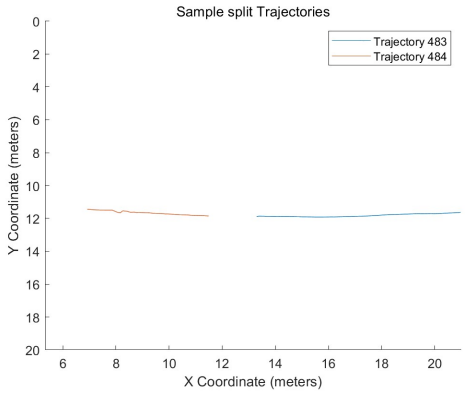

((b)) A Sample Split Trajectory of R1

Figure 4.3: Comparison of Sample Split Trajectory

Jump point fix

The third step of the trajectory fix is the jump point fix, where the jump point is caused by a detection error. This detection error causes the first half of the A trajectory to suddenly join the second half of the B trajectory at a certain point, and the first half of the B trajectory to join the second half of the A trajectory, making a crossover between the two as illustrated in Figure4.4(a).

The first step is to split the trajectory with jump points into two segments from the jump point and number them separately as shown in Figure4.4(b). The algorithm3 in appendixB.2.1 is designed to identify and process abnormal jumps in trajectory data. It begins by copying the original dataset D to D', then performs the following operations for each unique trajectory ID: calculating the distance between consecutive points in the trajectory, and if a distance exceeds the preset threshold d_{th}, marking that

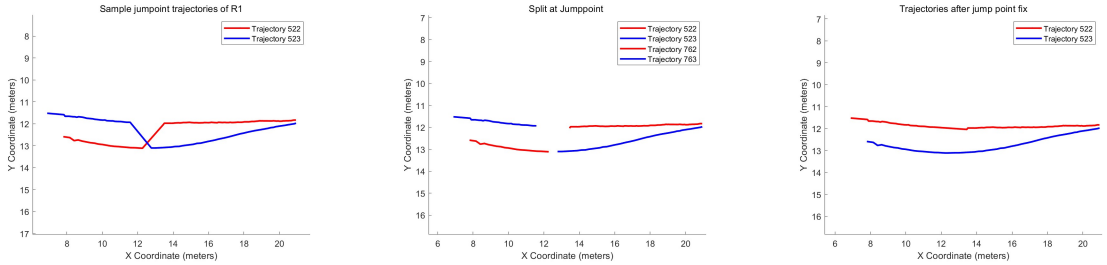

((a)) Jump Point Example of R1 **((b))** Split After Jump Point **((c))** Interpolation Trajectory

Figure 4.4: Explanation of the Jump Point fix Process

point as a jump point. For each detected jump point, the algorithm assigns all subsequent points to a new trajectory ID (starting from $newID$, which is incremented after each use). This process effectively separates trajectory segments following abnormal jumps.

The second step is to reconstruct the correct and complete motion trajectories as Figure4.4(c). The algorithm4 in appendixB.2.1 is designed for this task. It iterates through each unique trajectory ID in the split dataset D', performing the following steps for each trajectory: first, it finds the last point of the trajectory, then searches for the best matching next trajectory among the remaining trajectories. Matching conditions include a time difference not exceeding T_{th}, a spatial distance not exceeding D_{th}, and a Y-coordinate difference not exceeding Y_{th}. If a matching trajectory is found, the algorithm performs linear interpolation according to the missing time steps between the end point of the current trajectory and the start point of the matching trajectory, then merges the current trajectory, interpolated points, and the matching trajectory. If no matching trajectory is found, it retains the current trajectory. Finally, the algorithm removes duplicate time points within each trajectory, ensuring data uniqueness.

Scenario separation

After completing the error fix, the next step is to split the fixed data of each camera into separate scenarios based on the timestamp of each experimental scenario recorded on the day of the experiment. This step is performed to facilitate the subsequent process of merging trajectories from multiple cameras. Working with smaller, scenario-specific datasets during the trajectory merging step offers several advantages:

1. Easier error detection: When merging trajectories from multiple cameras, using smaller datasets makes it easier to identify and troubleshoot any inconsistencies or unreasonable outcomes that may arise during the merging process.
2. Simplified data analysis: Splitting the data into scenarios simplifies subsequent data analysis tasks, as researchers can focus on specific scenarios of interest without having to process the entire dataset.

4.1.7. Time synchronization

Time synchronization is a critical step in merging trajectories from multiple cameras. In this study, the first task is to calculate the precise Beijing time for each frame, as detailed in section 4.1.2, which is key to matching and merging trajectories. Despite synchronizing system times via the same WiFi on the day of the experiment, a time difference of one to two seconds between the cameras still occurred. Correcting this discrepancy is essential for accurate trajectory merging across cameras.

Since most experiment starting points were within the R1 camera's field of view, the R1 camera's time was used as the reference for aligning other cameras and the computer collecting IMU data. The correction process, though manual, is straightforward: using the overlapping areas between cameras (e.g., R1 and R2), a frame is selected where a participant appears within the overlapping region of both cameras. The pixel coordinates of the participant's red hat are manually extracted from both frames, allowing the precise times corresponding to those coordinates to be identified. The time error between the two cameras is calculated based on these matching times.

To determine the time difference between cameras, 5 trajectories from each camera from different

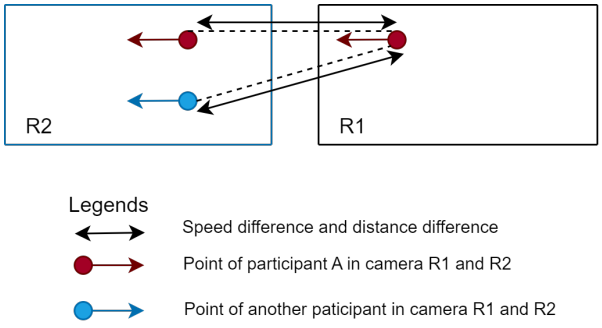

Figure 4.5: Speed and distance difference explnation

videos were randomly selected, allowing the calculation of an average time difference. As the time difference is constant over the whole experiment. We just need to do it once.

For the L1 and L2 cameras, the time error relative to R1 is determined by sequentially adding the time errors from overlapping cameras. Although L1 and R2 may not always overlap, this issue is minimal, as overlapping coverage exists at the beginning and end of the videos.

To synchronize the IMU data with the timing of R1, we identify extended periods of vehicle inactivity in both the IMU recordings and R1's video footage, during which the experimental vehicles remain stationary before initiating movement. By aligning these transitions from inactivity to motion, synchronization between the two systems is achieved with an accuracy of approximately one second.

4.1.8. Merging of multi-camera trajectories

In this study, the merging of camera trajectories is performed in two stages. The first stage involves merging cameras in pairs, while the second stage uses the common parts of the pairwise merged data as a bridge to merge trajectories from more than two cameras. The general merging principle is as follows: first, for a given trajectory, we identify two other closest trajectories. Where the closest is determined by the distance from the starting point of the given trajectory to the ending point of the other trajectory. We then select the trajectory that travels at a speed closest to the given trajectory as the best match, and finally, we merge these two trajectories.

The detail pairwise merging algorithm operates on the following way: when two cameras have overlapping coverage, the goal is to match trajectories from one camera to the other. Suppose experimental participant A is captured by camera R1 with a start time t_1 and an end time t_2, and by camera R2 with a start time t_3 and an end time t_4. After synchronizing the timestamps, if there is an overlap between the two cameras' fields of view, t_3 should be earlier than t_2. Therefore, we identify the time point t_2' in R2 that is closest to t_2, and retrieve the trajectory IDs in R2 that contain points at time t_2'.

However, due to overtaking behavior, multiple trajectories in R2 may exist at the same time t_2'. In this scenario, we calculate both the physical distance and velocity difference between all points in R2 at time t_2' and participant A's position in R1 at time t_2 as Figure4.5 shows. Initially, we retain the two trajectories with the smallest physical distance. From these, we select the trajectory with the smallest velocity difference. This identified trajectory is assumed to belong to participant A under camera R2. This process is referred to as trajectory matching in this study.

Once the matching is complete, the matched trajectories are merged.Trajectory merging involves deleting the data of A's trajectory in camera R2 before time t2' and shifting the remaining trajectory to the right so that it connects with A's trajectory under R1 end-to-end. This process is called trajectory merging. The specific algorithm design is as shown in Algorithm5 in appendixB.2.1.

After completing the pairwise merging, the next step is to merge trajectories from three or four cameras using the common overlapping regions. The algroithm6 in appendixB.2.1 is designed to achieve this. In this process, R2 serves as a bridge between R1 and L1 for merging. The same logic applies when using L1 as a bridge to merge with L2. To illustrate, we use R1, R2, and L1 as an example.

For each trajectory in the merged R1-R2 dataset, we know the R2 portion of that trajectory corresponds

to a specific original R2 trajectory. The algorithm6 proceeds by searching the R2-L1 dataset to find the trajectory in L1 that shares the same R2 portion. Once the corresponding trajectory in the R2-L1 dataset is found, the algorithm merges the R1-R2 trajectory with the R2-L1 trajectory based on their shared R2 segment.

The merging process retains only the common R2 portion in both trajectories to ensure continuity. Specifically, the algorithm6 first checks the temporal overlap by comparing the timestamps of the R2 segments in both datasets. Then, it ensures spatial continuity by applying offsets where necessary. After aligning the R1-R2 and R2-L1 trajectories at the R2 portion, the algorithm removes duplicate R2 points and assigns a new trajectory ID to the merged R1-R2-L1 trajectory.

4.1.9. Freezing point handle

The freezing point handle process was performed after merging the trajectories. This step is necessary. Because when browsing the data, the author discovered that some videos experienced frame freezing, where two consecutive frames in the video had exactly the same position, but the third frame jumped. This issue was found in some videos. The most likely cause of this problem is the limitations of the computer's performance during the video conversion process. To address this issue, the study employed the method described in algorithm7 for repair. The repair principle is as follows: if the i-th frame and the $(i+1)$-th frame are two consecutive identical frames, i.e., the X and Y coordinates are completely consistent, then the coordinates of the point corresponding to the $(i+1)$-th frame are replaced with the average value of the i-th frame and the $(i+2)$-th frame.

4.1.10. Accuracy validation

The primary objective of the accuracy validation process was to assess whether the processed trajectories accurately reflect overtaking behaviors, specifically in terms of micro-level variables like speed, speed difference, lateral distance, and longitudinal distance. The validation process primarily focused on evaluating the accuracy of positional data, as it serves as the basis for calculating position difference, speed, speed difference, and acceleration.

Due to the absence of a supplementary ground-truth trajectory system for direct comparison, an alternative method was employed. The experimental site, as outlined in Section 5.1, is paved with 60 cm by 60 cm tiles, which served as a basis for two indirect validation approaches:

To evaluate whether the trajectories could differentiate between overtaking pairs, a random sample of 10 overtaking pairs from each camera's footage was selected. At the moment the vehicles were parallel, the actual lateral distance between the overtaking and overtaken vehicles was estimated by counting the tile spans. These estimates were then compared with the lateral position differences calculated from the trajectory data, serving as an indirect validation of lateral accuracy. The main reason for choosing parallel moments to compare the distance between the two vehicles rather than comparing the difference in Y coordinates between one vehicle at one moment and another is that, unlike longitudinal movement, overall lateral movement is small, and because the floor tiles are supposed to be 60cm in length and width, it is difficult to get a better estimate of his movement in the Y direction by the number of tiles.

But this situation is different for the longitudinal direction, which, due to the much larger longitudinal speed and the longer distance of movement, employs for a rider moving in a straight line through the section (i.e., the stage where the overtaking maneuver has not yet been made or has already finshed), it can be easily verified by estimating the floor tiles in order to have a more accurate validation. For longitudinal validation, 10 rider from each camera was randomly selected, and the number of tiles they traversed over a one-second interval was recorded to determine the actual distance. This distance was then compared to the length of the corresponding trajectory segment. This approach directly validates the accuracy of the longitudinal accuracy of trajectory, also indirectly validates the rider's speed over the one-second timeframe.

We chose the methodology because direct validation of speed was not feasible without an additional precise positioning system, as it would require point-by-point comparison.

To address this, one-second intervals were used to calculate average speeds, which effectively smoothed out the fluctuations and provided a practical comparison metric. By ensuring that the trajectory-based

distance covered over one second aligns with the actual tile-measured distance, this method offers an indirect validation of average speed.

Though we can't directly validate the instant speed and acceleration, the effect of trajectory accuracy on speed and acceleration can be reasoned out, as they are both obtained through differencing position. A positional inaccuracies (up to 10 cm per point) can significantly impact instantaneous speed and acceleration calculations—up to 2 m/s and 40 m/s². However, these errors are non-cumulative, manifesting as fluctuations rather than sustained inaccuracies. The approach of averaging over a period of time could reduce such fluctuations, and in this validation process, this is the reason for using a range of tiles taken over a one-second walk-through. Another reason is due to the ease of finding video frames for a whole second when looking for the corresponding video frame in a video.

Regarding the acceleration, similarly there is no precise ground state system to help, but this part can be compared by way of literature, because the acceleration of E-bike and E-scooter has been studied in some literatures[28, 58], and we can compare the difference between the calculated acceleration and the acceleration in the literatures to judge whether it is reasonable or not.

4.1.11. Trajectory labelling

This labeling process is performed manually by watching the video footage and tagging each trajectory accordingly. For example, when a trajectory spans data from multiple cameras (e.g., R1, R2, and L1), it is sufficient to select data from only one of the cameras, such as R2, to label the entire trajectory. Each trajectory is then annotated with various attributes, including the corresponding ID, the participant's gender, the type of vehicle they are riding, and whether they are carrying an IMU device.

4.1.12. Synchronisation of IMU data and trajectory data

In the IMU output data, the precise Beijing time on the day of the experiment, along with the roll rate and roll angle data corresponding to each time point, are included. Since the IMU used in this study directly outputs roll rate and roll angle, no additional processing is required for these data before merging. The IMU data can be aligned with the trajectory data based on the precise timestamp. While the timestamps from both sources may not correspond exactly on a one-to-one basis, they can be synchronized by matching each trajectory data point with the nearest IMU timestamp.

4.2. Data analysis methodology

4.2.1. Scenario renumber

Before proceeding with the analysis of overtaking scenarios, to facilitate the subsequent comparison of seconds and scenes, this study re-numbered the scenarios according to the sequence on the day of the experiment. The details are presented in Table 4.1 below:

Table 4.1: Renumbered Overtaking Scenarios According to Experiment Sequence

New Scenario ID	Original Scenario Description
2	E-bike overtakes bike
3	E-bike overtakes E-scooter
4	E-bike overtakes E-bike
5	E-scooter overtakes bike
6	E-scooter overtakes E-bike
7	E-scooter overtakes E-scooter

Note: There is no Scenario 1 as it is the non-interactive scenario carried out first on the experiment date

4.2.2. Rationale for Per-Scenario Analysis

First, since this study involves the detection of many relationships, as shown in Figure, GLM and MANOVA can be used to detect multiple relationships or hypotheses simultaneously. Generalized linear model (GLM) is a flexible generalization of ordinary linear regression. The GLM generalizes linear regression by allowing the linear model to be related to the response variable via a link function

and by allowing the magnitude of the variance of each measurement to be a function of its predicted value[59]. Multivariate analysis of variance (MANOVA) is a procedure for comparing multivariate sample means. As a multivariate procedure, it is used when there are two or more dependent variables and is often followed by significance tests involving individual dependent variables separately[60].

However,this study adopts a per-scenario analysis approach, rather than using GLM or MANOVA, to explore the relationships within the conceptual framework. The decision to avoid using MANOVA was primarily due to the nature of the study design, which is not a full factorial design. MANOVA typically requires a full factorial setup to effectively assess the interactions between multiple factors across all possible combinations. Since our experimental design does not meet this criterion, the use of MANOVA would not be appropriate for analyzing the data.

Similarly, using GLM with interaction terms presents significant limitations when dealing with the complexity of this study. The research involves examining specific combinations of micromobility types and the influence of gender on decision-making within different overtaking contexts. For instance, we aim to compare the lateral distances when an E-bike overtakes an E-scooter, an E-bike, or a traditional bike, as well as the differences between scenarios where E-bikes or E-scooters overtake bikes. GLM can provide an overall assessment of such interactions but lacks the granularity to distinguish these specific overtaking combinations in sufficient detail. Likewise, when examining gender differences, GLM interaction terms may fail to accurately reflect how gender impacts decision-making across different scenarios due to the variability in context.

Moreover, incorporating numerous interaction terms in GLM increases the model's complexity and the risk of Type I errors, especially when the study design does not allow for balanced comparisons across all variable combinations. This makes it challenging to draw reliable conclusions about the unique effects of gender, micromobility type, and their interactions in each scenario.

To overcome these limitations, a per-scenario analysis approach was selected. This approach allows for a detailed investigation of each scenario independently, capturing the nuances and specific influences that might be missed by a generalized model. By analyzing each scenario separately, we reduce potential biases, minimize the risk of erroneous comparisons, and ensure a more accurate understanding of how gender, micromobility type, and other contextual variables influence overtaking behavior.

This method ultimately provides a clearer and more reliable understanding of the role of these variables in shaping rider decision-making and control strategies during overtaking interactions, which is crucial for understanding the variability in rider behavior across different scenarios.

4.2.3. Conceptual framework and hypothesis

In the practical execution of the experiment, only gender was feasible for study among demographic and experience factors, due to limitations in participant recruitment. Additionally, different types of E-bikes were included in the experiment, further refining the conceptual framework. As a result, the initial conceptual framework, shown in Figure 2.3, was adapted to more clearly reflect these considerations, leading to the updated framework presented in Figure 4.6.

Previous study have already segmented bicycle overtaking behavior into three distinct phases, including pre-passing, passing, and post-passing[29]. These phase concept has been adopted in the present study as moderating variables. The adoption is based on the following assumption: during different phases of overtaking, the influence of various attributes on micro variables may exhibit subtle yet significant differences. Of course, these three phases can also be used directly as an influencing attributes, for example, the difference in speed maintained between riders and the roll angle and roll rate due to different extent of control action may also be different in these three phases.

The aim of the data analysis is to test these potential relationships. This can be understood as a process of hypothesis testing using statistical methods to assess the significance of these factors. These hypotheses(the relationships) are further detailed as follows:

For non-interactive scenarios:

Speed/Deceleration:

Hypothesis 1: There is a significant difference in speed and deceleration between E-bikes and E-scooters in non-interactive scenarios.

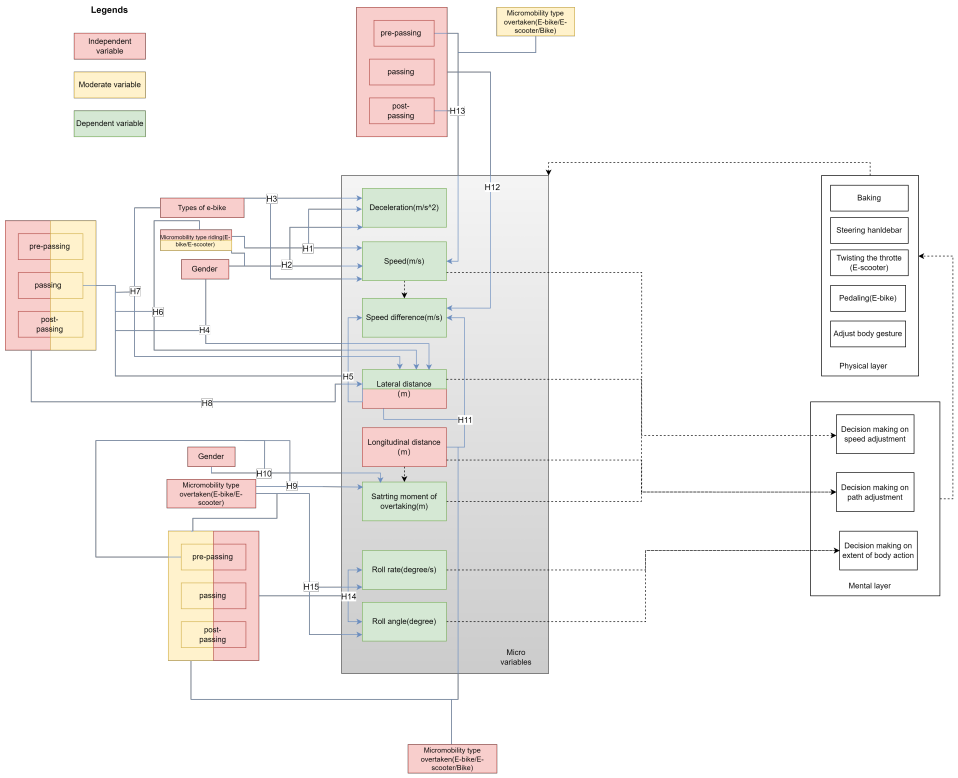

Figure 4.6: Conceptual framework before test

Scenario: Non-interactive scenarios
Independent Variable: Micromobility riding type (E-bike, E-scooter)
Dependent Variable: Speed/deceleration
Comparison: Across groups (E-bike vs. E-scooter)
Method: Independent t-test to compare the two vehicle types.
This hypothesis can be further refined:

- **H0 (Null Hypothesis 1.1)**: There is no significant difference in speed between E-bikes and E-scooters in non-interactive scenarios.
- **H1 (Alternative Hypothesis 1.1)**: There is a significant difference in speed between E-bikes and E-scooters in non-interactive scenarios.
- **H0 (Null Hypothesis 1.2)**: There is no significant difference in deceleration between E-bikes and E-scooters in non-interactive scenarios.
- **H1 (Alternative Hypothesis 1.2)**: There is a significant difference in deceleration between E-bikes and E-scooters in non-interactive scenarios.

Hypothesis 2: There is a significant gender difference in speed and deceleration within E-bike and E-scooter groups in non-interactive scenarios.
Scenario: Non-interactive scenarios
Independent Variable: Gender
Dependent Variable: Speed/deceleration
Comparison: Within group (separate comparisons within E-bike and E-scooter groups)
Method: Independent t-test within each micromobility group (E-bike and E-scooter).
This hypothesis can be further refined:

- **H0 (Null Hypothesis 2.1)**: There is no significant difference in speed between males and females within E-bike and E-scooter groups in non-interactive scenarios.
- **H1 (Alternative Hypothesis 2.1)**: There is a significant difference in speed between males and females within E-bike and E-scooter groups in non-interactive scenarios.

- **H0 (Null Hypothesis 2.2)**: There is no significant difference in deceleration between males and females within E-bike and E-scooter groups in non-interactive scenarios.
- **H1 (Alternative Hypothesis 2.2)**: There is a significant difference in deceleration between males and females within E-bike and E-scooter groups in non-interactive scenarios.

Hypothesis 3: There is a significant difference in speed among the three types of E-bikes in non-interactive scenarios.
Scenario: Non-interactive scenarios
Independent Variable: E-bike type (Regular E-bike, Fat E-bike, Foldable E-bike)
Dependent Variable: Speed/ deceleration
Comparison: Within group (among different E-bike types)
Method: ANOVA followed by post-hoc tests to compare the three types of E-bikes.
This hypothesis can be further refined:

- **H0 (Null Hypothesis 3)**: There is no significant difference in speed among the three types of E-bikes (Regular E-bike, Fat E-bike, Foldable E-bike) in non-interactive scenarios.
- **H1 (Alternative Hypothesis 3)**: There is a significant difference in speed among the three types of E-bikes in non-interactive scenarios.

For overtaking scenarios:
Lateral distance:
Hypothesis 4: There is a significant gender difference in lateral distance during passing phase.
Scenario: Scenarios 2, 3, 4, 5, 6, 7
Independent Variable: Gender
Dependent Variable: Lateral distance
Comparison: Within group (within each scenario, comparing males and females)
Method: Independent t-test for gender differences within each scenario.
This hypothesis can be further refined:

- **H0 (Null Hypothesis 4)**: There is no significant gender difference in lateral distance during the passing phase in each scenario.
- **H1 (Alternative Hypothesis 4)**: There is a significant gender difference in lateral distance during the passing phase in each scenario.

Hypothesis 6: There is a significant difference in the lateral distance when the same micromobility riding type overtakes a different type of overtaken micromobility and when different types of micromobility overtaking the same type of overtaken during passing phase.
Scenario: Scenarios 2, 3, 4, 5, 6, 7
Independent Variable: Micromobility type
Dependent Variable: Lateral distance
Comparison: Across groups (E-bike, E-scooter, Bike)
Method: ANOVA followed by post-hoc tests to compare micromobility types across different scenarios.
The hypothesis can be further refined as follows:

- **H0 (Null Hypothesis 6.1)**: There is no significant difference in lateral distance when the same micromobility type overtakes different types during the passing phase.
- **H1 (Alternative Hypothesis 6.1)**: There is a significant difference in lateral distance when the same micromobility type overtakes different types during the passing phase.
- **H0 (Null Hypothesis 6.2)**: There is no significant difference in lateral distance when different micromobility types overtake the same type during the passing phase.
- **H1 (Alternative Hypothesis 6.2)**: There is a significant difference in lateral distance when different micromobility types overtake the same type during the passing phase.

Hypothesis 7: There is a significant difference in lateral distance among different types of E-bikes during passing phase.
Scenario: Scenario 3
Independent Variable:E-bike type (Regular E-bike, Fat E-bike, Foldable E-bike)

Dependent Variable: Lateral distance
Comparison: Within group (among different E-bike types)
Method: ANOVA followed by post-hoc tests to compare lateral distance across E-bike types.
This hypothesis can be further refined:

- **H0 (Null Hypothesis 7)**: There is no significant difference in lateral distance among different types of E-bikes during the passing phase.
- **H1 (Alternative Hypothesis 7)**: There is a significant difference in lateral distance among different types of E-bikes during the passing phase.

Hypothesis 8: The maximum lateral distance occurs during the passing phase.
Scenario: Scenarios 2, 3, 4, 5, 6, 7
Independent Variable: Ovetaking phase (pre-passing, passing, post-passing)
Dependent Variable: Maximum lateral distance
Comparison: Within group (comparing across passing phases)
Method: Qualitative analysis method, identifying the maximum lateral distance point for each rider and determining in which phase (pre-passing, passing, or post-passing) the maximum distance occurs.
This hypothesis can be further refined:

- **H0 (Null Hypothesis 8)**: The maximum lateral distance does not occur during the passing phase.
- **H1 (Alternative Hypothesis 8)**: The maximum lateral distance occurs during the passing phase.

Starting position of overtaking:
Hypothesis 9:There is a significant difference in the overtaking starting position when the same micromobility riding type overtakes a different type of micromobility overtaken during passing phase.
Scenario: Scenarios 2, 3, 4
Independent Variable: Micromobility type
Dependent Variable: starting position of overtaking
Comparison: Across groups (E-bike, E-scooter, Bike)
Method: ANOVA followed by post-hoc tests to compare starting positions between different micromobility types.
This hypothesis can be further refined:

- **H0 (Null Hypothesis 9)**: There is no significant difference in the starting position of overtaking when the same micromobility type overtakes different types during the passing phase.
- **H1 (Alternative Hypothesis 9)**: There is a significant difference in the starting position of overtaking when the same micromobility type overtakes different types during the passing phase.

Hypothesis 10: There is a significant gender difference in the overtaking starting position within each scenario.
Scenario: Scenarios 2, 3, 4
Independent Variable: Gender
Dependent Variable: starting position of overtaking
Comparison: Within group (comparing males and females within each scenario)
Method: Independent t test to compare gender differences in the starting position of the passing.
This hypothesis can be further refined:

- **H0 (Null Hypothesis 10)**: There is no significant gender difference in the overtaking starting position within each scenario.
- **H1 (Alternative Hypothesis 10)**: There is a significant gender difference in the overtaking starting position within each scenario.

Speed difference
Hypothesis 5: There is a positive relationship between lateral distance and speed difference during passing phase.
Scenario: Scenarios 2, 3, 5, 6
Independent Variable: Lateral distance
Dependent Variable: Speed difference
Comparison: Within group (within each scenario)

Method: Pearson correlation, linear regression to explore the relationship between lateral distance and speed difference within each scenario.
This hypothesis can be further refined:

- **H0 (Null Hypothesis 5)**: There is no significant relationship between lateral distance and speed difference during the passing phase.
- **H1 (Alternative Hypothesis 5)**: There is a positive relationship between lateral distance and speed difference during the passing phase.

Hypothesis 11: Lateral distance, longitudinal distance, and micromobility type significantly influence the speed difference during the whole process of overtaking.
Scenario: Scenarios 2, 3, 4
Independent Variable: Lateral distance, longitudinal distance, micromobility type
Dependent Variable: Speed difference
Comparison: Across groups and variables
Method: Multiple linear regression to assess the impact of lateral distance, longitudinal distance, and micromobility type on speed difference.
This hypothesis can be further refined:

- **H0 (Null Hypothesis 11)**: Lateral distance, longitudinal distance, and micromobility type do not significantly influence speed difference during the overtaking process.
- **H1 (Alternative Hypothesis 11)**: Lateral distance, longitudinal distance, and micromobility type significantly influence speed difference during the overtaking process.

Hypothesis 12: There is a significant difference in speed difference across the three phases of overtaking.
Scenario: Scenarios 2, 3, 4
Independent Variable: passing phases (pre-passing, passing, post-passing)
Dependent Variable: Speed difference
Comparison: Within group (comparing speed differences across pre-passing, passing, and post-passing phases)
Method: ANOVA followed by post-hoc tests to compare speed differences across the three phases.

- **H0 (Null Hypothesis 12)**: There is no significant difference in speed difference across the three phases of overtaking (pre-passing, passing, post-passing).
- **H1 (Alternative Hypothesis 12)**: There is a significant difference in speed difference across the three phases of overtaking (pre-passing, passing, post-passing).

Speed of overtaken micromobility
Hypothesis 13 There is a significant change in the speed of the overtaken vehicle between the pre-passing phase and post-passing phase, and between the beginning and ending of the pre-passing phase.
Scenario: Scenarios 2, 3, 4
Independent Variable: passing phase (pre-passing, post-passing)
Dependent Variable: Speed of overtaken vehicle
Comparison: Within group (same vehicle, before vs. after passing)
Method: Paired t-test to compare the speed before and after passing for the same overtaken vehicle.
The hypothesis can be further refined as follows:

- **H0 (Null Hypothesis 13.1)**: There is no significant change in the speed of the overtaken vehicle between the pre-passing phase and the post-passing phase.
- **H1 (Alternative Hypothesis 13.1)**: There is a significant change in the speed of the overtaken vehicle between the pre-passing phase and the post-passing phase.
- **H0 (Null Hypothesis 13.2)**: There is no significant change in the speed of the overtaken vehicle between the beginning and the end of the pre-passing phase.
- **H1 (Alternative Hypothesis 13.2)**: There is a significant change in the speed of the overtaken vehicle between the beginning and the end of the pre-passing phase.

Roll rate and roll angle
Hypothesis 14 There is a significant difference in roll rate and roll angle across the three passing phases.
Scenario: Scenarios 3, 4, 5, 6
Independent Variable: passing phase (pre-passing, passing, post-passing)
Dependent Variable: Roll rate, roll angle
Comparison: Within group (comparing roll rate and roll angle across phases)
Method: ANOVA followed by post-hoc tests to compare roll rate and roll angle across different phases.
The hypothesis can be further refined as follows:

- **H0 (Null Hypothesis 14.1)**: There is no significant difference in roll rate across the three passing phases (pre-passing, passing, post-passing).
- **H1 (Alternative Hypothesis 14.1)**: There is a significant difference in roll rate across the three passing phases (pre-passing, passing, post-passing).
- **H0 (Null Hypothesis 14.2)**: There is no significant difference in roll angle across the three passing phases (pre-passing, passing, post-passing).
- **H1 (Alternative Hypothesis 14.2)**: There is a significant difference in roll angle across the three passing phases (pre-passing, passing, post-passing).

Hypothesis 15:There is a significant difference in roll rate and roll angle between E-bikes and E-scooters during each phase of overtaking.
Scenario: Scenarios 3, 4
Independent Variable: Micromobility type (E-bike, E-scooter)
Dependent Variable: Roll rate, roll angle
Comparison: Across groups (E-bike vs. E-scooter)
Method: Independent t-test to compare roll rate and roll angle between E-bikes and E-scooters during passing.
The hypothesis can be further refined as follows:

- **H0 (Null Hypothesis 15.1)**: There is no significant difference in roll rate between E-bikes and E-scooters during each phase of overtaking.
- **H1 (Alternative Hypothesis 15.1)**: There is a significant difference in roll rate between E-bikes and E-scooters during each phase of overtaking.
- **H0 (Null Hypothesis 15.2)**: There is no significant difference in roll angle between E-bikes and E-scooters during each phase of overtaking.
- **H1 (Alternative Hypothesis 15.2)**: There is a significant difference in roll angle between E-bikes and E-scooters during each phase of overtaking.

The hypotheses outlined above form the foundation of the data analysis approach used in this study. Each hypothesis is carefully tested using statistical methods tailored to the specific variables under consideration.

The following sections present the definitions of the moderating variables (phases) used in the analysis of the data for this study, as well as the calculations of speed, deceleration and the moment of the start of overtaking, and for the roll rate and roll angle.

4.2.4. Definition of passing phases

The concept of ”passing phases” which is similar to previous study[29] as mentioned in section2.5 was central to the data analysis. In this study, the overtaking process was primarily defined by the ”passing phase,” with additional phases identified before and after this critical period. The passing phase was defined as the time period when the longitudinal distance (X-difference) between the front of the overtaking vehicle and the rear of the overtaken vehicle was within 2 meters. The choice of a 2-meter threshold for defining the passing phase was based on ensuring that this distance could adequately cover all possible combinations of vehicles involved in the study. This threshold corresponds to approximately half the combined length of the overtaking and overtaken vehicles. While this value is indeed subject to variation—given that riders on E-bikes or bikes may lean forward or change posture, and e-scooter riders can stand in different positions—the 2-meter range provides a slight redundancy.

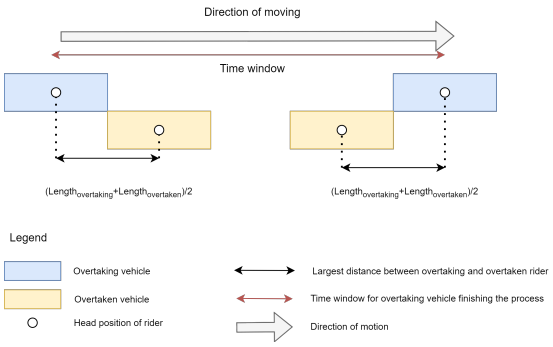

Figure 4.7: Explanation of passing phase

This redundancy is designed to account for these individual differences, ensuring that the threshold consistently encompasses the range needed for all rider and vehicle combinations in the experiment.

- Passing: The period when the longitudinal distance is within 2 meters.
- Pre-passing: The period before the passing phase begins, i.e., when the longitudinal distance is greater than 2 meters prior to the passing phase.
- Post-passing: The period after the passing phase ends, i.e., when the longitudinal distance exceeds 2 meters again following the passing phase.

Figure4.7 illustrates this definition of passing phase, showing how the longitudinal distance changes throughout the passing phase. This approach allows for a comprehensive analysis of rider behavior before, during, and after the critical passing phase, providing insights into how riders adjust their behavior throughout the entire overtaking process.

4.2.5. Speed and deceleration calculation

The speed calculation in this study was conducted using the Triangular Moving Average (TMA) method with a window size of 10, which corresponds to a 0.5-second span. This choice was based on a detailed comparison of various smoothing methods and window sizes, as documented in the AppendixE. TMA was selected because it offers a balanced approach to smoothing the data without sacrificing too much detail, providing a realistic representation of speed changes over time.

TMA is a type of weighted moving average, where data points near the center of the window are given more weight compared to those at the edges. In the context of this study, each point's speed is computed as a weighted average of the surrounding points, where the weights form a triangular distribution. This method helps to reduce short-term fluctuations caused by minor inaccuracies in trajectory data, while still capturing overall trends in speed. The window size of 10 (0.5 seconds) was chosen as it effectively balances smoothness with responsiveness to changes in speed, as confirmed through comparative testing. The calculation of acceleration is then consistent with speed using the TMA, window = 10 calculation.

4.2.6. Overtaking starting position

Detecting the initiation of overtaking for e-bikes and e-scooters is crucial for understanding their overtaking behavior, particularly in relation to the mental layer of the framework shown in Figure 4.6. This is especially important when riders decide to change their path and speed during overtaking.

The method for detecting overtaking initiation was based on observing when the lateral position difference between overtaking and overtaken vehicles began to increase significantly. This methodology using change rate of lateral distance has been used in a few studies about autonomous vehicles[61, 62, 63].Here, this thesis extends this method to the study of micromobility. The detection process consists of the following steps:

First, the change rate of lateral distance between the overtaking and overtaken vehicles is calculated at each time step using the following formula:

$$d(t) = \frac{y_{\text{overtaking}}(t) - y_{\text{overtaken}}(t) - (y_{\text{overtaking}}(t-1) - y_{\text{overtaken}}(t-1))}{\Delta t} \tag{4.2}$$

where $d(t)$ represents the rate of change in lateral distance at time t, $y_{\text{overtaking}}(t)$ is the lateral position of the overtaking vehicle at time t, $y_{\text{overtaken}}(t)$ is the lateral position of the overtaken vehicle at time t, and Δt is the time interval between measurements. After calculating the instantaneous rate of change, a moving average with a window size of 10(0.5S) is applied to smooth the data. This time window is the same with the one of speed calculation.

In the second step, a threshold for detecting significant lateral movement is established by performing a statistical analysis on the lateral position change rate during the pre-passing phase. The threshold is set as the mean minus one standard deviation (Mean - 1σ) of the lateral position change rate during these non-overtaking periods. The first moment when the rate of change of lateral distance is greater than that of (Mean - 1σ) is the starting position of overtaking.

The selection of Mean - 1σ as the threshold for detecting the initiation of overtaking maneuvers in e-bikes and e-scooters is based on two primary considerations:

1. Statistical Robustness: Utilizing the mean and standard deviation of lateral position change rates during non-overtaking periods establishes a statistically sound baseline. This approach accounts for the natural variability in rider behavior while enabling the detection of significant deviations. The Mean - 1σ threshold strikes an optimal balance between sensitivity and specificity, allowing for the identification of genuine overtaking initiation events while minimizing false positives from routine movements.
2. Visual Validation: While direct quantitative validation was not possible due to the lack of a ground truth dataset, the effectiveness of the Mean - 1σ threshold was assessed through a visual analysis process. This involved plotting the relative coordinates of the overtaking pair (e-bike or e-scooter and the overtaken vehicle) over time. By visually inspecting these marked points in relation to the trajectory data, the reasonableness of the detected overtaking initiation moments could be observed. For a subset of trajectories, five were randomly selected from each scenario for validation, ensuring a representative sample across different contexts. Although qualitative, this method provides practical insights and an verification step.

4.2.7. Roll rate and roll angle

The experimental design and data collection procedures in this study presented certain limitations that influenced the analysis. A critical technical issue arose from the placement of the E-scooter's inertial measurement unit (IMU) on the continuously rotating stem. This positioning resulted in roll angle and roll rate measurements that do not accurately represent the E-scooter's true lateral tilt relative to its direction of travel. This technical limitation significantly impacts our ability to directly compare the dynamic behavior of E-bikes and E-scooters during overtaking maneuvers, particularly when these vehicles are overtaking similar vehicle types.

Despite this limitation, the study utilized the collected data to analyze E-scooter behavior when overtaking different types of vehicles. However, it is crucial to exercise caution when interpreting these results. The data still provide valuable insights into the general patterns of E-scooter movement during overtaking, but the specific magnitudes and timings of roll angles and rates may not be directly comparable to those of E-bikes or accurately reflect the E-scooter's true motion relative to the ground.

In this study, mean absolute value was used for all roll angle and roll rate data, which is consistent with study[28, 27].

5

Implementation of experiment design

This Section details the preparatory steps and execution process of the experiment. Initially, Section 5.1 outlines the selection process for the experiment field.Following this, Section 5.2 introduces the specific models of e-scooters and e-bikes used in the experiment. Section 5.3 covers the actual recruitment of participants for the experiment. Subsequently, Section 5.4 elaborates on the detailed experimental plan, which is based on the actual availability of e-bikes and e-scooters. Section 5.5 then discusses the models of data collection equipment used in the experiment and their setup. Section 5.6 describes the events and procedures that took place on the day of the experiment, providing insights into the practical implementation of the study.

As the execution of this experiment in China, while the author was primarily based in the Netherlands, necessitated significant collaboration with local teams. Moreover, the author's supervisor, Yufei, shared the role of experimental supervisor and implementer with the author during the execution of the experiment. Every step of the implementation has contributions from both Chinese team and the supervisor. All of their detail contribution and the joint work are in AppendixC.

5.1. Experiment field location

The experimental site is a square area located at the Hebei University of Water Resources and Electric Engineering in Cangzhou, China, as shown in the red rectangle part of figure5.1. The measurements

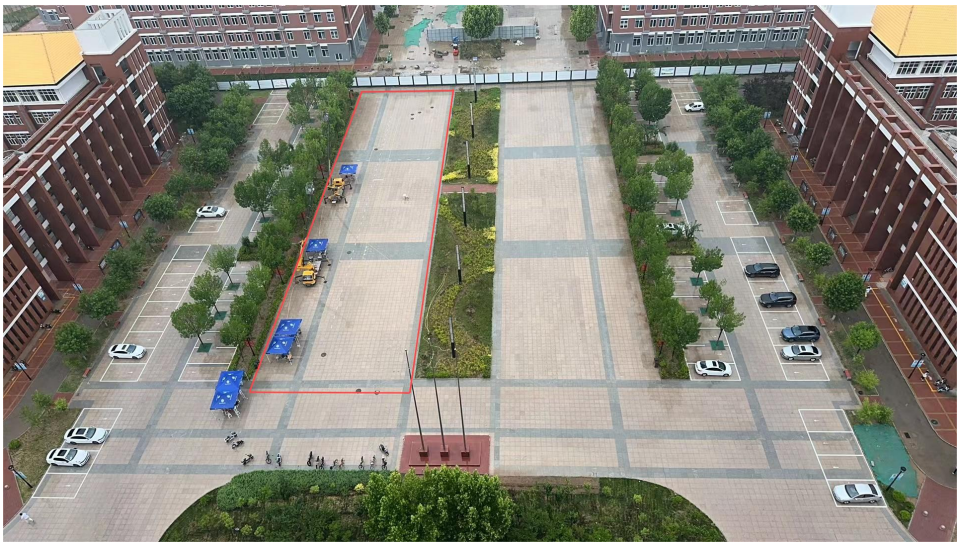

Figure 5.1: Experiment field

of this square are about 25 meters in width and 80 meters in length. In the actual experiment, the track

Figure 5.2: Main track and middle line

in figure3.1 was achieved by means of ground tape, where the boundary line of the road was taped in yellow and black, and the dotted line in the middle of the road was realized by using white ground tape as show in Figure5.2. The ground taping is achieved with the help of the supervisor and the local team as in AppendixC.1.

In this experiment, video recognition techniques are used to extract the trajectory data of the e-bike and e-scooter riders. The video extraction technique requires the camera to be set up in a high place, and in this experiment, the aerial work platforms are used to lift the cameras. In order to ensure that the data obtained by the video extraction technique is accurate and consistent, two groups of cameras are used. Before the experiment started, the position of the two aerial trucks, as well as the exact height of the lift, were adjusted to achieve the optimal position based on the real-time output from the camera. Figure5.3 shows the position of the two aerial trucks during the experiment, as well as the track on the ground, which was taped out with yellow&black tapes and white tapes. The area is covered with standard square tiles of size 60 x 60 cm.It is regularly used by pedestrians, bicycles, and motor vehicles within the campus. Therefore, the surface type can resemble real-world riding/cycling conditions.

Figure 5.3: One shot during the experiment

5.2. Micromobilty vehicles used in experiment

For practical reasons, we ended up obtaining three e-scooters on our own, the model being the Ninebot E9 as shown in figure 5.4, with a top speed of 20 km/h. For the e-bikes as shown in figure5.5, we finally obtained 4 e-bikes. Two of the e-bikes were regular ones; one was foldable, and the other one was a fat

e-bike. This implies that the variety within the same e-modes (particularly e-bikes) should be critically considered when analyzing the data.

The decision on these vehicles are done by the author, while the purchase and renting are done by Chinese teams as in AppendixC.2

Figure 5.4: E-scooter

5.3. Participant recruitment

Regarding rider personal characteristics, combined with the actual recruitment of the experimental participants, a broad coverage in age, and the equal level in gender and riding experience were difficult to realize because the participants were mainly university students, with very little difference in age. Most of them had similar experience in using e-scooter and e-bike but varying in familiarity level.

In terms of specific arrangements for the participants, two days prior to the experiment, the author explained how they would be asked to ride on the day of the experiment. After the briefing, participants were allowed to voluntarily choose the type of vehicle they wanted to ride. The participants who have more experience in certain modes had the priority of using the corresponding mode in the experiment. Finally, the male/female ratios are 9/3, 8/4, and 9/3 for e-scooter, e-bike, and e-moped, respectively. Although it is not 50/50, the effect of rider gender on micromobility interactions can be accommodated.

According to their willingness, the author group the participants. Once the e-scooter and e-bike groups were formed, each participant was assigned a micromobility vehicle based on their height order. This measure was taken because the limited number of e-bikes required three people to share one vehicle, and similar heights ensured that they did not need to adjust the seat height throughout the experiment. After completing the grouping, the participants familiarized themselves with and test drove the vehicles they would use during the experiment.

After completing group assignment, participants familiarized themselves with and test drove the vehicles they would use during the experiment, ensuring they were qualified as riders of the assigned modes, despite varying levels of user experience and familiarity. According to[64],riding a bicycle involves a combination of tasks executed based on rules for performing maneuvers and automatic actions for split-second control of the bicycle. We posit that a similar operational process of actions and reactions applies to micromobility traffic. By providing participants with the opportunity and sufficient time to familiarize themselves with riding the vehicles (particularly e-scooters and e-bikes), their riding and interactive maneuvers are expected to reflect their natural behavior under split-second decision-making conditions.

((a)) E-bike a

((b)) Foldable e-bike b

((c)) E-bike c

((d)) Fat e-bike d

Figure 5.5: E-bikes

And a unique ID system is used to identify the participants during the experiment, the design of this system, is a joint work by the author and the supervisor. And the recruitment of the participants is a joint of author and the local team. Then the instruction, grouping and measurement of the height is joint work of the author, local team and the supervisor. The details on each one's contribution is shown in AppendixC.3.

5.4. Experiment schedule

Although a theoretical schedule for each scenario's duration was initially outlined in section3.7, these planned durations proved to be excessive for each scenario in practice. To minimize the potential effects of learning bias, it was necessary to reduce the riding time. The actual schedule implemented during the experiment is presented in Table5.1.

It's important to note that while the scenario numbers and names remain consistent with those in section3.7, the actual order of implementation differed during the experiment. As mentioned in section3.7, if transitions between scenarios and rounds were executed efficiently, the actual duration could be shorter than the planned time.

Table5.2 displays the true duration of each scenario upon completion of the experiment. The scenario numbers here are the order in which the experiments were actually performed on the day of the experiment. This data provides a realistic picture of the time required for each experimental scenario, reflecting the adjustments made to optimize the experimental process and reduce potential learning effects among participants.

Table 5.1: Schedule used on experiment day
Where Rd stands for Round;ovt stands for overtaking; ovn stands for overtaken,; Dur.Rd. stands for duration of a round;Dur.Sc. stands for duration of a scenario

Sc. No	Sc. Name	Rd. No	EB		ES		B	Dur. Rd.	Dur. Sc.(min)
			ovt	ovn	ovt	ovn	ovn		
2	Ov-bike2	1	3	-	-	-	3	5	20
		2	3	-	-	-	3	5	
		3	3	-	-	-	3	5	
		4	3	-	-	-	3	5	
3	Ov-inter2	1	3	-	3	-	-	5	20
		2	3	-	3	-	-	5	
		3	3	-	3	-	-	5	
		4	3	-	3	-	-	5	
4	Ov-intra2	1	2	2	-	-	-	5	30
		2	2	2	-	-	-	5	
		3	2	2	-	-	-	5	
		4	2	2	-	-	-	5	
		5	2	2	-	-	-	5	
		6	2	2	-	-	-	5	
5	Ov-bike2	1	-	3	-	3	-	5	20
		2	-	3	-	3	-	5	
		3	-	3	-	3	-	5	
		4	-	3	-	3	-	5	
6	Ov-inter2	1	-	3	3	-	-	5	20
		2	-	3	3	-	-	5	
		3	-	3	3	-	-	5	
		4	-	3	3	-	-	5	
7	Ov-intra2	1	-	2	1	-	-	5	30
		2	-	1	2	-	-	5	
		3	-	1	2	-	-	5	
		4	-	1	2	-	-	5	
		5	-	1	2	-	-	5	
		6	-	1	2	-	-	5	

Where scenario 1 is non-interactive scenario

5.5. Data Collection equipment setup

5.5.1. Cameras setup

The experiment finally used four cameras of Dahua as shown in Figure5.6(a). The four cameras are divided into two sets to cover the whole range with overlapping area to trajectory stitching purposes. Before the start of the experiment, the camera was secured to the railing of the aerial truck, which was physically mounted using wire as shown in figure5.6(b). The offset angle and focal length of the camera, as well as the position of the aerial work truck and the final operating height, were all adjusted repeatedly according to the output picture of the camera, which was accomplished after achieving the effect of clear video effect and reasonable coverage. The final four cameras all output video in 1920*1080, 20fps format, where each focal length is set as shown in the table5.3.

The acquisition and transport of the camera was done with the assistance of the Beijing team, and the setup is a joint work of the author and the supervisor both software and hardware as shown in AppendixC.4.

5.5.2. IMU

The Figure5.7shows the IMU device mounted on the e-scooter's steering stem. BNO-055 has a built-in Kalman filter algorithm that directly outputs roll, yaw, and pitch angle and rate data.

It is worth noting that due to the limitation of the number of IMU devices. During the experiment, only one e-scooter, number two in table AppendixF.2, carried the device; for the e-bike, it was equipped only on the e-bike in figure5.5(a). And throughout the experiment, neither vehicle is treated as the overtaken vehicle.

Table 5.2: Actual Scenarios Duration

Scenario No.	Start Time	End Time	Duration (min)
2	08:58:00	09:27:00	29
3	09:27:00	09:42:00	15
4	09:59:00	10:24:00	25
5	10:25:00	10:45:00	20
6	10:50:00	11:10:00	20
7	11:11:00	11:27:00	16

Where scenario 1 is non-interactive scenario

((a)) Cameras

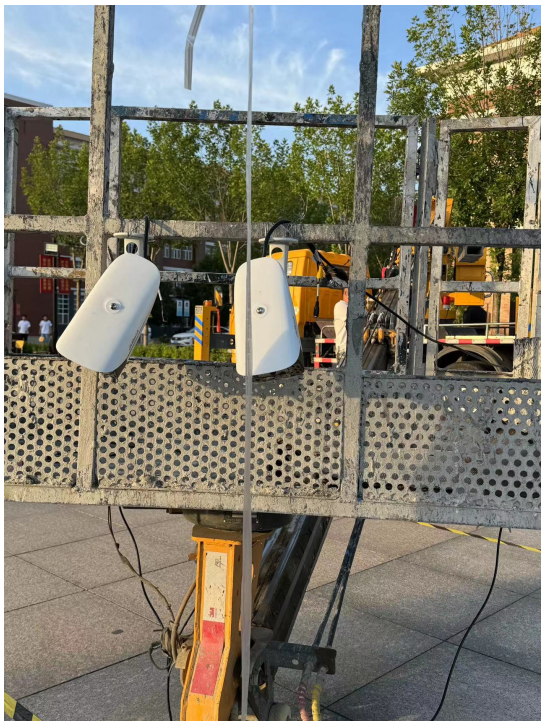

((b)) Cameras mounting on the railing

Figure 5.6: Comparison of different camera setups

The IMU device were provided by the Beijing team including the setup as shown in AppendixC.5.

5.6. Experiment execution

The experiment was conducted on May 26, 2024, at the Hebei University of Water Resources and Electric Engineering. Participants were provided with white T-shirts and red caps, as shown in Figure5.9, which they wore throughout the experiment to ensure consistent visibility in camera images. Each participant was assigned a unique identification code, consisting of a specific shape and a Roman numeral, as described in section5.3.

This identification code was implemented in two forms. One set was affixed to the T-shirts, serving to assist supervisors in monitoring the experimental process. The second set was placed on the caps, with the code size on the cap brim designed to be sufficiently large for camera visibility. The cap-mounted codes were primarily intended to aid in trajectory calibration, allowing for easy identification of vehicle types and gender information during data analysis.

For most design scenarios, participants were instructed to perform their riding tasks in a sequential order, eliminating the need for participants to wait for others to complete a lap before entering the track.

Table 5.3: Camera Settings

Name of camera	Zoom Step Length	Focus Step Length	Camera Height
L1	560	1988	14,5 m
L2	560	1926	14.5 m
R1	560	1982	15.1 m
R2	560	1976	15.1 m

Figure 5.7: E-scooter with IMU

This arrangement expedited most overtaking and bypassing scenarios.

To ensure sufficient interactive maneuvers were triggered and captured by cameras in designated areas, multiple vehicles were simultaneously present on both paths shown in Figure3.3, rather than just one vehicle per path. The specific number of vehicles for each scenario and round is detailed in Table5.1. Furthermore, as mentioned in section3.5, experiment supervisors could slightly control the timing of participants re-entering the designed track after completing a lap, maximizing the likelihood of triggering overtaking maneuvers.

On the day of the experiment, to more effectively capture the overtaking behavior of e-bikes and e-scooters, the experimental path was modified to the form shown in Figure5.8. Unlike the initially designed complete circular path, the modified experimental path no longer required participants to overtake spontaneously. Instead, experimental monitors were stationed on both sides of the field, responsible for controlling the entry timing of overtaking and overtaken participants in each round of the experiment to ensure the occurrence of overtaking behavior. The main reason for adopting this strategy lies in the relatively small sample size of e-bikes and e-scooters. By controlling the entry timing, the time consumed by experimental participants to complete sufficient overtaking behaviors through meaningless riding can be saved. This meaningless riding may lead to the emergence of the learn

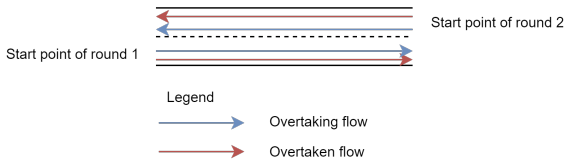

Figure 5.8: Path of intra mode overtaking

effect, which could affect the validity of the experimental results.

By modifying the experimental path and introducing the control of experimental monitors, this study minimizes the influence of the learn effect while ensuring the acquisition of sufficient overtaking behavior samples. This adjustment in the experimental design helps to improve the efficiency of data collection and ensures that the collected data can more accurately reflect the true behavioral characteristics of e-bikes and e-scooters during the overtaking process.

The cameras and IMU units began recording simultaneously after camera parameter adjustments. The researcher then guided participants on the appropriate times to enter the designed track according to the pre-defined schedule. Once on the track, participants followed their designated paths and performed their assigned tasks.

This detailed experimental setup and execution process demonstrates the careful planning and real-time management required to ensure the collection of relevant data for analyzing micromobility interactions, particularly overtaking behaviors.

((a)) Caps **((b))** T-shirt

Figure 5.9: Caps and T-shirts

During the whole experiment, the video was recorded without a break, and the experimental researcher was closely monitoring the experiments to prevent accidents or disruptions to the experimental plan. Figure5.10 shows one shot from camera L2 during one e-scooter overtake one bicycle.

Figure 5.10: One shot from camera L2 during overtaking

Throughout the course of the experiment, the actual riding time of the riders was only about one-fifth of the total length of the experiment, and the fatigue level of the experimenters was very low because of the small amount of physical energy needed to be consumed to ride the e-scooter and e-bike. Moreover, there were sufficient sunshades for experimental participants to rest during their free time, and the local logistic team provided sufficient logistic support for the participants, including purchasing and providing watermelons, beverages, and snacks. Therefore, the learning effect due to exhaustion was artificially absent in this study.

Second, the learning effect due to mutual learning and familiarity with the same task was also eliminated as much as possible. In this experiment, each participant engages in different scenarios, completing four laps within each scenario. During these laps, participants perform four overtaking maneuvers, providing multiple data points per individual under consistent conditions.

This design effectively controls for learning effects by introducing variation across scenarios, so while each participant encounters only one session per scenario, the repeated overtakes within each session help capture intra-scenario behavior. The four laps per scenario allow us to observe consistent overtaking patterns and subtle behavioral differences within a single context, thereby balancing the need for representativeness and capturing individual behavior variability.

The object of overtaking is different each time. In addition, the learning effect due to observing the behavior of other experimental participants was also objectively weakened, according to the researchers' observation that the vast majority of experimental participants were playing with their cell phones, etc., in their free time.

Of course during the trial there was some joint work, especially in terms of logistics support, which is shown in AppendixC.6.

5.7. Clarify on contribution

During the execution of the experiment, the author received help from the supervisor and the Chinese team.

The team from China provided the purchase and rental of almost all equipment, including cameras, IMUs, and experimental vehicles. The Chinese team also provided participant recruitment and logistical support during the experiment. The setup of the IMU and the data collection of IMU during the experiment were also handled by the Chinese team.

The author and his supervisor are mainly responsible for the specific implementation of each step. The author of this thesis arrived at the test site a week before the experiment date, received the equipment and set them up. During the preparation week, the author communicated with the supervisor timely about the situation to make up for the selection and purchase of some equipment, such as shirts and caps. And jointly, after grouping the experimenters, the author and the supervisor conducted training participants and measured heights, and jointly served as experimental supervisors on the day of the experiment. Of course, in the specific implementation process, the author and the supervisor also received help from the Chinese team, especially in transporting equipment and providing venues.

The details of every single step is shown in the AppendixC.

6

Data processing

This section describes, the specific implementation of the video data processing process. The sequence of execution follows exactly the data flow described in section4.1. The results of the data processed through this sequence are used to support the data analysis in the next section.

6.1. Video data processing

6.1.1. Video format conversion

This research employs HandBrake, a free video conversion tool, to convert HEVC format video files to MP4 format. Handbrake can process most common multimedia files and any DVD sources that do not contain any kind of copy protection, and it could output .MP4 videos with H.264, MPEG-4 encoding[65].

Through this step, video files that originally could only run on specific computers can now be processed and analyzed on various computers with different configurations. This not only improves the portability of the video files but also lays a solid foundation for subsequent research work.

6.1.2. Pixel trajectory extraction

Figure6.1 shows the working of MODT tool in identifying a pair of overtaking pairs. Figure6.2 shows the sample trajectory extracted from one video of each camera.

For calculating the exact start time of each video, Figure 6.3, which contains two images, shows an example. As can be seen, the time in the upper right corner transitions from 10:12:32 to 10:13:33. By manually extracting the first fifty frames, we are able to count them manually and find that at frame 13, the video time changes from 10:13:32 to 10:13:33. Given that the video frame rate is 19.98 FPS (frames per second), we can calculate the exact start time of the video as follows:

$$\text{10:13:33.000} - \left(\frac{1000}{19.98}\right) \times 12 = \text{10:13:32.400}.$$

Thus, we can determine the exact start time of each video.

After completing the preliminary extraction, the data format was first organized and the data was integrated into a table. There are six columns in total, namely X coordinate (unit: pixel), Y coordinate (unit: pixel), and trajectory ID, relative video time, frame number, precise Beijing time. The relative video time and frame number are retained to prepare for time alignment in the subsequent process. The trajectory extracted in the first step has detection errors, including the detection of some non-experimental research objects, detection errors, trajectory disconnection due to shadow interference, etc. These errors will be fixed during subsequent processing.

The parameters used in this process include RGB values, standard deviation, camera detection range, and the precise start time of each video are in table Appendix G.1, G.2 and G.3,G.4,G.5 and ,G.6.

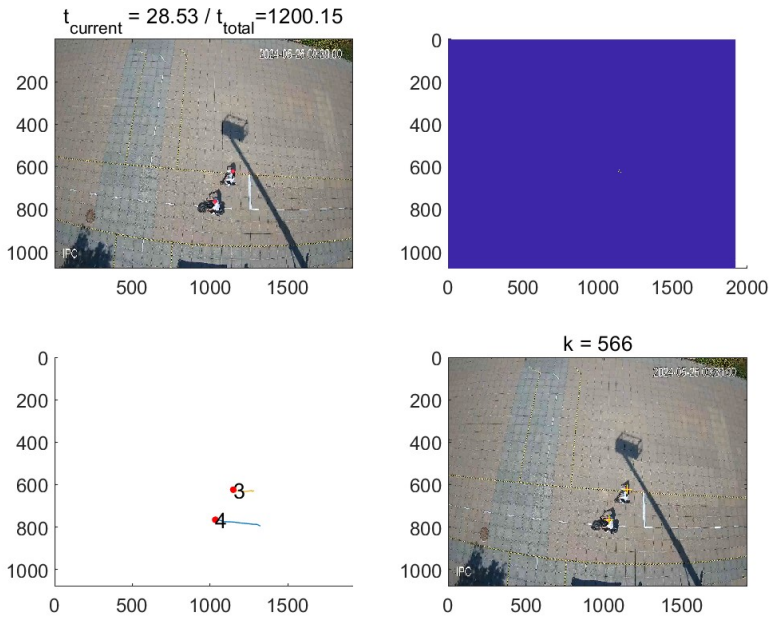

Figure 6.1: A snapshot when MODT tool extracting pixel trajectory from L1 camera

Table 6.1: Scale table

Camera	R1	R2	L1	L2
Scale	0.012	0.012	0.013	0.013

6.1.3. Image Correction

Figure6.4 and Figure6.5 respectively show the uncorrected pictures and corrected pictures of the four cameras R1-R2-L1-L2 (order from right to left) as shown in Figure3.4. And the table6.2 shows the parameter used for the Figure6.4 and Figure6.5. The R1 and R2 parameters in table6.2 are the parameters used for all videos.The parameters for L1 and L2 will be put in an independent Excel file in the name of ParameterImageCorL1 and ParameterImageCorL2, as there are too many columns and rows.

In Figure 6.5, the black border is present because during the transformation of the original image, some of the transformed pixel values exceed the range of 1920*1080. To ensure that the trajectories are not lost after the transformation, a larger canvas is needed to accommodate the image, and the black base serves as this canvas. In this study, the canvas size was chosen to be 2560*1600, which is the screen resolution of the computer used by the data processing personnel.

By calculating the average scale from the video frames, a scale table6.1 was obtained for these four cameras. The scale parameter is an average value, which is calculated by manually counting the number of standard-sized floor tiles and determining the total physical length in the X direction, then dividing it by the pixel length of 1920 in the X direction.

It is important to highlight that the aerial work platform, which held the L1 and L2 cameras in a fixed position, experienced a gradual tilting motion throughout the experiment. This tilting was not uniform; it included a sudden tilt from the right to the left, followed by a slow tilt from the left back to the right. This continuous change in camera orientation presented a significant challenge for data processing and analysis. To address this issue, each video captured by the L1 and L2 cameras was divided into ten equal segments. This segmentation approach was necessitated by the constantly changing camera angles, which meant that a single set of parameters could not be used to convert the entire video to a vertical downward perspective. Instead, parameters needed to be adjusted continuously to account for the changing viewpoint. The decision to divide each video into ten segments was based on several

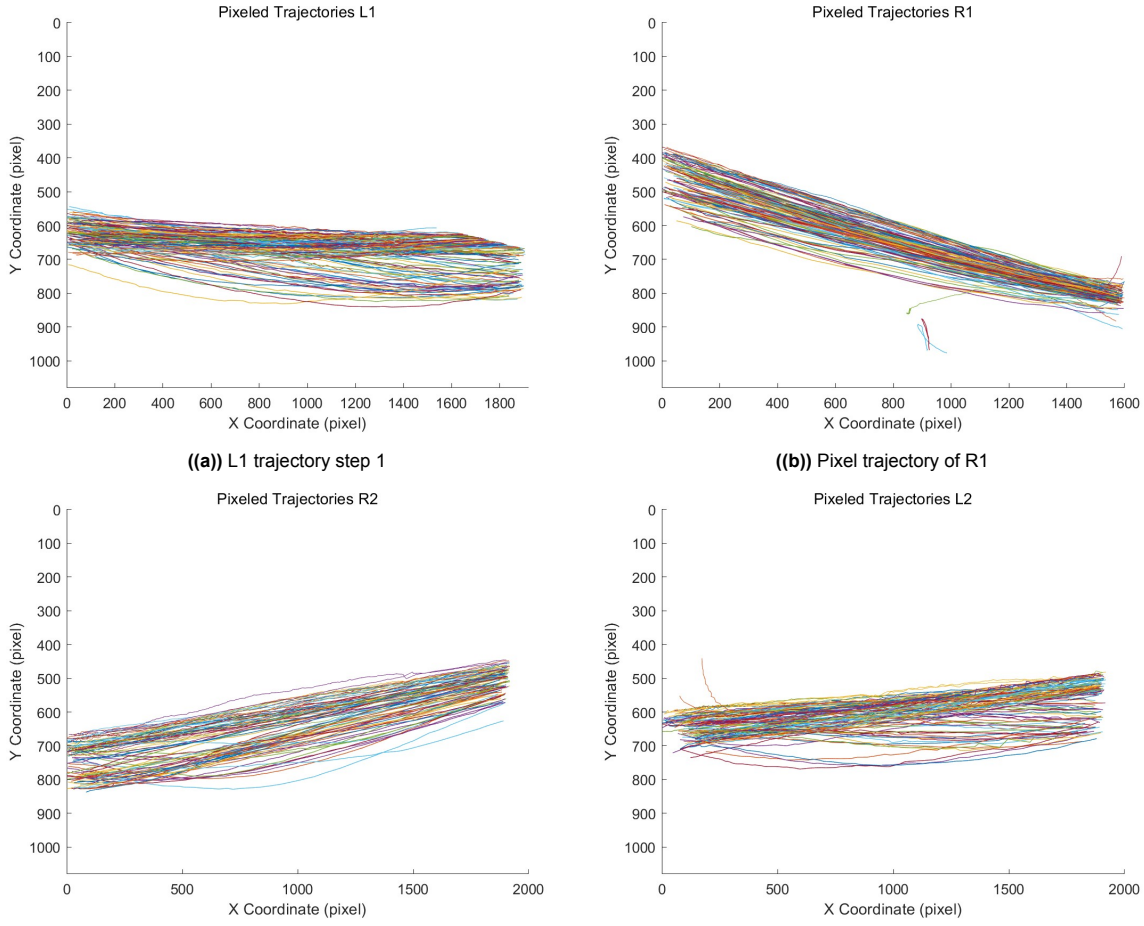

((a)) L1 trajectory step 1

((b)) Pixel trajectory of R1

((c)) Pixel trajectory of R2

((d)) Pixel trajectory of L2

Figure 6.2: Samples of extracted Trajectories of L1, R1, R2, and L2

factors:

1. Video Duration: Each video was approximately 20 minutes long.
2. Observational Data: Practical observations indicated that within a 2-minute timeframe, the camera shift was not significantly noticeable.
3. Balance Between Accuracy and Efficiency: Dividing the videos into 10 segments (approximately 2 minutes each) struck a balance between capturing the changing camera angles with sufficient accuracy and maintaining computational efficiency in the data processing pipeline.

This segmentation approach allowed for more accurate transformation of the video data to a consistent vertical perspective, despite the ongoing changes in camera orientation. By applying different correction parameters to each segment, we were able to mitigate the effects of the platform's tilting motion on our trajectory data.

Figure6.6shows the comparison of the trajectory data of the first video from the R1 camera before and after correction.

6.1.4. Height projection

The input parameters required for the height projection algorithm include the camera height in meters, the camera coordinates in meters, and the height of the detected object that needs to be height-projected. The camera height is measured on the day of the experiment. The camera position is actually an intermediate calculated value in the Imagetracker tool in step 2.The camera position calculated in the image correction step is relative to the center of the 2560x1600 canvas. However, the

Figure 6.3: Time change for an example video

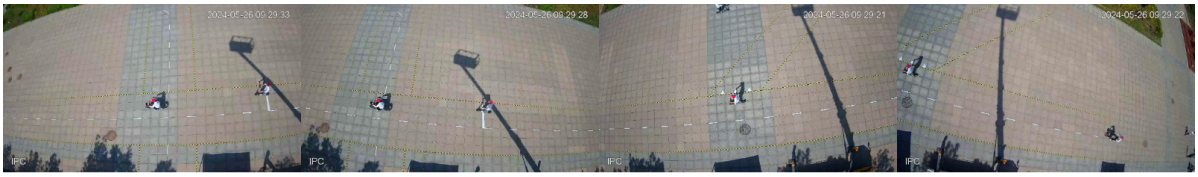

Figure 6.4: Camera image before transform

origin of the trajectory position is located at the top-left corner of the 2560x1600 canvas. Figure6.7 shows these two coordinates.

To align the camera coordinates with the trajectory coordinate system, we need to perform a coordinate transformation by equation6.1.Where x' and y' represent the camera position calculated in step 2.

$$\begin{aligned} x &= x' + \frac{2560}{2} \cdot \text{scale} \\ y &= y' + \frac{1600}{2} \cdot \text{scale} \end{aligned} \tag{6.1}$$

After determining the camera coordinates, another input parameter that needs to be determined is the height of the tracked object. On the day of the experiment, the sitting or standing height of each participant was measured for each type of vehicle involved. Based on the vehicles involved in each video, an average height approach is adopted in this study. The specific parameter table can be found in the Appendix tableG.7 and G.8.

the scene, eliminating the distortion introduced by the camera's elevated viewpoint. Figure6.8 shows the change in a trajectory with an ID of 2 from the R1 camera after height projection. It can be observed that due to the lower position of the camera, the trajectory shifts downward as a whole after the height

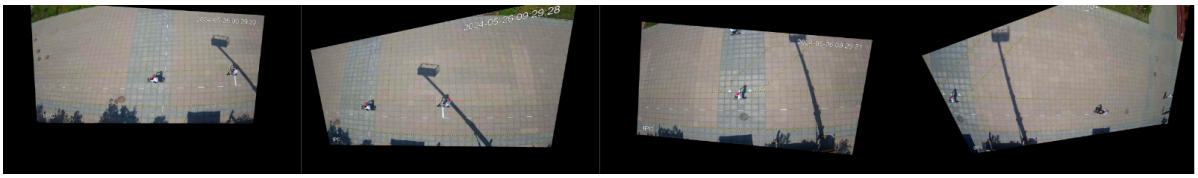

Figure 6.5: Camera image after correction

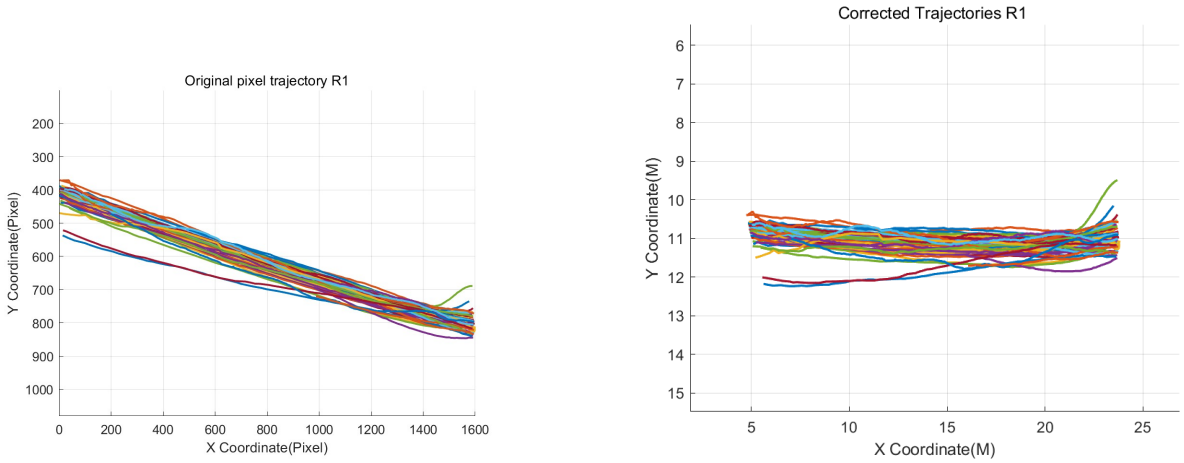

((a)) R1 first video's trajectory before correction

((b)) R1 first video's trajectory after correction

Figure 6.6: Comparison of R1 trajectory before and after correction

Table 6.2: Camera Parameters for Image Correction (R1 and R2)

Parameter	R1 Value	R2 Value	L1 Value	L2 Value
Rotation (degrees)	15	-5.5	6	-2.5
Wedge Angle X (degrees)	-22	-4	-11	1
Wedge Angle Y (degrees)	-14	-1	-16	1.5
Elevation (units)	1258	1258	1,115	1,115

The parameters used for for image correction for R1 and R2 cameras; they are also used for the example. The parameter for L1 and L2 will be put in an independent Excel file, as there are too many columns and rows

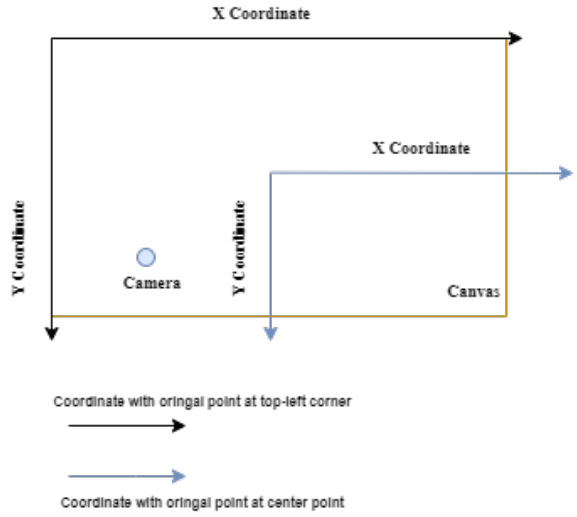

Figure 6.7: Camera position with two coordinates

projection. To verify the reasonableness of this process, Figure6.8 presents one frame of the trajectory with an ID of 2 from the R1 camera. It can be seen that the trajectory after height projection should indeed be located lower.

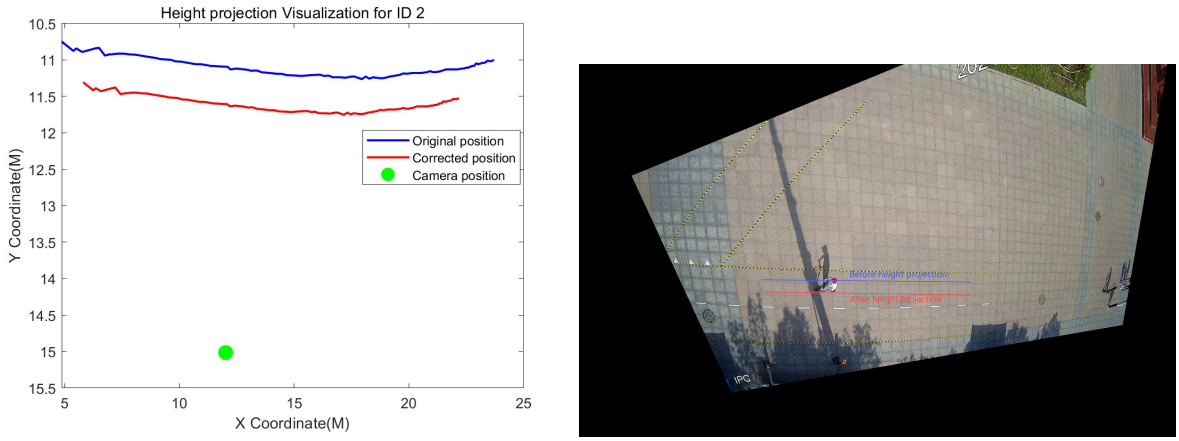

((a)) Height projection visualization

((b)) Verification on reasonableness of height projection

Figure 6.8: Height projection example

6.1.5. Combine video files from the same camera

The selection of distance and time thresholds D and T of algorithm1, set at 6 meters and 2 seconds respectively, was based on careful consideration of the experimental conditions and data characteristics. The time threshold of 2 seconds was primarily determined by the inherent limitations of the computer processing capabilities, which resulted in a minimal gap between consecutive videos of approximately 2 seconds. The spatial coverage of each camera was limited, with fast-moving vehicles typically appearing in a single camera's field of view for only 3 to 4 seconds. Analysis of fast-moving vehicle trajectories from R2 camera between 8:58:26 and 9:25:20 revealed an average trajectory duration of 3.3 seconds. In contrast, slower vehicles exhibited an average dwell time of 9.8 seconds, with a mean velocity of 2.2 meters per second. Given these parameters, the algorithm was primarily designed to detect and reconcile fragmented trajectories of slower vehicles. The trajectories of faster vehicles, due to their brief duration closely matching the inter-video intervals, were less likely to require merging across video segments.

However, post-implementation analysis, including manual verification, revealed that the actual need for trajectory merging was minimal. This can be attributed to two main factors:

1. The limited scale of the experiment resulted in few instances of trajectories spanning across video segments.
2. The intervals between successive videos often exceeded 3 seconds, sometimes extending to over 10 seconds, which surpassed our initial estimations.

Consequently, the algorithm's execution on the current dataset did not identify any trajectories requiring merging. Nevertheless, the inclusion of this algorithm in the processing pipeline remains valuable for potential future scenarios where experimental conditions or data characteristics may necessitate its application.

Figure 6.9 illustrates the final picture of all the video data from the four cameras after image correction and height projection. However, it is evident that the tracks still contain a significant number of errors. These errors will be addressed and corrected in the subsequent step of the data processing pipeline.

6.1.6. Fixes for trajectory errors

Manual Trajectory Filtering and U-turn Handling

For the detected U-turn behaviors, the method of handling them is to truncate the U-turn portion of the trajectory. Figure 6.10(a) illustrates the detection of U-turns, early exits, and non-experimental subjects,

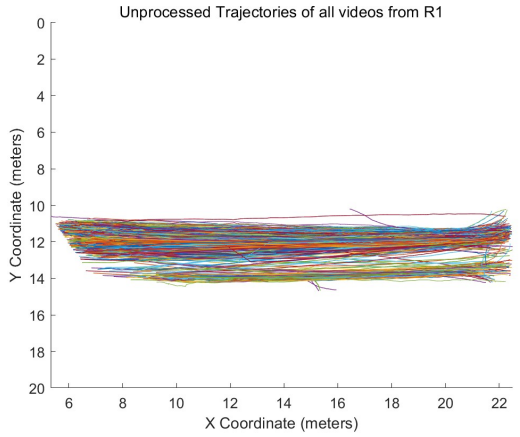

((a)) R1 trajectories after image correction and height projection

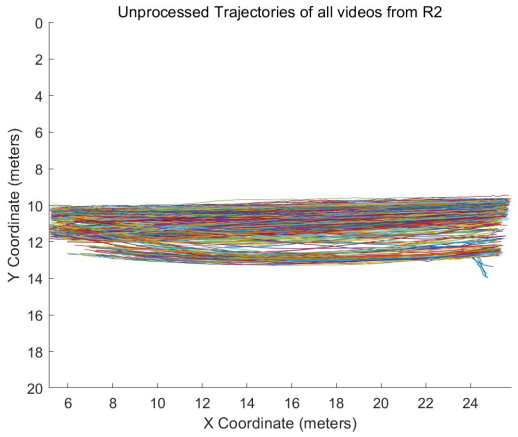

((b)) R2 trajectories after image correction and height projection

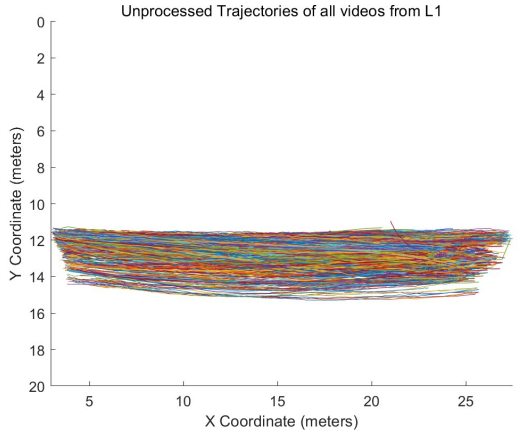

((c)) L1 trajectories after image correction and height projection

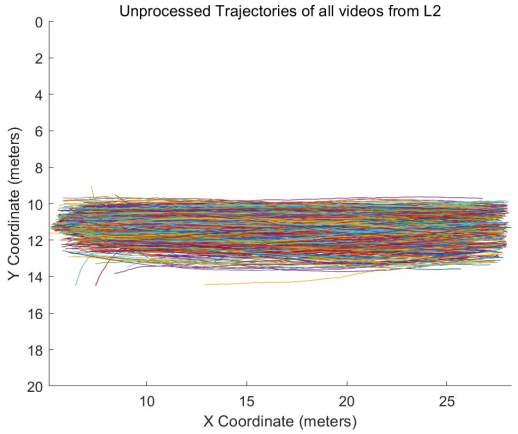

((d)) L2 trajectories after image correction and height projection

Figure 6.9: Unprocessed trajectories from cameras R1, R2, L1, and L2. Note: Trajectories shown are raw and have not undergone error detection.

all of which are highlighted within the red circles in the image.

The rightmost red circle denotes U-turn. The red circles with X-coordinates between 16 and 18 meters indicate participants who prematurely exited the experiment. The annotations with X-coordinates between 14 and 16 meters represent detected objects that were not part of the experimental cohort (in this instance, these were experimenters wearing hats who traversed the area during the idle time between two scenarios).

Figure 6.10(b) presents the trajectories after manually processing these errors. The trajectory images of the remaining three cameras after deletion are shown in Figure6.11.

Handle split trajectory

After removing the obviously erroneous trajectories, the second step of the processing pipeline involves handling trajectories that are fragmented due to shadows.

Two thresholds were established for the algorithm2:a temporal threshold and a spatial threshold. Visual analysis of the image4.3(a) revealed that the shadow coverage typically spanned approximately three standard tiles, equating to a length of 1.8 meters. Consequently, the spatial threshold was set at 3 meters. This extended threshold accounts for potential variations in shadow length and the discrete nature of frame-by-frame analysis. The temporal threshold was set at 2 seconds, derived from the estimated time required for a slow-moving vehicle to traverse the 3-meter spatial threshold. This estimation considers that the shadow effect might persist across multiple frames (approximately five frames in our observations), potentially extending the affected area beyond the observed 1.8 meters

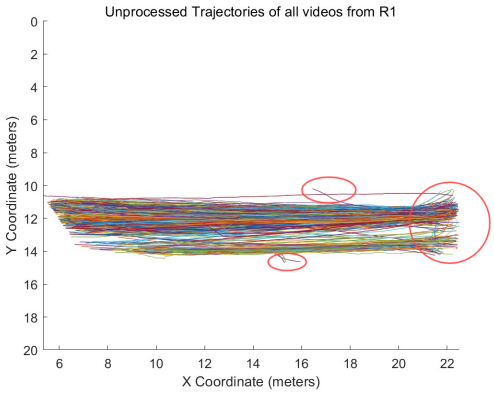

((a)) All R1 Trajectories with Errors

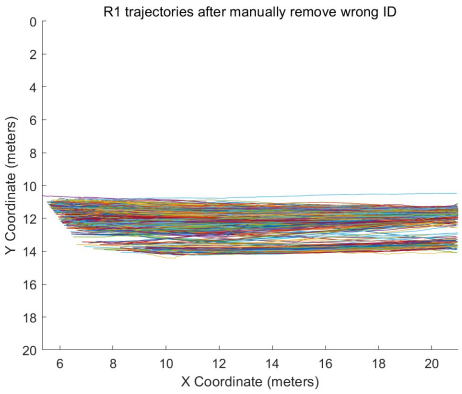

((b)) R1 Trajectory After Manually Removing Wrong IDs

Figure 6.10: Comparison of R1 Trajectories

((a)) R2 Trajectories After Manual ID Removal

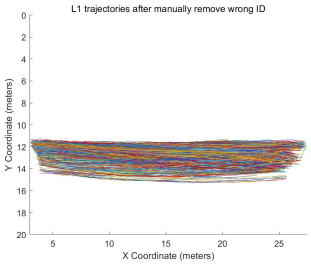

((b)) L1 Trajectories After Manual ID Removal

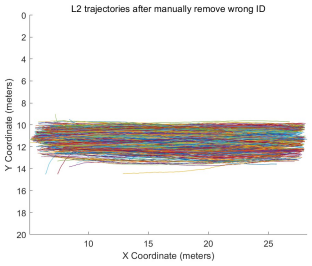

((c)) L2 Trajectories After Manual ID Removal

Figure 6.11: Comparison of Trajectories After Manual ID Removal

due to the discrete sampling inherent in frame-by-frame analysis.

Figure 6.12 illustrates the results of trajectory processing for camera R1, where trajectories were initially disrupted by shadows. This phenomenon was observed across multiple cameras, with the processed trajectory data for the remaining cameras presented in the Appendix figureG.1(b). The algorithm can handle 100% of all trajectories that are split by shadows.

Jump point fix

The process of setting distance thresholds for separation Algorithm3 involves a largely manual approach. By utilizing MATLAB's visualization tools and considering the relatively small number of trajectories, we can identify all of the trajectories with jump points as shown in figure4.4(a). After calculating the distance from the jump point i to $i+1$ of these trajectory with jump points, the selected threshold values should be less than the minimum calculated distance. This is to ensure that we can split all of the error trajectories shown by figure4.4(a) at the jump point. Finally, the thresholds are selected 0.7 meters for the two cameras on the right side and 0.9 meters for the two cameras on the left side.

When setting the distance threshold for match and merge Algorithm4, it is essential to ensure that the threshold is larger than the distance between the jump point i and the next point $i+1$ in the correct ID part. For example, in Figure6.12(b) this means the distance between ID 522 and ID 763(where 763 is the bule trajectory with Y coordinates lie between 11m and 12m) This can be roughly calculated using MATLAB's interactive plotting tool. In this study, a distance threshold of 2 meters was ultimately adopted for all cameras.

Regarding the time threshold, the minimum speed of slow vehicles was taken into consideration. Since the minimum speed of slow vehicles is sometimes could reach 2 m/s,If the slowest car passes through the breakpoint, it takes 1s, and the time threshold is chosen to be greater than one second. a time threshold of 2 seconds(the first whole value larger than 1) was chosen.

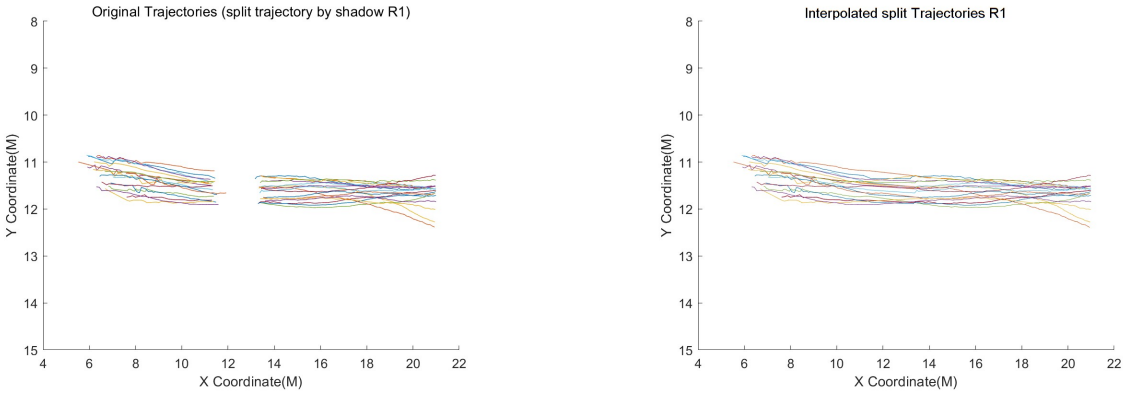

((a)) Split Trajectory R1

((b)) Interpolated Split Trajectories R1

Figure 6.12: Split and Interpolated Split Trajectories for R1

As for the Y-axis threshold, it is based on the assumption that the movement direction should be consistent within a short time for the same trajectory. Therefore, a threshold of 0.5 meters was selected, which corresponds to an angle of approximately 20 degrees calculated by arctan(Δy/Δx).The trajectory after jump point fix of R1 is shown in Figure6.13.

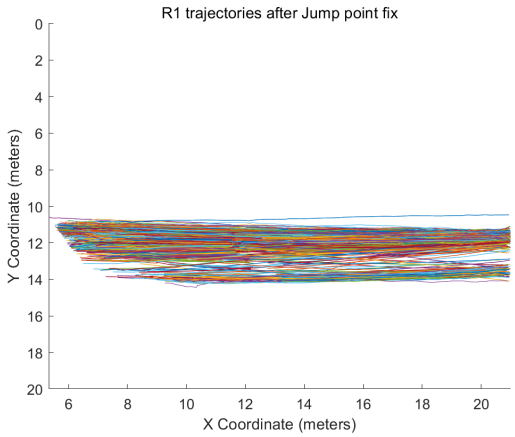

Figure 6.13: Trajectory after jumpoint fix R1

Scenario separation

The Table6.3 shows the result of the scenario separation. Each scenario has a separate file.This table also shows which cameras recorded the different scenarios respectively.

During the experimental procedure, data loss occurred in specific scenarios due to technical limitations of the recording equipment. Specifically, the computer responsible for video capture from both cameras in region R2 failed to record data for scenarios 5, 6, and 7. Additionally, region R1 experienced data loss for scenario 1. The most probable cause of this data loss is attributed to the performance constraints of the laptop computers utilized for storage, resulting in incomplete video preservation. Given the irretrievable nature of the lost data, it was not feasible to reconstruct the missing information. Consequently, our methodological approach adhered to the principle of maximizing data utilization within the constraints of the available information. This principle was consistently applied throughout the subsequent data processing and analysis phases.

6.1.7. Time synchronization

Figure6.14 shows an example to fix the time between R1 and R2. To determine the time difference between the rider's positions in the R1 and R2 data, we can utilize the precise timestamps obtained

Table 6.3: Scenario Time and Captured Cameras

Scenario No.	Start Time	End Time	Captured Cameras
2	08:58:00	09:27:00	R1, R2,L1, L2
3	09:27:00	09:42:00	R1, R2,L1, L2
4	09:59:00	10:24:00	R1, R2,L1, L2
5	10:25:00	10:45:00	R1, L1, L2
6	10:50:00	11:10:00	R1, L1, L2
7	11:11:00	11:27:00	L1, L2

Where number 1 is non-interactive scenario starting from 08:40:00 until 08:55:00

((a)) Time fix example of camera R1

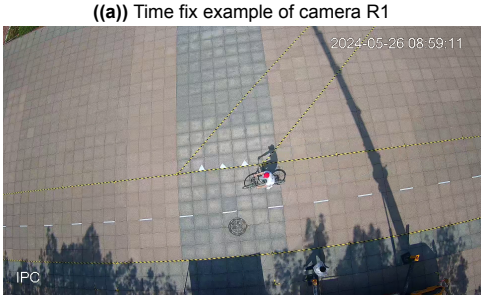

((b)) Time fix example of camera R2

Figure 6.14: Time fix examples for cameras R1 and R2

from the pixel trajectory extraction process described in Section 4.1.2. By manually identifying the rider's position using the red hat as a reference point, we can associate these positions with their corresponding timestamps in the R1 and R2 data. The precise timestamp for the rider in the R1 data is 8:59:12.992, while in the R2 data, the timestamp is 8:59:12.069. By calculating the difference between these two timestamps, we can determine the time offset between the R1 and R2 data for this specific rider. Let t_{R1} and t_{R2} denote the timestamps for the rider in the R1 and R2 data, respectively. The time difference Δt can be calculated as follows:

$$\Delta t = t_{R1} - t_{R2} = 8:59:12.992 - 8:59:12.069 = 0.923 \text{ seconds} \tag{6.2}$$

Therefore, based on the manual identification of the rider's position using the red hat and the precise timestamps obtained from the pixel trajectory extraction, we can conclude that there is a time offset of 0.923 seconds between the R1 and R2 data for this particular rider.

It is important to note that when attempting to identify the exact position where an experimental participant appears simultaneously in the overlapping field of view of two cameras, perfect alignment is often unattainable. This discrepancy primarily arises from the discrete nature of video images, which are captured at specific frame rates rather than continuously. Consequently, it is challenging to guarantee a perfect matching point between the two camera feeds. To mitigate this issue and ensure the highest possible accuracy in position matching, we implemented a methodological approach. For each camera, we extracted a sequence of 20 frames surrounding the target time. From these frame sequences, we then identified the pair of frames (one from each camera) that exhibited the closest spatial correspondence for the participant's position. This method allows us to approximate the optimal matching point

within the constraints of the discrete frame-based nature of video data.

6.1.8. Merging of multi-camera trajectories

In the pairwise merging algorithm, there is an important threshold called the time threshold. The time threshold is used to find the closest t2' (the time point in R2 that is closest to t2 in R1), and its significance lies in several aspects. Firstly, although the timestamps in the dataset are precise to the millisecond, the video frames correspond to discrete time points rather than being perfectly continuous. As a result, the closest t2' found may not be exactly equal to t2. Therefore, a threshold is needed to accommodate this discrepancy. In this study, the time threshold is set to 0.2 seconds.

Furthermore, due to the offset between the two cameras on the left side (L1 and R2), there is a period when L1 and R2 do not have an overlapping range. Consequently, a reasonable time matching range needs to be set to ensure that trajectories can still be matched even when there is no overlap. In this case, the threshold is set to 6 seconds. The main reason for setting the threshold to 6 seconds is that the maximum non-overlapping range between L1 and R2 is close to 12 meters, and the minimum speed of slow vehicles could read 2m/s, then it took 6s. By allowing a time matching range of 6 seconds, the algorithm can still effectively match trajectories even when there is a significant spatial gap between the camera views.

During the pairwise merging process, the author discovered that the merging of trajectories from cameras L1 and L2 often produced unreasonable results. This issue manifested as a significant number of trajectories in each scenario having merged lengths much greater than the expected real-world lengths as shown in the green rectangle of Figure6.15. The root cause of this phenomenon lies in the fact that the precise time corresponding to each frame is the primary variable determining whether two trajectories can be reasonably merged in the pairwise merging algorithm. When the time of one of the cameras is problematic, the matching and merging results will be affected, as time is used as the first matching dimension.

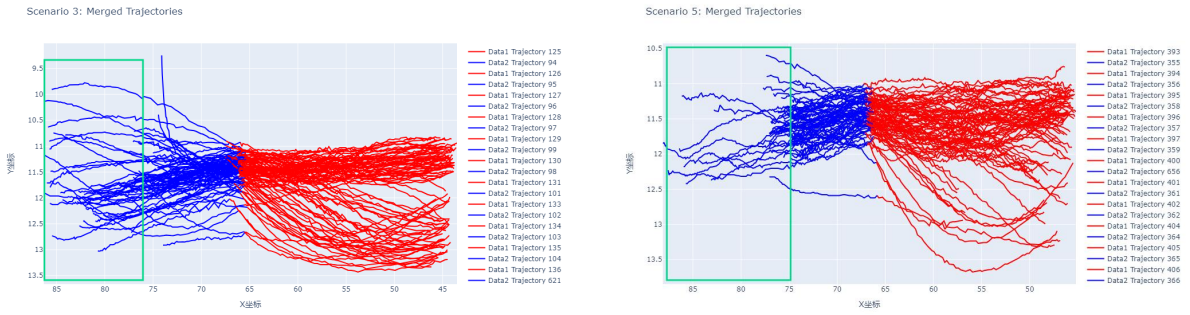

((a)) The L1-L2 merger process for Scenario 3

((b)) The L1-L2 merger process for Scenario 5

Figure 6.15: The merged result of camera L1 and L2

For example, if a trajectory in L1 has a calculated end time of tL1, theoretically, there should be a corresponding point with the same time tL1 in the L2 camera data after time correction. These two points should have the same physical coordinates, meaning they should be within the overlapping range of the cameras. However, the frame rate of the video recorded by the L2 camera was not stable. Although the overall frame rate of L2 videos could be maintained at around 20 frames per second, some parts had higher frame rates while others had lower and more fluctuating frame rates. This led to many trajectories having calculated precise Beijing times that did not match the actual situation. Sometimes, the calculated time was later than the actual Beijing time, causing the theoretical corresponding physical coordinates of tL1 in L2 to fall outside the overlapping range of the cameras, resulting in an elongation of the overall merged trajectory. This issue was present in almost all scenarios' data, and the calculated time was difficult to repair due to its nature as a computed value. Considering the actual data situation, where most overtaking behaviors were completed before the L2 camera, and the large overlapping range between L1 and L2 (with L1 covering half of L2's range), the data from the L2 camera was discarded in subsequent processing.

Figure6.16(a) and Figure6.16(b) show results of the processing of R2-L1 in scenarios 2 and 3. Where green represents data from R2, red represents data from L1, and black represents the connection part.

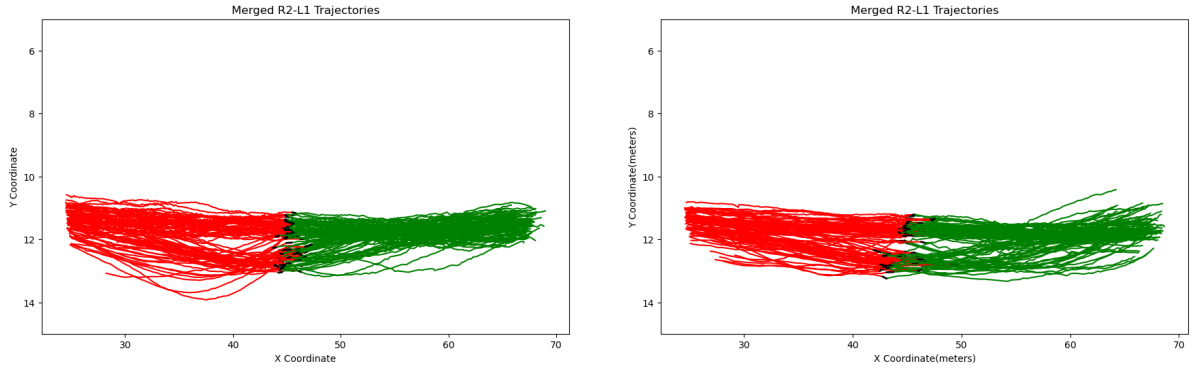

((a)) Merged Trajectories for R2-L1 Scenario 2

((b)) Merge of R2-L1 Scenario 3

Figure 6.16: EXample R2-L1 merged trajectories in scenario 2 and 3

After completing the two-by-two merger, the work of combining the trajectories of the three cameras R1R2L1 based on the common portion of R2 as a medium is to be carried out. Figure6.17 shows result of triple camera merging of scenario 3.

6.1.9. Freezing point handle

In this step, the algorithm 7 will first detect consecutive points with the same position on each trajectory and replace the X, Y coordinates of the first of these points that stays in place. Table6.4 and Table6.5 shows an exapmle of the standsstill point and its result after smoothing.

Table 6.4: Original Trajectory (Stationary Point)

Trajectory ID	X Coordinate	Y Coordinate	Timestamp	Camera
12	28.761	11.070	34 206.673	**R2**
12	28.761	11.070	34 206.723	**R2**
12	29.006	11.092	34 206.773	**R2**

Note: All points are stationary with identical or minimal coordinate changes.

6.1.10. Accuracy validation

Figure 6.18 demonstrates the principle of lateral accuracy validation. The blue lines in the image represent the actual lateral distance between two experimental participants. Visual inspection indicates that this distance spans approximately two floor tiles, which corresponds to 1.2 meters. We can corroborate this visual estimation by examining the coordinate data for the corresponding frame, as shown in Table

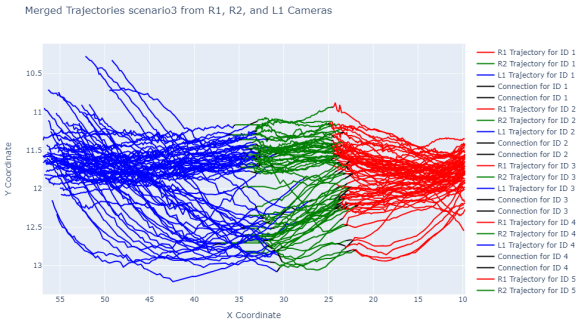

Figure 6.17: R1R2L1 merged result of scenario3

Table 6.5: Transformed Trajectory (Moving Points)

Tajectory ID	X Coordinate	Y Coordinate	Timestamp	Camera
12	28.761	11.070	34 207.023	**R2**
12	28.884	11.081	34 207.073	**R2**
12	29.006	11.092	34 207.123	**R2**

Note: Points have been transformed to indicate movement.

6.6. The data reveals a difference in Y-coordinates of 1.2206 meters, which closely aligns with our visual assessment.

Figure 6.18: An example of accuracy validation of camera L1

Table 6.6: Position Data for Frame 102 of L1

Frame Number	Y (meters)
102	14.1371
102	12.9044

Figure 6.19 demonstrates the principle of longitudinal accuracy validation. The two red lines in Figure6.19(a) and in Figure6.19(b) in the image represent the actual longitudinal distance traveled by one participant during one second. Visual inspection indicates that this distance spans approximately 3 floor tiles, which corresponds to 1.8 meters. We can corroborate this visual estimation by examining the coordinate data for the corresponding frame, as shown in Table 6.7. The data reveals a difference in X-coordinates of 1.61 meters, which aligns with our visual assessment.

Through multiple comparisons of this nature, we can establish confidence in the accuracy of our trajectory data.For both the X and Y directions, thirty data were selected. For the Y direction, the average error was 0.094 meters. For the X direction, the overall difference was 0.196 meters. In percentage terms, the error/actual value in the X-direction and Y-direction is 6.1% and 7.8%, respectively, as detailed in the table of data in the AppendixD.1 and D.2. Regarding speed, direct validation is not possible. However, in validating the longitudinal direction, we only selected thirty trajectories that closely followed linear motion. Assuming the speed is directed along the X-axis, the error of 0.196 meters would result in a similar magnitude of error when calculating the average speed per second, which is 0.196 meters/second. The same applies to acceleration. However, this is an average calculated over one second; when calculating the value at each point, there should still be considerable fluctuations. These fluctuations can be addressed using a moving average method. In the subsequent data analysis process, the average speed and deceleration we calculated align with the performance levels of the vehicles we purchased and the values found in related literature. These points will be discussed in detail in Section 7.1.

This validation process confirms that the data obtained after our series of processing steps adequately reflects the riders' behaviors. The close correspondence between visual cues and processed data coordinates substantiates the reliability of our methodology in capturing and representing the spatial relationships of participants throughout the experiment. This validation approach not only verifies the

((a)) An example of accuracy validation of camera R2 (Image 1) **((b))** An example of accuracy validation of camera R2 (Image 2)

Figure 6.19: Accuracy validation of camera R1

Table 6.7: Position Data for Frame 460 and 480 of R2

Frame Number	X (meters)
460	14.5824
480	12.9711

accuracy of our data processing pipeline but also reinforces the validity of subsequent analyses based on these trajectories. It provides a crucial foundation for the interpretation of rider behaviors and interactions derived from this dataset.

6.1.11. Trajectory Labeling

Table6.8 shows the available overtaking pairs in each of the six scenarios involving overtaking. Ideally, each scenario should have 48 overtaking pairs, meaning that each of the 12 experimental participants has four overtaking behaviors. However, the author discovered some issues during the labeling process that led to fewer than 48 pairs in multiple scenarios. These reasons include:

1. Due to the relatively large interval between two consecutive videos, as mentioned earlier, one or two pairs in each scenario were not recorded or only partially recorded the trajectory of the overtaken vehicle.
2. In some cases, the camera suddenly blurred, resulting in the failure to record the trajectories that occurred precisely during this situation.

These reasons contributed to the final missing one or two overtaking pairs in some scenarios. However, overall, the vast majority of experimental participants were recorded performing four overtaking behaviors, although some scenarios did not capture complete overtaking behaviors due to data loss.

Table 6.8: Number of Overtaking Pairs in Different Scenarios

Sce No	Sce Vehicle	Number of Overtaking Pairs Finally
2	EB-B	47
3	EB-ES	47
4	EB-EB	48
5	ES-B	47
6	ES-EB	46
7	ES-ES	48

Where scenario 1 is non-interactive scenario

In general, after a series of data processing steps, a relatively reliable trajectory data set was obtained for the next step of data analysis. However, due to missing data, especially the missing R2 camera data, the data in the E-scooter overtaking scenarios could not be used in many hypothesis tests. Therefore, in the subsequent data analysis, E-bike-related scenarios would be dominated.

7

Data analysis

This section performs the data analysis process of section4.2 based on the output data from the data processing. This series of analysis was performed to verify the influence of gender factor and micro-mobility factor on cyclist behaviour. By testing the hypotheses in the 4.2, we examined the influence of the upper level factors in the Figure2.3 on the decision-making level and the physical level. section7.8 Answers to subquestion 1,2.5 are given.

7.1. Descriptive statics

Before proceeding to detailed hypothesis testing, this section presents some descriptive statistics for the micro variables.

Speed

In non-interactive conditions, the average traveling speed for E-bikes was 18.51 km/h (SD = 4.58 km/h), while E-scooters traveled at an average speed of 15.38 km/h (SD = 3.72 km/h). These values, illustrated in Figure7.1, indicate that E-bikes maintain a higher average speed than E-scooters under non-interactive conditions. Whether it is statistically significant needs further verification, though.

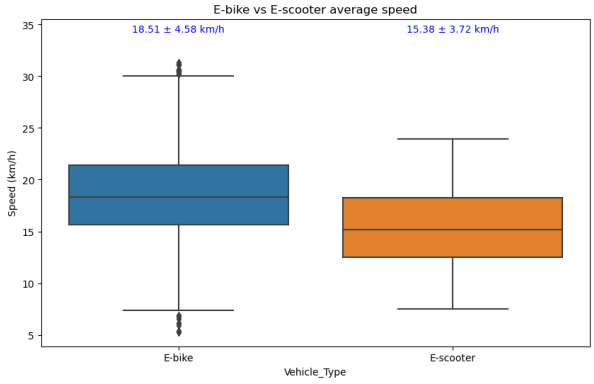

Figure 7.1: Non-interactive E-bike and e-scooter riding speed

In non-interactive conditions, the average deceleration for E-bikes was 3.83 m/s² (SD = 1.46 m/s²), while E-scooters had an average deceleration of 3.24 m/s² (SD = 0.97 m/s²) as shown in Figure7.2. These findings align with existing research, such as the study by [58], which reported e-scooter deceleration rates between -3.39 m/s² and -3.84 m/s².

Lateral distance

The lateral distance during the passing phase is particularly important in this study, as it reflects the

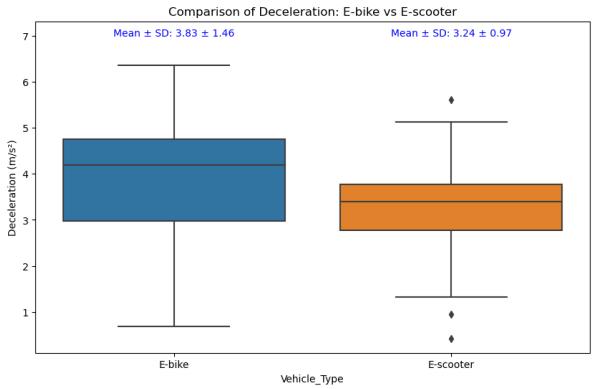

Figure 7.2: E-bike and E-scooter deceleration

overtaker's lateral avoidance strategy, an essential aspect of path selection. The mean and standard deviation of lateral distances for each overtaking scenario are shown below and in Figure7.3:

- **E-bike overtaking bike**: Mean ± SD: 1.25 ± 0.26 m
- **E-bike overtaking e-bike**: Mean ± SD: 1.31 ± 0.35 m
- **E-bike overtaking e-scooter**: Mean ± SD: 0.89 ± 0.34 m
- **E-scooter overtaking bike**: Mean ± SD: 1.21 ± 0.35 m
- **E-scooter overtaking e-bike**: Mean ± SD: 1.06 ± 0.31 m
- **E-scooter overtaking e-scooter**: Mean ± SD: 1.08 ± 0.40 m

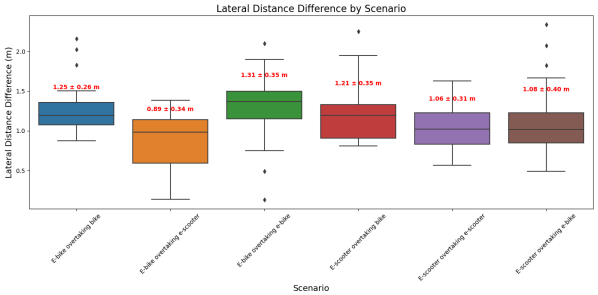

Figure 7.3: Lateral distance of differenct scenario

Overtaking starting position

The overtaking start moment refers to the longitudinal distance between the overtaker and the overtaken vehicle at the initiation of the overtaking maneuver. Due to missing pre-passing phase data in Scenarios 5, 6, and 7 (E-scooter overtaking bike, E-scooter overtaking e-scooter, and E-scooter overtaking e-bike), this analysis only includes Scenarios 2, 3, and 4. The means and standard deviations for these scenarios are as follows and in Figure7.4:

- **Scenario 2 (E-bike overtaking bike)**: Mean = 9.75 m, SD = 2.86 m
- **Scenario 3 (E-bike overtaking e-scooter)**: Mean = 10.19 m, SD = 3.62 m
- **Scenario 4 (E-bike overtaking e-bike)**: Mean = 7.80 m, SD = 4.93 m

Roll rate and roll angle

This study uses the absolute mean values of roll rate and roll angle, consistent with the methods of [28, 27]. Notably, due to incorrect IMU placement for E-scooters and missing trajectory data for Scenarios 5, 6, and 7, only data from Scenarios 3 and 4 were analyzed. Figure 7.5 and Figure7.6 show the variation of roll angle and roll rate across three phases in Scenarios 3 and 4.

Scenario 3:

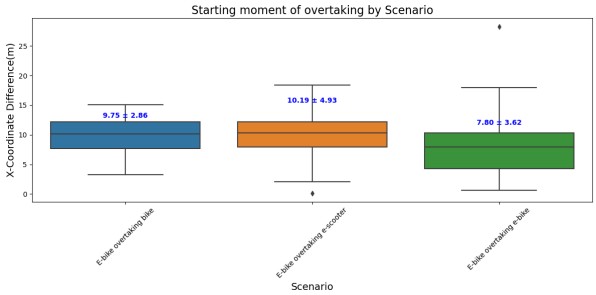

Figure 7.4: starting position of overtaking

- **Roll Angle (absolute mean):**
  - Before: Mean = 4.03°, SD = 2.56°
  - During: Mean = 6.66°, SD = 3.71°
  - After: Mean = 4.67°, SD = 2.65°
- **Roll Rate (absolute mean):**
  - Before: Mean = 26.17°/s, SD = 3.64°/s
  - During: Mean = 36.73°/s, SD = 11.57°/s
  - After: Mean = 24.68°/s, SD = 7.56°/s

Scenario 4:

- **Roll Angle (absolute mean):**
  - Before: Mean = 4.48°, SD = 2.87°
  - During: Mean = 7.04°, SD = 4.46°
  - After: Mean = 4.43°, SD = 4.16°
- **Roll Rate (absolute mean):**
  - Before: Mean = 30.41°/s, SD = 6.52°/s
  - During: Mean = 36.21°/s, SD = 25.33°/s
  - After: Mean = 27.49°/s, SD = 12.59°/s

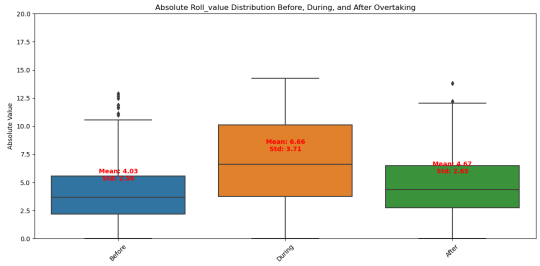

((a)) Roll angle across different phases in Scenario 3

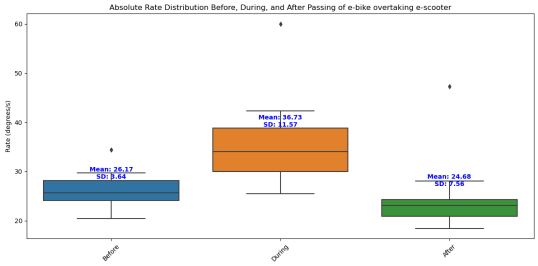

((b)) Roll rate across different phases in Scenario 3

Figure 7.5: Comparison of roll angle and roll rate across different phases in Scenario 3

Figure7.7 shows an example of the change in roll angle and roll rate over time for a trajectory in Scenario 4.

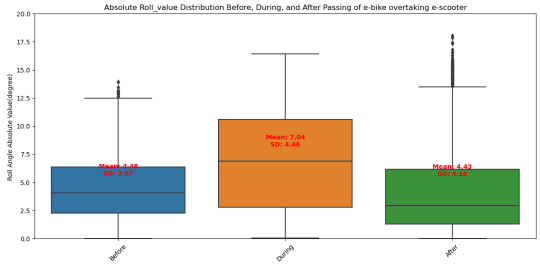

((a)) Roll angle across different phases in Scenario 4

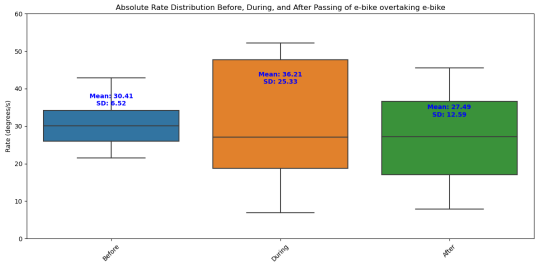

((b)) Roll rate across different phases in Scenario 4

Figure 7.6: Comparison of roll angle and roll rate across different phases in Scenario 4

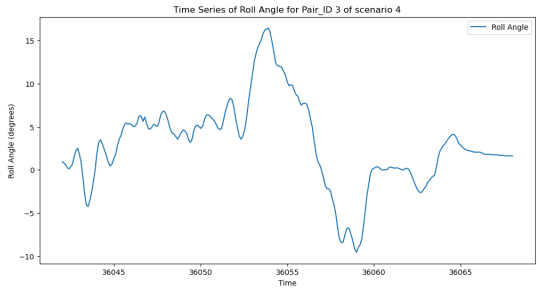

((a)) Roll angle over time of Pair 3 in scenario 4

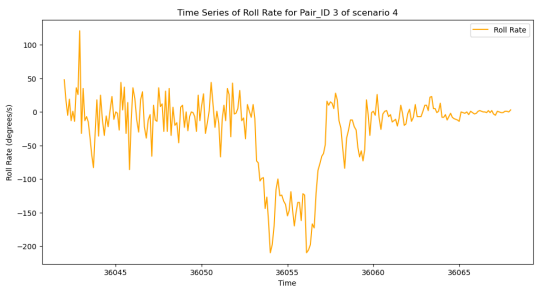

((b)) Roll rate over time of Pair 3 in scenario 4

Figure 7.7: Roll angle and roll rate over time example

7.2. Travel speed and dcceleration

7.2.1. Travel speed

This section first addresses Hypothesis 1, which examines the speed difference between e-bikes and e-scooters in non-interactive scenarios. The goal is to test whether significant speed difference exist between these two types of micromobility vehicles. The average traveling speed of e-bikes was 18.51 km/h, while the average traveling speed of e-scooters (Camera=R2 section) was 15.38 km/h. This comparison confirms the hypothesis that there is a significant difference in speed between these two micromobility types with p-value= 0.0000. This means that we accept alternative hypothesis 1.1.

This finding is also consistent with the actual specifications of the experimental vehicles we selected. The e-scooter we chose has a maximum speed of only 20 km/h, while the e-bike has a minimum speed limit of 25 km/h, even when using the pedaling mode. The reason the observed speeds are lower than the maximum is that we are not asking the riders to reach their top speed. Instead, we are asking them to maintain a speed that feels normal to them during regular riding.

Next, in line with Hypothesis 2, we examined gender differences in speed within e-bike and e-scooter groups.

Figure7.8(a) shows the average speed of male and female riders using e-scooters. Gender was found to have a significant influence on the average e-scooter riding speed. The results revealed that the average riding speed of male riders was significantly higher than that of female riders, with male riders having an average speed of 16.21 km/h and female riders having an average speed of 13.93 km/h,with t-statistic of 4.1970 and a p-value of 0.0000 We performed the same analysis for e-bikes as shown in Figure7.8(b). However, the results showed no significant difference between male and female riders in terms of average riding speed for e-bikes, with male value of 19.70 m/s and female of 17.77 m/s, with t-statistic of 1.602 and a p-value of 0.1170. We conditionally accept the alternative hypothesis 1.2, as it is supported for e-scooters but not for e-bikes.

Moving forward, Hypothesis 3 explores the differences in speed among the three types of e-bikes (regular, fat-tire, and foldable e-bikes). The ANOVA analysis on different types of e-bikes as Figure7.9 showed significant differences in the mean travel speeds between the three types of e-bikes ($F(2, 37) = 4.3$, $p = 0.0210$).

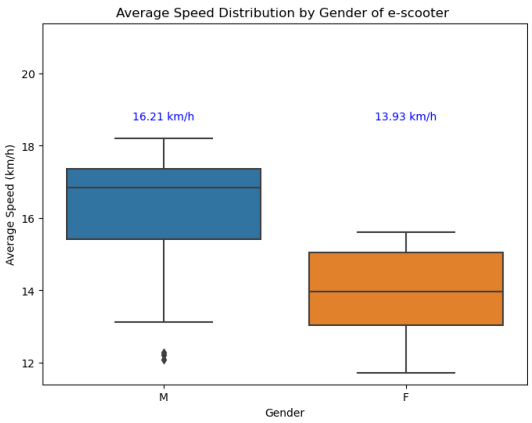

((a)) Average speed of e-scooter by gender

36 Male and 12 Female

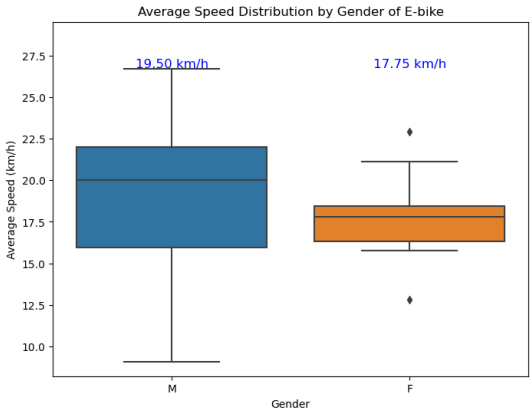

((b)) Average speed of e-bike by gender

32 Male and 16 Female

Figure 7.8: Comparison of average speeds by gender for different electric vehicles

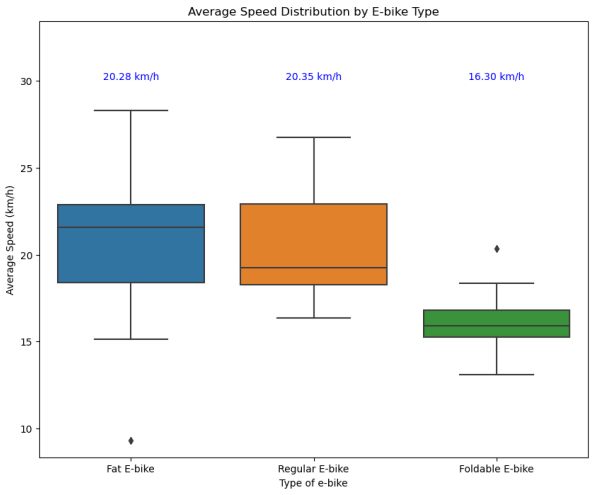

Figure 7.9: Speed of e-bike by e-bike type

Regular sample size: 21 Fat E-bike sample size: 11 Foldable E-bike sample size: 8

The results of Tukey's HSD post hoc test are shown in the table below:

Table 7.1: Tukey HSD table for speed comparison of different types of e-bikes

Group 1	Group 2	Mean Diff	p-adj	Lower	Upper	Reject
Fat e-bike	Foldable E-bike	-1.1067	0.061	-2.2555	0.042	False
Fat e-bike	Regular E-bike	0.0177	0.9988	-0.9024	0.9379	False
Foldable E-bike	Regular E-bike	1.1245	0.0293	0.0973	2.1516	True

The post hoc test results indicate that there is no significant difference in mean travel speed between regular e-bikes (mean speed = 20.28 m/s) and fat-tire e-bikes (mean speed = 20.35 m/s) ($p = 0.9988$). However, the mean travel speed of foldable e-bikes (mean speed = 16.30 m/s) is significantly lower than that of regular e-bikes ($p = 0.0293$), but not significantly different from that of fat-tire e-bikes ($p = 0.0610$). We accept the null hypothesis 3.

It is important to note that the sample sizes for the different types of e-bikes in this study are relatively small, particularly for fat-tire e-bikes (n=11) and foldable e-bikes (n=8). Larger sample sizes could provide more reliable and robust results. Additionally, factors such as rider characteristics, battery

capacity, motor power, and terrain may influence the observed differences in average travel speed between different types of e-bikes.

7.2.2. Deceleration

The deceleration analysis also first addresses the hypothesis about deceleration, which compares speed and deceleration differences between e-bikes and e-scooters in non-interactive scenarios. The results indicated that there was a difference in the deceleration capabilities between the two micromobility modes. The E-bike had an average deceleration rate 3.8262m/s^2 and the E-scooter with an average deceleration 3.2449m/s^2, with a t statistic: 2.1668 and a p-value: 0.0332. Therefore, we accept the alternative hypothesis 2.1.

Furthermore, Hypothesis 2 concerning gender differences in deceleration was also tested for e-bikes and e-scooters. The results indicated no statistically significant gender differences in deceleration for either vehicle type, suggesting that both male and female riders display similar braking behaviors. We accept the null hypothesis 2.2.

7.3. Lateral distance

7.3.1. Gender impact on Lateral distance

The analysis of lateral distance during overtaking connects to Hypothesis 4, which explores gender differences in lateral distance during overtaking. A series of T-tests were conducted to compare male and female riders across various scenarios. No significant gender differences were observed in all scenarios involving E-scooters.We therefore accept null hypothesis 4.

7.3.2. Speed difference impact on Lateral distance

The Hypothesis 5, which posits a positive relationship between speed difference and lateral distance during passing, is addressed through the analysis of Pearson correlation coefficients across scenarios where E-scooters overtook bikes(scenario 5) and where E-scooters overtook e-bikes(scenario 6). The test results are presented in Table7.2.

Table 7.2: Correlation Analysis Results for E-scooter Overtaking Scenarios

Scenario	Pearson Correlation Coefficient	P-value
E-scooter overtakes E-bike	0.3118	0.0000
E-scooter overtakes bike	0.6061	0.0000

In analyzing the correlation between lateral distance and speed difference across two scenarios, the scenario 5 yielded a correlation coefficient of 0.3118, indicating a moderate positive correlation. This suggests that as the speed difference increases, the lateral distance during overtaking tends to increase, albeit at a relatively lower strength. The scenario 6 presented a correlation coefficient of 0.6061, signifying a strong positive correlation. This stronger association indicates that in this scenario, a greater speed difference is more significantly linked to an increase in lateral distance.

The data points for lateral distance and speed difference were specifically collected during the passing phase of the overtaking maneuver. This phase represents the moment when the overtaking vehicle is actively passing the overtaken vehicle, which is critical for analyzing the dynamics of the interaction. By focusing on this phase, we capture the most relevant data reflecting the relationship between speed difference and lateral distance as the overtaking maneuver is executed. Additionally, this phase likely represents the moment when the overtaker maintains the maximum distance from the overtaken vehicle, thereby emphasizing the importance of lateral distance for ensuring safe maneuvering.

In order to further verify this phenomenon, two E-bike scenarios, Scenario 2 and Scenario 3, were also selected for this correlation. The same analysis was done and the results are in Table 7.3. E-bike analyses show the same trend. The Figure7.10 further shows the results of linear regression and polynomial regression for the lateral position difference and speed difference of scenario 2 and scenario 3, respectively. Figure7.11 shows the relationship between each group of speed difference and the corresponding transverse positional differences after grouping them.

For scenario 2, the groups are 0.5170m/s to 2.0126m/s(low),2.0126m/s to 2.6965m/s(medium-low),2.6965m/s to 3.5450m/s(medium high), and 3.5450m/s to 5.2349m/s(high). For scenario 3, the groups are 0.0071m/s to 1.7042m/s(low),1.7042m/s to 2.5108m/s(medium-low),2.5108m/s to 3.0769m/s(medium high), and 3.0769m/s to 6.8409m/s(high).

Table 7.3: Correlation Analysis Results for E-bike Overtaking Scenarios

Scenario	Pearson Correlation Coefficient	P-value
E-bike overtakes bike	0.4110	0.0000
E-bike overtakes E-scooter	0.4063	0.0000

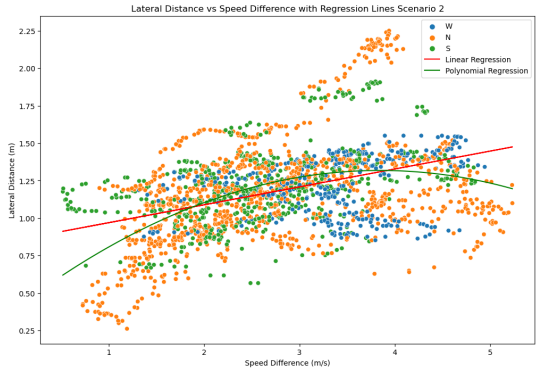

((a)) Regression result scenario 2

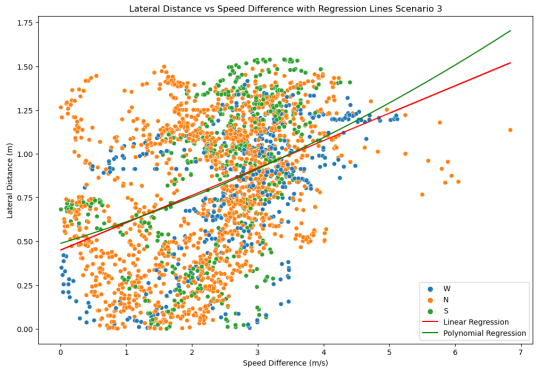

((b)) Regression result scenario 3

Figure 7.10: Overall Regression Results for scenario 2 and scenario 3

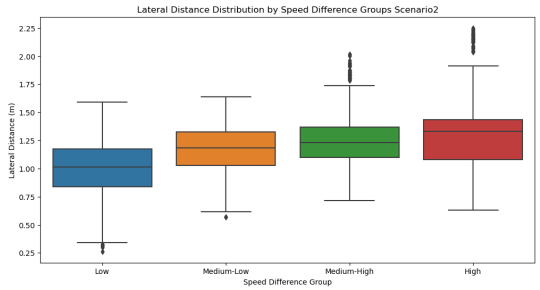

((a)) Lateral Speed Distribution by group for Scenario 2

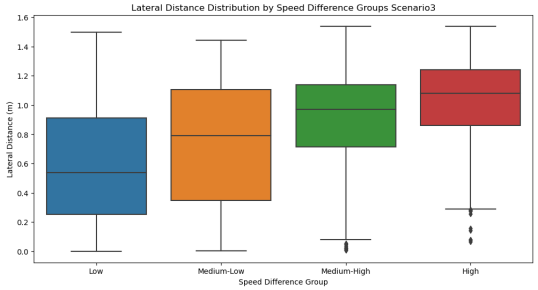

((b)) Lateral Speed Distribution by group for Scenario 3

Figure 7.11: Overall Lateral Speed Distributions by group

The correlation analysis in both E-scooter overtakes E-bike and E-scooter overtakes bike scenarios reveals a moderate and statistically significant positive relationship between speed difference and lateral distances during overtaking. This means that we accept the alternative hypothesis 5. Additionally, in the E-bike overtakes bike and E-bike overtakes E-scooter scenarios, a similar moderate positive correlation was observed. These findings support the notion that higher speed difference contribute to larger lateral distances, which may be indicative of safer overtaking practices by providing greater maneuvering space to avoid collisions. Furthermore, the significant gender differences observed in E-scooter scenarios highlight the influence of rider speed on overtaking behavior, underscoring the importance of considering both device type and rider characteristics in traffic safety analyses.

7.3.3. Micromobility type's impact Lateral distance

Hypothesis 6, which explores differences in lateral distance among micromobility types, was tested using ANOVA.

First we compared the lateral distance difference between the same vehicle when overtaking different types of vehicles. The results are shown in the table7.4 and the Figure7.12

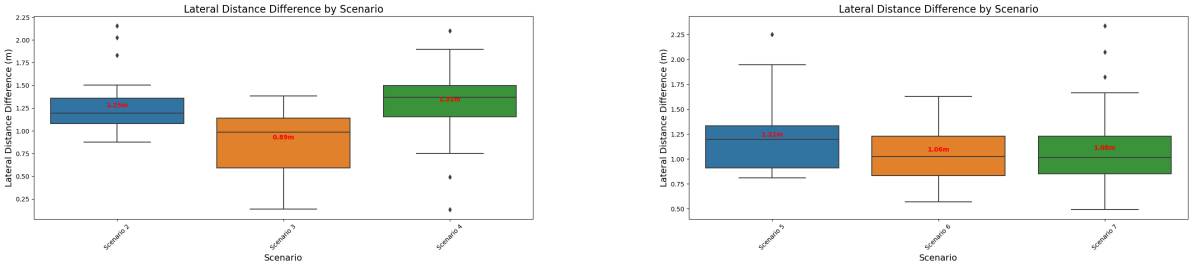

((a)) ANOVA analysis of e-bike

((b)) ANOVA analysis of e-scooter

Figure 7.12: Comparison of ANOVA analyses for e-bike and e-scooter scenarios

Table 7.4: Tukey's HSD Test Results for E-bike Overtaking Different Vehicles

Group 1	Group 2	Mean Diff	p-adj	Lower	Upper	Reject
Scenario 2	Scenario 3	-0.3289	0.0000	-0.4880	-0.1697	True
Scenario 2	Scenario 4	0.0643	0.5933	-0.0918	0.2203	False
Scenario 3	Scenario 4	0.3931	0.0000	0.2389	0.5473	True

The results of Tukey's HSD test reveal significant differences in lateral distance between Scenarios 2 and 3, as well as Scenarios 3 and 4, during e-bike overtaking maneuvers. In Scenario 2, the lateral distance maintained by e-bikes while overtaking is approximately 0.3289 meters smaller than in Scenario 3. Similarly, the lateral distance in Scenario 3 is about 0.3931 meters less than in Scenario 4. However, no statistically significant difference was observed between Scenarios 2 and 4. The mean lateral distances for Scenarios 2, 3, and 4 were 1.2491, 0.8946, and 1.3058 meters, respectively. These findings suggest that the lateral distance adopted by e-bikes during overtaking varies depending on the type of vehicle being overtaken. Notably, e-bikes tend to maintain a smaller distance when overtaking e-scooters compared to bicycles and other e-bikes. This behavior may be attributed to the visual similarity between e-bikes and traditional bicycles, as well as the significantly larger volume occupied by these vehicles in comparison to e-scooters, potentially prompting riders to choose a greater lateral distance during overtaking maneuvers.

In contrast, the ANOVA analysis for e-scooter overtaking scenarios across three different vehicle types (Scenarios 5, 6, and 7) did not yield statistically significant differences in mean lateral distances. The mean lateral distances for Scenarios 5, 6, and 7 were 1.2076, 1.0577, and 1.0778 meters, respectively. We therefore conditionally accept alternative hypothesis 6.1.

The lack of significant variation in lateral distance during e-scooter overtaking maneuvers may be explained by several factors. Firstly, riders' spatial perception may influence their judgment of the space required for safe overtaking based on their perception of their own vehicle's size and that of the vehicle being overtaken. Given the smaller size of e-scooters, riders may believe that they can safely overtake other vehicles even in narrow spaces, thus not requiring significant adjustments in lateral distance. Secondly, the agility and maneuverability of e-scooters may further enhance riders' confidence in their ability to control the vehicle with smaller lateral distances, reducing the need for substantial adjustments. This effect may be particularly pronounced in the present experiment, where e-bike riders were instructed to use pedal-assist mode, while e-scooter riders operated in fully electric mode throughout the study.

Based on the information provided in Figure 7.12(a), it is evident that Scenario 3 exhibits a larger range of variation in lateral distance compared to the other scenarios. This increased variability may be attributed to the presence of different types of e-bikes within the e-bike category, namely Fat e-bikes, Regular e-bikes, and Foldable e-bikes. To further investigate this observation, an additional ANOVA analysis was conducted to compare the lateral distances maintained by these three e-bike types within Scenario 3.

The results of this analysis, presented in Figure 7.13, indicate that there are no statistically significant differences in the mean lateral distances among the three e-bike types. However, it is noteworthy that

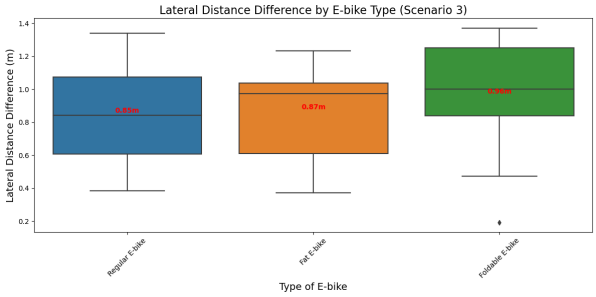

Figure 7.13: Lateral distance by E-bike type(E-bike overtaking e-scooter)

the presence of Foldable e-bikes appears to contribute to a larger overall standard deviation within the scenario. This finding suggests that while the mean lateral distances may not differ significantly across e-bike types, the inclusion of Foldable e-bikes introduces greater variability in the lateral distances maintained by riders during overtaking maneuvers. The design of Foldable e-bikes often prioritizes compactness and portability, which may come at the expense of performance, including acceleration capabilities. Foldable e-bikes may have lower-powered motors, and their folding structure can affect the rigidity of the frame, impacting stability during acceleration. These factors may lead Foldable e-bike riders to adopt a more conservative approach during overtaking maneuvers, resulting in greater variability in lateral distances.

Following this, we made a comparison of the differences between various types of vehicles when overtaking the same type of vehicle. The results indicate that significant differences were observed only in the context of E-bikes/E-scooters overtaking e-bikes. Specifically, E-bikes maintained a notably larger lateral distance during the maneuver, with a T-statistic of 3.152 and a P-value of 0.0027. We therefore conditionally accept alternative hypothesis 6.2.

The smaller lateral distance observed when E-scooters overtook may primarily result from the riders' perception of their vehicle's smaller size. E-scooter riders might feel that, due to the compact nature of their vehicle, they can safely complete the overtaking maneuver with less space. This perception likely leads E-scooter riders to opt for a smaller lateral gap compared to E-bikes.

Additionally, the modifications to the experimental path could also have influenced this behavior. To efficiently collect data with the limited number of E-bikes, a shorter experimental path was used, which necessitated that E-bike riders achieve higher speeds to overtake within the design constraints. However, E-scooters on this path likely did not need to adapt to higher speeds as E-bikes did, and thus could choose a smaller lateral distance at relatively lower speeds. This smaller lateral distance reflects not only the E-scooter's size advantage but also the differing speed and space requirements imposed by the path design. Therefore, the reduced lateral distance for E-scooters may result from a combination of both path adjustments and the riders' perception of their vehicle's size.

7.3.4. Maximum lateral distance position

The examination of Hypothesis 8, which posits that the maximum lateral distance occurs during the passing phase, was tested through custom analysis. Analysis of the data across multiple scenarios as shown in table7.5 revealed varying degrees of support for the hypothesis.

Table 7.5: Percentage of Max Lateral Distance Moments within Overtaking phase

Scenario	Percentage (%)
Scenario 2	88.64
Scenario 3	55.56
Scenario 4	71.43
Scenario 5	91.67
Scenario 6	88.57
Scenario 7	76.32

The maximum lateral distance during an overtaking maneuver occurs within the overtaking period. The percentage of maximum lateral distance moments occurring within the overtaking period ranged from 55.56% to 91.67% across the scenarios studied. Notably, Scenario 3 exhibited the lowest concordance with the hypothesis at 55.56%. This scenario also demonstrated the smallest average lateral distance(0.8956m) among all scenarios examined. A plausible explanation for this observation is the reduced spatial perception of e-scooters by e-bike riders during overtaking maneuvers. The compact profile of e-scooters may lead to an underestimation of the necessary lateral clearance by e-bike riders, resulting in closer passing distances and potentially altering the typical overtaking dynamics. The data provides support for our hypothesis across multiple scenarios. Specifically, in Scenarios 2, 5, and 6, a high proportion of maximum lateral distance moments (88.64%, 91.67%, and 88.57% respectively) occurred within the overtaking period. Scenarios 7 and 4 also showed considerable alignment with our hypothesis, with 76.32% and 71.43% of maximum lateral distance moments occurring during overtaking.

These findings suggest that while the alternative hypothesis 8 is generally accepted, there is considerable variability across different overtaking scenarios. The observed differences, particularly in Scenario 3, underscore the importance of considering vehicle type and rider perception in micro-mobility interactions as mentioned in section7.3.3.

7.4. Overtaking starting position

The starting position is a relative position in the x-direction. We first implemented a comprehensive visual validation of our overtaking detection threshold. This process involved creating detailed plots of the relative coordinates of the overtaking pairs (e-bike or e-scooter and the overtaken vehicle) over time. On these plots, we marked the detected overtaking initiation points, as illustrated in Figure 7.14. After validation by randomly selecting 10 for each scenario, it was shown that the selection of (Mean - 1σ) is justified. The choice is because 10 is already greater than 20 percent of the dataset and is representative.

((a)) Overtaking moment of pair 3 in scenario 2

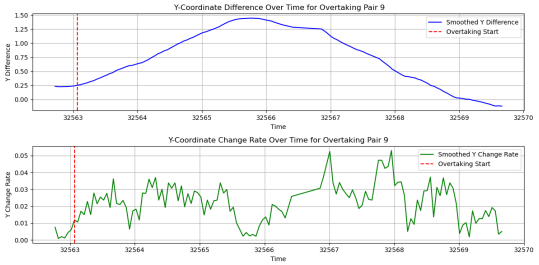

((b)) Overtaking moment of pair 9 in scenario 2

Figure 7.14: Comparison of overtaking moments for different pairs in scenario 2

7.4.1. Micromobility's impact

The findings in this section relate directly to Hypothesis 9, which proposed that micromobility type would influence the overtaking starting position.For Hypothesis 9, an ANOVA test and subsequent Tukey's HSD post-hoc analysis were conducted to assess differences in the overtaking starting positions among various micromobility types. The results of this analysis are presented in Table 7.6.

Table 7.6: ANOVA Results for Relative Overtaking Times

Statistic	Value	p-value
F-value	4.1921	0.0171

For scenario 2 (E-bike overtaking bike) the mean value is 9.75 m, with SD 2.86 m; for scenario 3 (E-bike overtaking e-scooter), the mean value is 10.19 m, with SD 3.62 m; for scenario 4 (E-bike overtaking e-bike), the mean is 7.80 m, with SD 4.93 m. The ANOVA results indicate a statistically significant difference in relative overtaking times between scenarios (F = 4.2474, p = 4.2474). This

p-value, being less than the conventional significance level of 0.05, suggests that there are indeed significant differences in overtaking behavior across the different micromobility scenarios tested.

To further investigate which specific scenarios differ from each other, a post-hoc analysis using Tukey's Honest Significant Difference (HSD) test was performed. The results of this test are presented in Table 7.7.

Table 7.7: Tukey's HSD Test Results of starting position of overtaken

Group 1	Group 2	Mean Difference	p-adj	Lower	Upper
Scenario 2	Scenario 3	0.4387m	0.8587	-1.5380	2.4154
Scenario 2	Scenario 4	-1.8717m	0.0716	-3.8710	0.1276
Scenario 3	Scenario 4	-2.3104m	0.0183	-4.2987	-0.3221

The Tukey's HSD test reveals that:

1. There is no statistically significant difference between Scenario 2 and Scenario 3 (p-adj = 0.8587).
2. The difference between Scenario 2 and Scenario 4 is not statistically significant (p-adj = 0.0716), although there is a trend towards shorter overtaking starting position in Scenario 4 (mean difference = -1.8717).
3. There is a statistically significant difference between Scenario 3 and Scenario 4 (p-adj = 0.0183). Scenario 4 has a shorter overtaking starting position in Scenario 4 (mean difference = -2.3104m).

The analysis reveals intriguing patterns in overtaking behavior across different micromobility scenarios. E-bike riders tend to initiate overtaking later when passing e-bikes. We therefore accept alternative hypothesis 9.

The phenomenon of e-bike riders initiating overtaking maneuvers later when passing other e-bikes can be primarily attributed to two key factors:

1. Familiarity and Predictability: E-bike riders likely possess a more nuanced understanding of the performance characteristics and typical behaviors of other e-bikes. This familiarity engenders a sense of predictability, allowing overtaking riders to feel more at ease when initiating the maneuver at a closer distance. The shared experience of riding e-bikes may contribute to a mutual understanding of acceleration patterns, speed maintenance, and potential reactions to traffic conditions. This implicit knowledge could lead to a more confident approach to overtaking, resulting in later initiation of the maneuver.
2. Confidence in Acceleration: E-bikes are equipped with electric assistance, providing them with the capability for rapid acceleration.Additionally, Section 7.2 confirms that the normal riding speed of e-bikes is faster. In fact, the experimental equipment used on the day of testing showed that the maximum speed of e-bikes was indeed higher than that of e-scooters. Overtaking riders may leverage this feature, feeling assured in their ability to swiftly increase speed and execute the overtaking maneuver efficiently, even when initiating it at a closer proximity to the vehicle being overtaken. This confidence in the e-bike's performance characteristics may allow riders to delay the start of their overtaking action, knowing they can rely on the bike's electric boost to complete the maneuver safely and effectively.

These factors combined suggest that e-bike riders, when overtaking other e-bikes, may feel a greater sense of control and predictability in the overtaking process. This increased comfort level, coupled with the confidence in their vehicle's capabilities, could explain the observed tendency to initiate overtaking maneuvers at a later point and closer distance compared to overtaking other micromobility modes.

7.4.2. Gender's impact

In terms of Hypothesis 10, which examined the effect of gender on overtaking starting positions, no significant gender differences were detected in these scenarios. We therefore accept null hypothesis 10. This suggests that gender does not significantly impact when the overtaking maneuver begins. While gender was tested in earlier sections, no notable differences emerged, indicating that the type of vehicle being overtaken plays a more crucial role than gender in this context.

7.5. Regression analysis on speed difference

This section addresses Hypotheses 11 and 12, which explore the influence of lateral and longitudinal position differences, vehicle types, and overtaking phases on speed difference during the whole overtaking process.

Multiple Regression Analysis

First, for Hypothesis 11, a multiple regression analysis was conducted to assess the relationship between speed difference and position differences (both lateral and longitudinal), as well as vehicle type. The results, as detailed in the regression equation:

$$\text{Speed difference} = 6.4167 + 0.2567X + 1.2394Y + 0.8093T_2 - 0.8093T_3 \tag{7.1}$$

Where X is the longitudinal position difference, Y is the lateral position difference, and T_2 and T_3 represent overtaken vehicle types e-bike and e-scooter respectively (relative to the reference type bike). The model's R^2 value is 0.1240.

The analysis results reveal significant influences of position differences, vehicle types, scenarios, and overtaking phases on speed difference. We therefore accept the alternative hypothesis 11. Several key findings warrant further discussion:

1. Lateral vs. Longitudinal Position Difference: The lateral position difference shows a greater impact (coefficient: 1.2394) on speed difference compared to the longitudinal position difference (coefficient: 0.2567). This aligns with our expectations of overtaking behavior. The overtaking process typically involves the rider accelerating in the initial phase, maintaining a higher speed during the passing maneuver, and then decelerating after completion. Throughout this process, the speed difference difference generally increases as the lateral distance increases, and decreases as it narrows, given that lateral distance difference is always positive.

   Conversely, the longitudinal distance difference transitions from positive (before overtaking) to negative (after overtaking). In the pre-passing phase, the positive longitudinal difference corresponds to the acceleration stage, resulting in a positive change in speed difference. Post-overtaking, as the longitudinal difference becomes negative, the speed difference naturally decreases.
2. Vehicle Type Influence: The results indicate that when an E-bike overtakes another E-bike, the speed difference is greater than when overtaking a bicycle. Conversely, when an E-bike overtakes an E-scooter, the speed difference is lower than when overtaking a bicycle. These findings suggest that the type of vehicle being overtaken significantly influences the overtaking dynamics.

   This pattern could be attributed to several factors. E-bike riders might be more comfortable maintaining higher speeds when overtaking similar vehicles (other E-bikes).The lower speed difference when overtaking E-scooters could indicate a more cautious approach due to the perceived instability or unpredictability of E-scooters.

Phase-wise Comparison Analysis of Overtaking

Moving forward, Hypothesis 12 examined differences in speed difference across the overtaking phases (before, during, and after) as in Figure7.15.

An ANOVA analysis on this data revealed a significant effect of overtaking phase on speed difference ($F = 4.7211$, $p = 0.0009$). Subsequent Tukey HSD post-hoc tests yielded the following results:

- Significant difference between After and During phases ($p = 0.0009$)
- Difference between Before and After phases approaching significance ($p = 0.2371$)
- No significant difference between Before and During phases ($p = 0.2922$)

These results unveil distinct patterns of speed difference dynamics across overtaking phases:

- In Scenario 2, speed difference shows a gradual decrease from the Before phase to the After phase.

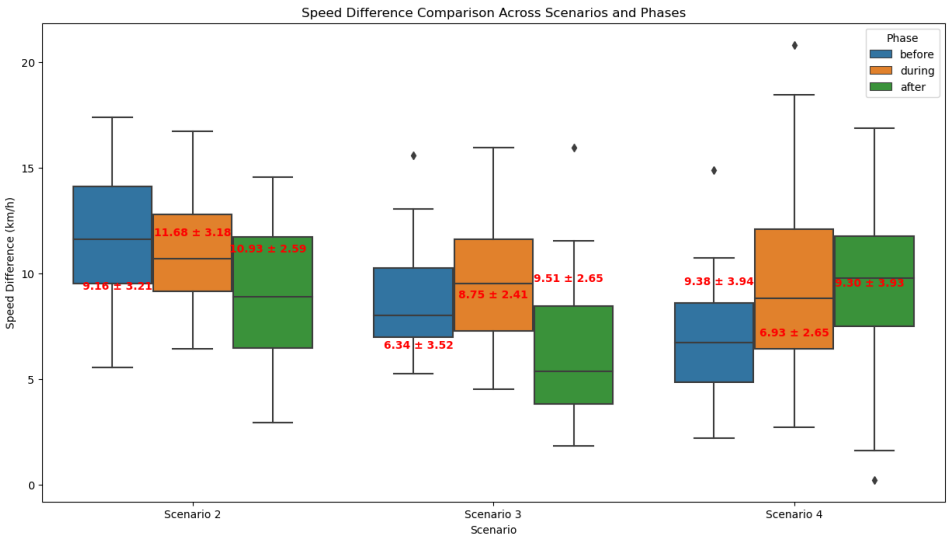

Figure 7.15: Phase-wise Comparison Analysis of Overtaking

- Scenario 3 exhibits a unique pattern where speed difference peaks during the During phase, followed by a significant decrease in the After phase.
- Scenario 4 demonstrates a trend of increasing speed difference from the Before phase to the After phase.

These phase-wise variation patterns reflect differences in driver behavior across different overtaking scenarios. For instance, the gradual deceleration in Scenario 2 might indicate drivers adopting a more cautious strategy after completing the overtaking maneuver. Conversely, the speed increase trend in Scenario 4 could suggest specific traffic or environmental factors prompting drivers to accelerate progressively during the overtaking process.We therefore accept alternative hypothesis 12.

A plausible explanation for the observed trend in scenario 2 stems from the experimental conditions. During the bike overtaking experiments, the number of bicycles on the red overtaken path was notably higher than in other scenarios, with at least 5 and sometimes 6 bicycles present. Despite efforts by experiment supervisors to moderate the conditions, there were instances where two or three bicycles occupied the main track simultaneously. This higher density of bicycles significantly altered the dynamics of the overtaking process. In some cases, overtaking vehicles were not merely passing a single bicycle but were engaged in consecutive overtaking maneuvers involving two bicycles in close succession. This scenario introduces a more complex overtaking behavior where the overtaking vehicle initiates the maneuver to pass the first bicycle at its typical speed, but upon approaching the second bicycle in close proximity, adopts a more cautious approach. Rather than maintaining or increasing speed to complete the second overtaking maneuver quickly, the driver opts for a slight deceleration. This deceleration during the second overtaking phase results in a lower speed difference between the overtaking vehicle and the bicycle being overtaken, which is reflected in the data and contributes to the observed trend of lower speed difference in scenario 2.

In Scenario 4, which focuses on overtaking e-bikes, the utilization of a smaller circular path, as illustrated in Figure 5.8, in the experimental design is particularly noteworthy. By comparing the path length used in this scenario to the natural encountering distance in other scenarios, it becomes apparent that the shorter path could potentially create a perceived time constraint for the participants to complete the overtaking process.

7.6. Change of overtaken mode motion

7.6.1. Compare pre-passing and post-passing phase

This section relates to Hypothesis 13, which addresses the speed changes of overtaken riders before and after being overtaken. The study investigates whether there is a significant difference in the behav-

ior of overtaken vehicles after overtaking, with a focus on how different types of micromobility vehicles respond to overtaking events.

To test Hypothesis 13, paired t-tests were conducted to compare the speeds of overtaken riders before and after overtaking across Scenarios 2, 3, and 4. The results showed that only scenario 4 exhibited a significant difference, with an overall trend of acceleration. The T-value is -3.1412 and p-value is 0.0031.

However, upon examining the paired comparison boxplots for the three scenarios as in Figure7.16, it was observed that both acceleration and deceleration accounted for a certain proportion in each scenario. In scenarios 2 and 3, the proportions of acceleration and deceleration were similar, resulting in no significant overall change in speed. We therefore accept null hypothesis 13.1.

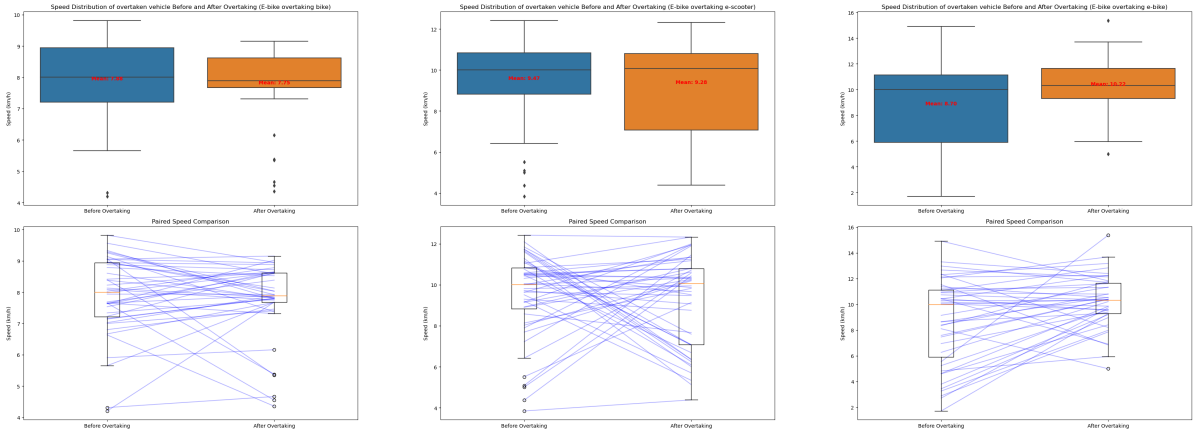

((a)) Scenario 2 **((b))** Scenario 3 **((c))** Scenario 4

Figure 7.16: Speed distribution of overtaken modes across different scenarios

To address this phenomenon more comprehensively, we conducted a detailed analysis of individual speed changes within each scenario. While the aggregate data showed significant acceleration only for e-bikes across all scenarios, we found that in Figure7.16 that this might be due to the offsetting effects of individual accelerations and decelerations within each group. To test this hypothesis, we performed a more granular analysis. For every scenario, we calculated the proportion of cases where the absolute speed change after overtaking phase exceeded 2 km/h. This threshold was chosen because it represents a substantial change (approximately 20%) relative to the average speeds of overtaken vehicles, which ranged from 7.88 km/h to 10.22 km/h across scenarios. We categorized these significant speed changes into acceleration cases and deceleration cases. Figure 7.17 illustrates the proportions of significant acceleration and deceleration cases among all cases of each scenario. This analysis reveals the percentage of overtaken riders who exhibited notable acceleration or deceleration post-overtaking, providing a more nuanced understanding of individual behavioral responses.

Interestingly, it was found that overtaken bicycle riders typically experienced minimal speed changes, with a low percentage of significant changes. In contrast, e-scooter and e-bike riders showed much larger variations in speed.

This difference may be related to vehicle type and rider behavior. E-scooters and e-bikes are equipped with electric assist systems, making it easier for riders to accelerate using the electric system when being overtaken. On the other hand, traditional bicycles rely on human power, making it more difficult for riders to significantly accelerate or quickly adjust their speed when being overtaken.

Additionally, psychological factors of the riders may play a role. E-scooter and e-bike riders may feel the need to adjust their position or avoid potential risks by accelerating or decelerating when being overtaken. Traditional bicycle riders may not feel the same pressure or may be limited in their ability to accelerate, resulting in a weaker response.

Another possible reason is that the average speed of e-scooters and e-bikes is typically faster than that of traditional bicycles. At relatively higher speeds, changes in vehicle speed may appear more

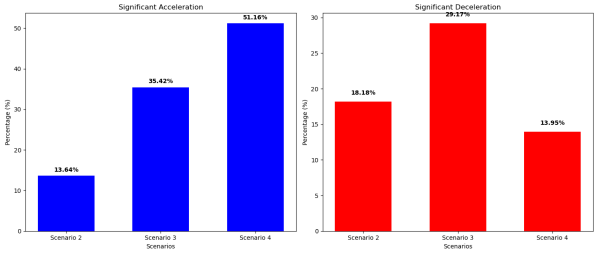

Figure 7.17: Percentage of riders with significant change on speed in three scenairos

pronounced.

Notably, the high proportion of significant acceleration among e-bike riders may be largely attributed to individual rider behavior habits. During the process of trajectory labelling through some of the L1 videos,the authors noticed three male E-bike riders frequently accelerating while being overtaken.

7.6.2. Compare the speed change between beginning and ending of the pre-passing phase

The purpose of this comparison remains focused on analyzing the behavior of the overtaking rider. However, in this case, we are specifically examining the rider's behavior at the start position of being overtaken, which corresponds to the end of the pre-passing phase. This phase represents the point at which the overtaken rider becomes aware that they are about to be passed. We aim to determine whether any speed changes—either deceleration or acceleration—occur compared to the beginning of the pre-passing phase.

The results indicate that both E-bikes and E-scooters exhibit a slight acceleration at the end of the pre-passing phase, whereas bikes show no significant change. The speed changes observed in the three scenarios are as follows:

- E-bike overtaking bike: p-value = 0.4933, Mean speed difference = -0.21 km/h
- E-bike overtaking E-scooter: p-value = 0.0591, Mean speed difference = 1.02 km/h
- E-scooter overtaking bike: p-value = 0.0001, Mean speed difference = 2.32 km/h

Overall, the alternative hypothesis 13.2 is accepted. Although some acceleration is observed, the magnitude of these acceleration changes remains relatively small. In the study by [66], it was shown that 38.3% of bicyclists accelerate when being overtaken. However, there is currently almost no comparison of E-bike and E-scooter as overtaken modes. Considering that E-bikes and E-scooters are either assisted or fully electric, it is a reasonable outcome that they generally exhibit acceleration due to a higher percentage of acceleration. This adjustment can be seen as a natural reaction to being overtaken, facilitated by the stronger acceleration capabilities of these vehicles

7.7. Roll angle and roll rate

This section examines the changes in roll angle and roll rate during the overtaking process, as hypothesized in Hypotheses 14 and 15, which focus on the differences in roll dynamics across different phases of overtaking and the influence of micromobility type on these dynamics.

The first analysis on different phases inside each scenario shows that in all scenarios, the rate of change in roll angle during the overtaking phase is higher than in the pre-passing and post-passing phases. A similar trend is observed in the roll angle itself, indicating that vehicles experience larger angle changes and more intense rates of angle change during the overtaking process. We therefore accept alternative hypothesis 14.1 and 14.2.

This phenomenon may be attributed to the following reasons: During overtaking, riders need to rapidly change position to avoid collisions with the overtaken vehicle, inevitably leading to larger angle changes. Completing an overtaking maneuver within limited lane width requires riders to make more abrupt and pronounced steering actions.

In the comparison between E-bikes overtaking E-scooters (Scenario 3) and E-bikes overtaking E-bikes (Scenario 4), Scenario 4 exhibits a significantly higher lateral angle change rate in the pre-passing phase. The roll angles for scenario 3 in the three overtaking phases were 4.03, 6.66, and 4.67 degrees, respectively. The roll rate is 26.17, 36.73, and 24.68 degree/s for scenario 3. The roll angles for scenario 4 in the three overtaking phases were 4.48, 7.04, and 4.43 degrees, respectively. The roll rate is 30.41,36.21, and 27.49 degree/s for scenario 4. The results of the T-tests for roll rate and roll angle (absolute values) during the before-overtaking phase are as follows:

- **Roll Rate (Absolute)**: The t-statistic is -3.2385 and the p-value is 0.0012, indicating a statistically significant difference.
- **Roll Angle (Absolute)**: The t-statistic is -2.7336 and the p-value is 0.0063, also indicating a statistically significant difference.

Therefore we accept the alternative hypothesis 15.1 and 15.2. There is no significant difference between the other phases in terms of either roll rate or roll angle.

This finding aligns with previous analysis results: in Scenario 4, overtakers tend to initiate overtaking maneuvers at closer positions to the overtaken vehicle but ultimately maintain a larger lateral distance difference than in Scenario 3. This behavior pattern implies that riders need to complete larger lateral movements in a shorter time, which is likely the direct cause of the higher roll rate in the pre-passing phase of Scenario 4 compared to Scenario 3. This phenomenon may reflect the strategy differences of E-bike riders when facing different types of overtaken vehicles. E-bike riders may be more familiar with the performance characteristics of other E-bikes, thus exhibiting more confidence and willingness to adopt more aggressive overtaking strategies. E-bike riders might underestimate the speed difference difference with other E-bikes, causing them to realize the need for overtaking at a closer distance, necessitating more abrupt maneuvers.

7.8. Summary

This chapter first compares the normal driving speeds and deceleration capabilities of vehicles in non-interactive scenarios. The results revealed significant speed differences between E-bikes and E-scooters, with E-bikes traveling at notably higher speeds. However, no distinction was observed in their deceleration capabilities. Gender differences in speed were only significant in E-scooter riders, where male riders consistently exhibited higher speeds than females.

To explore the influence of gender factors and the combination of overtaking and overtaken vehicles on overtaking behavior, the study analyzed the lateral position difference. The findings indicate that the maximum lateral distance difference mostly occurs within the passing phase. During this phase, the overtaker's choice of lateral distance is influenced by speed difference; higher speed differences correspond to larger maintained lateral distances. This reflects the riders' adaptation to safety requirements based on speed differentials.

The study then compared the behavioral differences of overtaking vehicles when passing different vehicle types. These differences were less pronounced for E-scooters but more evident for E-bikes, potentially reflecting the overtaking riders' perceptions of their own vehicle's size and that of the overtaken vehicle. Additionally, when comparing different vehicles overtaking the same type, a significant difference emerged only when E-bikes and E-scooters overtook E-bikes, with E-bikes maintaining a larger lateral distance. This increased lateral distance was likely due to that e-scooter riders may perceive themselves as occupying less space and thus more maneuverable compared to e-bike riders, prompting them to feel more comfortable overtaking with a smaller lateral gap. However, it may also be influenced by modifications to the experimental path, which required higher speeds and, consequently, greater spacing to ensure safety.

Using an analysis of the rate of change in lateral position difference, the study detected the initiation points for overtaking maneuvers in E-bikes overtaking E-scooters and E-bikes. Interestingly, E-bikes initiated overtaking of E-scooters at a greater distance compared to overtaking other E-bikes, without significant gender influence.

Combining these findings with the maximum lateral distance difference tests provides an overview of E-bike overtaking patterns for E-scooters and E-bikes, as illustrated in Figure 7.18. Generally, E-bikes

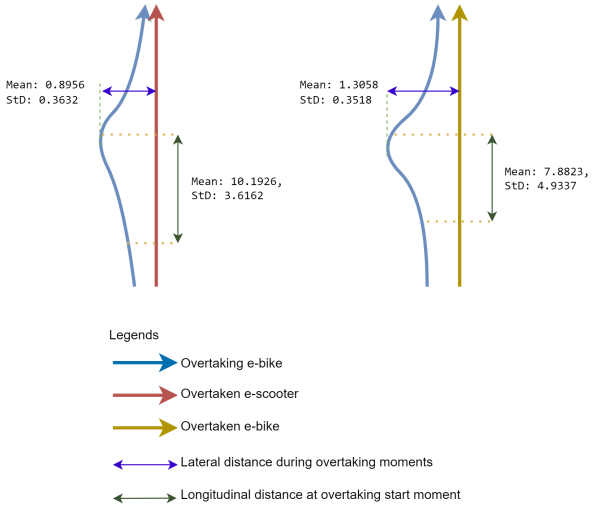

Figure 7.18: Overtaking pattern of e-bike overtaking e-scooter and e-bike

initiate overtaking E-scooters from a greater distance but maintain a smaller maximum lateral distance during the process. Conversely, when overtaking other E-bikes, they initiate the maneuver closer but choose a larger lateral spacing.

This pattern is further corroborated by the phase-wise comparison of roll rates and roll angles' absolute values across different overtaking scenarios. Additionally, this comparison reveals a common motion characteristic: roll rates and roll angles reach their maximum values during the passing phase.

To further understand the differences between pre-passing, overtaking, and post-overtaking phases, the study compared average speeds during these phases for E-bikes overtaking bikes, E-scooters, and E-bikes. These results revealed some experimental design flaws, such as an excess of vehicles on the bike lap leading to continuous deceleration while overtaking two bicycles consecutively(scenario2), and inappropriate timing control during internal overtaking experiments resulting in continuous acceleration during overtaking(scenario4). In Scenario 2, an overtaker may accelerate to a high speed to overtake the first vehicle and then realize that there is a second overtaken vehicle, but instead of accelerating further, he slowly decelerates to overtake the second low-speed vehicle. In scenario 4, since the experimental requirement is to complete the overtaking inside the design track, it may result in the overtaking vehicle that starts later needing to keep accelerating in order to complete the overtaking maneuver before the end of the deisgn track, this phenomenon may also occur in scenario 7, but due to the missing data of 7, it is not possible to test it.

Furthermore, the study examined the behavior of overtaken vehicles during the overtaking process, particularly focusing on speed changes before and after the passing phase, and within the pre-passing phase. When comparing the speed between the pre-passing phase and post-passing phase, E-scooters and E-bikes showed a significantly higher proportion of noticeable speed changes compared to bikes. Due to some E-bike riders' personal preferences, E-bikes as overtaken vehicles demonstrated a markedly higher proportion of acceleration after being overtaken. when comparing within pre-passing phase, e-bike and e-scooter exhibit a slight acceleration at the end of the pre-passing phase, showing that riders alter their speed as a form of defensive or adaptive behavior when interacting with others in close proximity.

The final test results of the relationships in the Conceptual framework are shown below in Figure7.19 is the conceptual framework that has been tested.

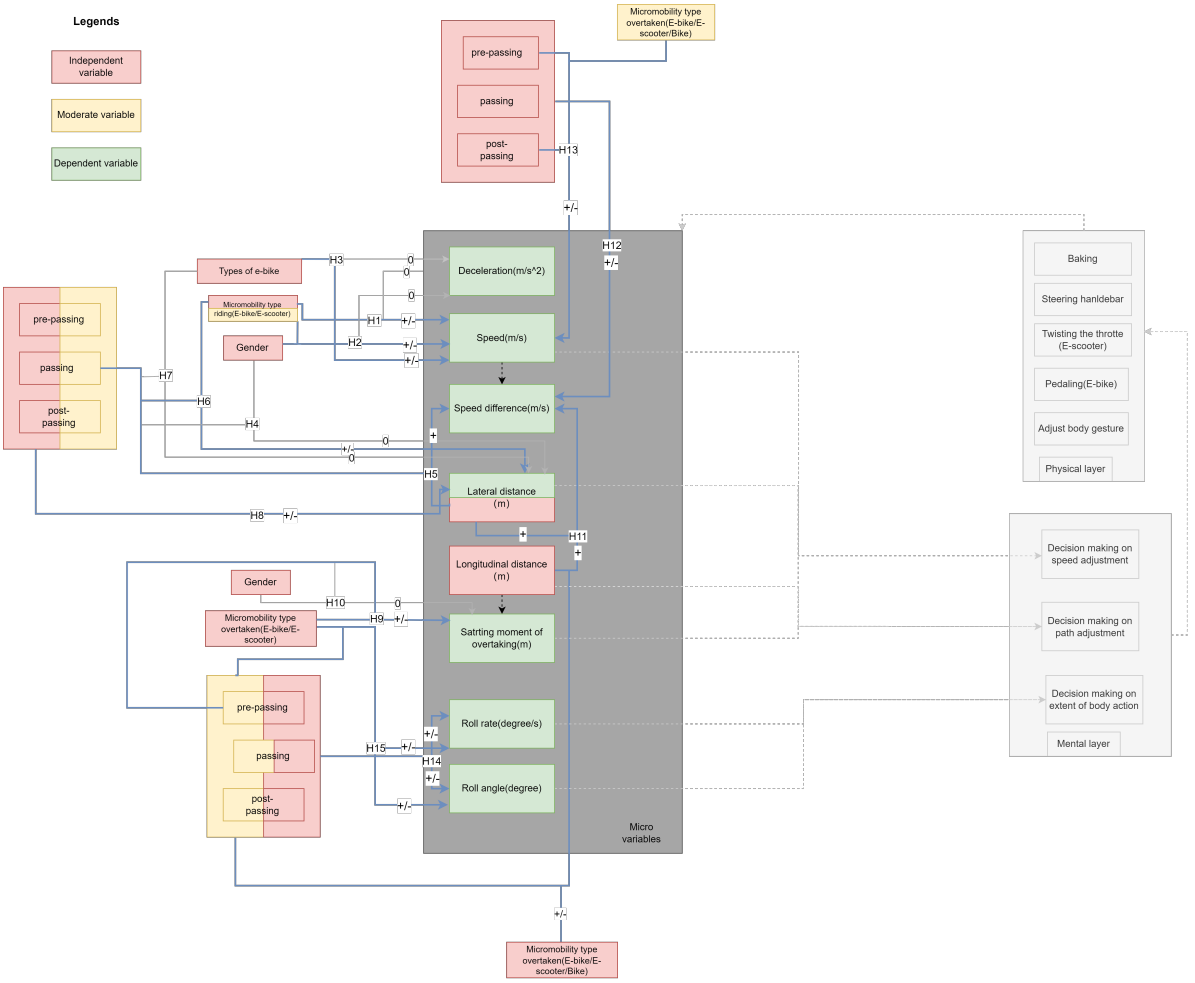

Figure 7.19: Conceptual framework after test

Where + means there is significant positive relationship, +/- means there is significant relationship but whether it is postive or negative is up to the characteristic, 0 means there is no significant relationship

8

Conclusion and discussion

This thesis aims to investigate the individual behavior of micromobility users, specifically e-bike and e-scooter riders, during their interactions with regular bicycles and with each other. To study and understand rider behavior during overtaking scenarios, this research designed and implemented a controlled experiment to collect trajectory data of e-scooter and e-bike riders through video recording during overtaking maneuvers, along with data on roll angle and roll rate from IMU sensors. After processing the video data, trajectory data of the participants were obtained, which were then synchronized with the IMU data on a common timeline. From these trajectory data, micro-level variables such as lateral position difference, longitudinal position difference, and speed difference were derived. The study then employed statistical methods, including t-tests, ANOVA, Pearson correlation analysis, and regression models, to examine the effects of gender, vehicle type, and other influencing factors on these micro-level variables. Ultimately, the results revealed several behavioral characteristics and patterns during the overtaking process, providing key insights into how different micromobility types and individual characteristics influence rider behavior.

8.1. Answers to the main research question

"How do different combinations of ridden types of micro-mobility vehicles and overtaken types of micro-mobility vehicles and individual characteristics of the rider affect individual behavior during overtaking?".

In this study, the individual characteristics is speficed to gender.

8.1.1. Affect of micro-mobility type combination

In the context of overtaking behavior, micromobility vehicle type had a substantial impact. E-bike riders, when overtaking e-scooters, initiated the overtaking maneuver from a greater distance but maintained a smaller maximum lateral distance throughout the maneuver. Conversely, when overtaking other e-bikes, riders initiated the overtaking maneuver closer to the overtaken vehicle but maintained a larger lateral distance, indicating more caution and space in similar-vehicle interactions.

The vehicle type also influenced the speed difference dynamics during the overtaking process. As the multiple regression analysis, lateral position differences were more strongly correlated with speed difference than longitudinal differences, confirming that riders prioritize lateral safety margins when overtaking. The type of overtaken vehicle also affected the speed, with e-bikes maintaining higher speed diference when overtaking other e-bikes compared to when overtaking e-scooters, demonstrating that vehicle-type familiarity influences rider behavior.

The roll rate and roll angle peaked during the passing phase. Moreover, in the process of E-bike overtaking E-bike, the roll angle and roll rate are significantly larger in the pre-phasing stage when E-bike overtakes E-scooter because more lateral movement has to be accomplished in a shorter period of longitudinal distance.

8.1.2. Gender affect

Gender differences in riding behavior were clearly observed in non-interactive driving, especially for e-scooter riders, where male riders showed significantly higher speeds than female riders. However, no gender-based differences were found for e-bike riders in similar conditions, suggesting that vehicle type plays a role in how gender impacts driving behavior.

Initially, it was hypothesized that gender might influence lateral distance decisions during overtaking, particularly for e-scooter riders. However, subsequent analysis revealed no significant gender-based differences in lateral distances maintained during overtaking maneuvers. This finding suggests that while gender may influence riding speed in non-interactive scenarios, it does not significantly affect spatial decisions during overtaking.

Furthermore, gender had no significant impact on the initiation of overtaking maneuvers. These results collectively indicate that factors such as vehicle type and speed may be more influential than gender in determining both the timing and spatial characteristics of overtaking behaviors.

8.1.3. Key findings overall

Several key findings emerged regarding rider behavior as follows:

1. speed difference and Lateral Distance: There was a consistent positive correlation between speed difference difference and lateral distance, with higher speeds associated with larger lateral distances during overtaking. This indicates that riders adapt their lateral space for safety based on speed differences.
2. Maximum Lateral Distance Timing: The maximum lateral distance typically occurred during the passing phase, though there was some variation across scenarios . In scenarios where e-bikes overtook e-scooters, this pattern was less consistent, suggesting that e-bike riders may underestimate the space needed when overtaking smaller vehicles like e-scooters.
3. Phase-Wise Speed Differences: The phase-wise comparison of speed difference revealed that in some scenarios, speed difference gradually decreased after overtaking, while in others, the speed difference continued to increase post passing. This could reflect environmental factors or experimental design conditions, such as the number of vehicles on the track.
4. Behavior of Overtaken Vehicles: Electrically-powered vehicles like e-bikes and e-scooters exhibited more speed variation when overtaken compared to bicycles. Notably, some e-bike riders increased their speed after being overtaken, indicating individual behavioral preferences or reactions to being passed. And at the start moment of being overtaken, the e-bike and e-scooter rider have a noticeable acceleration.
5. The roll rate and roll angle were consistently higher during the passing phase across all scenarios. In the case of an E-bike overtaking another E-bike, the overtaking began with a later start and maintained a greater lateral distance. Consequently, both the roll rate and roll angle were larger in the pre-passing phase compared to another overtaking scenario(E-bike overtaking E-scooter), reflecting the increased maneuvering needed to initiate the overtaking maneuver with a safe lateral buffer

8.2. Societal Contributions

The findings from this research can have several significant applications in guiding infrastructure development, informing traffic regulations, and enhancing the design of traffic simulation models, especially with the growing popularity of micromobility vehicles like e-bikes and e-scooters. The following are some key areas where this research can be applied:

1. Wider and Safer Lanes: Based on the findings that micromobility users, particularly e-bike riders, tend to maintain larger lateral distances when overtaking other vehicles, the study suggests that wider cycling lanes should be considered in urban planning. This would provide adequate space for safe overtaking and reduce the risk of collisions, particularly in areas with high mixed-use traffic involving micromobility vehicles. Wider lanes could ensure safer maneuverability for both overtaking and overtaken riders, especially in congested areas. In the past, the recommended width for two-way bicycle paths in the Netherlands was 2 meters[67], based on the assumption of a

minimum lateral spacing of 0.75 meters between two bicycles. This study, however, recommends increasing the minimum width to 2.3 meters, as the observed average maximum lateral spacing in this research was 1.1 meters.

Coincidentally, in 2022, the CROW Design Manual for Bicycle Traffic updated the recommended width for one-way bicycle paths in the Netherlands from 2 meters to 2.35 meters[68]. However, CROW did not explicitly cite the introduction of e-bikes or e-scooters as a reason for this change; instead, the update was motivated by the potential safety benefits of wider paths. This study's findings further validate the reasoning behind CROW's recommendation, as larger lateral spacing can accommodate various micromobility types and contribute to overall riding safety.

2. Overtaking Distance Guidelines: The analysis of lateral distances and speed differences during overtaking demonstrates the need for clearer guidelines on safe overtaking distances between different types of micromobility vehicles. Transport authorities can use these findings to develop minimum overtaking distance standards for micromobility users. Such guidelines could be integrated into traffic laws, ensuring that riders are aware of the necessary space required to safely overtake other vehicles, ultimately enhancing road safety for all users.
3. Traffic Calming Measures: The differences in speed and acceleration between e-scooters, e-bikes, and traditional bicycles could be used to design more effective traffic calming measures. Implementing speed limits tailored to different types of micromobility vehicles and creating designated overtaking zones could help reduce conflicts between riders and minimize high-risk overtaking behaviors. This approach could also prevent scenarios where slower bicycles are overtaken in unsafe conditions, thus mitigating potential hazards.
4. Micromobility Integration into Traffic Systems: Given the increasing integration of e-bikes and e-scooters into urban transportation, the study's insights into overtaking behavior could inform traffic simulation models that reflect real-world dynamics of mixed micromobility interactions. These models could be used by transportation planners and engineers to simulate and optimize the flow of micromobility vehicles in urban traffic systems, allowing for the development of infrastructure that accommodates the unique behaviors of these vehicles, leading to safer and more efficient traffic networks.

8.3. Research contribution

This study presents a comprehensive experimental design process that can serve as a reference for future researchers undertaking similar investigations in the field of micromobility behavior. The methodology developed here offers a systematic approach to studying complex interactions between different types of micromobility vehicles and users.

Moreover, this research has resulted in the development of a robust video data processing pipeline. This pipeline is characterized by its adaptability to datasets of varying quality, making it particularly suitable for studies where data collection conditions may not be ideal. The process is designed with a focus on reproducibility, allowing other researchers to apply and build upon this methodology in their own work.

The video processing workflow developed in this study addresses common challenges in micromobility research, such as multi-camera trajectory merging, time synchronization across different data sources, and trajectory smoothing. By providing solutions to these technical hurdles, this research contributes to the standardization of data processing methods in micromobility studies. Furthermore, the approach taken in this study to define and analyze overtaking phases offers a nuanced framework for examining micromobility interactions. This framework can be adapted and refined by future researchers to explore various aspects of micromobility behavior beyond overtaking.

In summary, the methodological contributions of this study - including the experimental design, data processing pipeline, and analytical framework - provide a solid foundation for future research in micromobility behavior. These tools and approaches can enhance the rigor and comparability of studies in this rapidly evolving field.

8.4. Limitations and recommendation for future research

This study provides valuable insights into micromobility overtaking behavior. However, several limitations should be recognized and addressed in future research. Each limitation highlights areas for improvement and suggests potential avenues for further investigation:

1. **Cultural and Market Context:** This study was conducted within the unique micromobility landscape of China, where e-mopeds dominate and e-bikes are less common, with e-scooters primarily used in specific areas such as university campuses. While participants were given time to adjust to the vehicles, their behavior may not fully reflect that of experienced riders in regions like Europe, where e-bikes are more prevalent and used in diverse settings. These contextual factors may have influenced overtaking behaviors specific to the Chinese market. Future research should consider cross-cultural comparisons in regions with established e-bike ecosystems to examine if local factors and cultural norms shape rider behavior, ultimately determining if findings are generalizable or if region-specific safety guidelines are necessary.
2. **Experimental Design Constraints:** The simultaneous presence of multiple slow-moving vehicles in the study may have impacted participant behavior, particularly when e-bikes overtook bicycles. This multi-target environment might have inadvertently altered overtaking decisions, introducing confounding variables. To address this, future studies should control for individual overtaking events by isolating specific scenarios. For example, carefully staged setups or virtual simulations could allow researchers to capture single overtaking actions without additional distractions, thereby providing a clearer understanding of specific overtaking initiation behaviors across micromobility types.
3. **Data Collection Challenges:** Several technical issues impacted data quality and analysis:
    - **Camera Positioning:** Non-vertical camera placements, combined with the absence of calibration images, led to edge distortions that compromised visual data accuracy. Future research should prioritize comprehensive camera calibration, possibly using pre-calibration with a chessboard or software that automatically corrects distortions. Advanced video processing tools, such as motion-capture software, could further enhance data fidelity.
    - **Equipment Setup:** Extended multi-camera recordings highlighted the need for more robust data capture systems. To address issues such as data loss during transfer and the need for frequent camera synchronization, future studies could use high-performance setups, including Power over Ethernet (PoE) collect station and backup systems to preserve data integrity. Real-time monitoring of data collection could further ensure recording reliability.
    - **IMU Data Collection:** Incorrect sensor placement on the e-scooter's stems led to incorrect roll rate and angle measurements, as the data did not reflect the travel direction. Future research should focus on calibrating and securing IMU devices in a way that aligns the sensor measurements with the vehicle's travel direction, ensuring that the roll rate and angle data are consistent with the e-scooter's actual movement. Testing and validating sensor orientation and placement prior to data collection can help improve the accuracy of dynamic measurements for micromobility vehicles.
4. **Data Processing and Analysis:** Although this study developed a novel video data processing pipeline, further refinements could improve robustness. Future research should enhance this pipeline, specifically targeting improvements in distortion correction and multi-camera trajectory merging. Applying machine learning algorithms for trajectory tracking and pattern recognition could yield deeper insights. Additionally, automated data alignment solutions could simplify the data processing workflow, supporting the scalability of future studies on micromobility interactions.

To build on these findings, future research should focus on:

1. Conducting cross-cultural studies in various micromobility markets to understand behavioral differences.
2. Designing experiments that isolate individual overtaking maneuvers to minimize external influences.

3. Enhancing data collection methodologies, with attention to camera calibration, sensor placement, and real-time equipment monitoring.
4. Developing sophisticated data processing techniques, such as machine learning-based trajectory analysis.
5. Exploring long-term studies on how rider behaviors evolve with increased exposure to different micromobility vehicles.

By addressing these limitations and implementing the recommended improvements, future research can contribute to a more comprehensive understanding of micromobility overtaking behaviors and inform the development of safety guidelines tailored to diverse rider groups and regions.

References

[1] Zoi Christoforou et al. “Who is using e-scooters and how? Evidence from Paris”. In: *Transportation research part D: transport and environment* 92 (2021), p. 102708.

[2] Michelangelo-Santo Gulino et al. “Exploring Performances of Electric Micro-Mobility Vehicles and Behavioural Patterns of Riders for In-Depth Accident Analysis”. In: *Designs* 5.4 (2021). ISSN: 2411-9660. URL: https://www.mdpi.com/2411-9660/5/4/66.

[3] Rijwiel en Automobiel Industrie Vereniging. *Number of electric bicycles sold in the European Union (EU-28) from 2006 to 2022 (in 1,000 units)*. Statista. Retrieved March 31, 2024, from https://www.statista.com/statistics/397765/electric-bicycle-sales-in-the-european-union-eu/. 2023.

[4] ZIV. *E-bike sales volume in Germany from 2011 to 2022*. Statista. Retrieved March 10, 2024. 2023. URL: https://www.statista.com/statistics/1265760/e-bikes-sold-number-germany/.

[5] Giulia Oeschger, Páraic Carroll, and Brian Caulfield. “Micromobility and public transport integration: The current state of knowledge”. In: *Transportation Research Part D: Transport and Environment* 89 (2020), p. 102628. ISSN: 1361-9209. DOI: https://doi.org/10.1016/j.trd.2020.102628. URL: https://www.sciencedirect.com/science/article/pii/S1361920920308130.

[6] Statistisches Bundesamt. *Number of pedestrian, cycling and e-scooter traffic crash injuries in Germany from 2019 to 2022, by mode*. Statista. Retrieved March 09, 2024. 2023. URL: https://www.statista.com/statistics/1399153/active-and-micro-mobility-traffic-crash-injuries-germany-by-mode/.

[7] GITNUX. *E-Bike Accident Statistics*. URL: https://gitnux.org/e-bike-accident-statistics/ (visited on 03/10/2024).

[8] E. M. J. Verstappen et al. “Bicycle-related injuries in the emergency department: a comparison between E-bikes and conventional bicycles: a prospective observational study”. In: *European Journal of Trauma and Emergency Surgery* 47.6 (2021), pp. 1853–1860. DOI: 10.1007/s00068-020-01366-5.

[9] Katja Schleinitz et al. “The German Naturalistic Cycling Study–Comparing cycling speed of riders of different e-bikes and conventional bicycles”. In: *Safety science* 92 (2017), pp. 290–297.

[10] Divera Twisk et al. “Speed characteristics of speed pedelecs, pedelecs and conventional bicycles in naturalistic urban and rural traffic conditions”. In: *Accident Analysis & Prevention* 150 (2021), p. 105940.

[11] Patrícia Baptista et al. “From on-road trial evaluation of electric and conventional bicycles to comparison with other urban transport modes: Case study in the city of Lisbon, Portugal”. In: *Energy Conversion and Management* 92 (2015), pp. 10–18.

[12] Marco Dozza, Giulio Francesco Bianchi Piccinini, and Julia Werneke. “Using naturalistic data to assess e-cyclist behavior”. In: *Transportation research part F: traffic psychology and behaviour* 41 (2016), pp. 217–226.

[13] Lu Han. “Perceived Risk of Interaction with E-Bikes”. Master’s thesis. Delft: Delft University of Technology, Oct. 2023. URL: http://resolver.tudelft.nl/uuid:8c9c976a-2ed6-45a6-b2bd-85e1dfb4ae60.

[14] Alejandra Sofía Fonseca-Cabrera et al. “Micromobility Users’ Behaviour and Perceived Risk during Meeting Manoeuvres”. In: *International Journal of Environmental Research and Public Health* 18.23 (2021). ISSN: 1660-4601. URL: https://www.mdpi.com/1660-4601/18/23/12465.

[15] Arthur James et al. “Comparison of Injuries Associated With Electric Scooters, Motorbikes, and Bicycles in France, 2019-2022”. In: *JAMA Network Open* 6.6 (June 2023), e2320960–e2320960. ISSN: 2574-3805. DOI: 10.1001/jamanetworkopen.2023.20960. eprint: https://jamanetwork.com/journals/jamanetworkopen/articlepdf/2806716/james_2023_oi_230620_1687536392.30391.pdf. URL: https://doi.org/10.1001/jamanetworkopen.2023.20960.

[16] A. James et al. “Comparison of Injuries Associated With Electric Scooters, Motorbikes, and Bicycles in France, 2019-2022”. In: *JAMA network open* 6.6 (2023), e2320960. DOI: 10.1001/jamanetworkopen.2023.20960. URL: https://doi.org/10.1001/jamanetworkopen.2023.20960.

[17] Matteo della Mura et al. “E-Scooter Presence in Urban Areas: Are Consistent Rules, Paying Attention and Smooth Infrastructure Enough for Safety?” In: *Sustainability* 14.21 (2022). ISSN: 2071-1050. DOI: 10.3390/su142114303. URL: https://www.mdpi.com/2071-1050/14/21/14303.

[18] Mohammed Hamad Almannaa et al. “A comparative analysis of e-scooter and e-bike usage patterns: Findings from the City of Austin, TX”. In: *International Journal of Sustainable Transportation* 15.7 (2021), pp. 571–579.

[19] Qingyu Ma et al. “E-Scooter safety: The riding risk analysis based on mobile sensing data”. In: *Accident Analysis & Prevention* 151 (2021), p. 105954.

[20] Rijksoverheid. *Welke regels gelden voor mijn elektrische fiets (e-bike)?* 2023. URL: https://www.rijksoverheid.nl/onderwerpen/fiets/vraag-en-antwoord/welke-regels-gelden-voor-mijn-elektrische-fiets-e-bike (visited on 03/12/2024).

[21] Himo Bikes. *E-Bike Laws in Europe, Specifically Germany*. 2023. URL: https://www.himobikes.com/blogs/news/e-bike-laws-in-europe-specifically-germany (visited on 03/12/2024).

[22] Euronews. *Electric scooters: What are the rules across Europe and where are injuries highest?* Sept. 2023. URL: https://www.euronews.com/next/2023/09/01/electric-scooters-what-are-the-rules-across-europe-and-where-are-injuries-highest (visited on 03/12/2024).

[23] Willem Vlakveld et al. “Traffic conflicts involving speed-pedelecs (fast electric bicycles): A naturalistic riding study”. In: *Accident Analysis & Prevention* 158 (2021), p. 106201.

[24] A. Gavriilidou et al. “Modelling cyclist queue formation using a two-layer framework for operational cycling behaviour”. In: *Transportation Research Part C: Emerging Technologies* 105 (2019), pp. 468–484. ISSN: 0968-090X. DOI: https://doi.org/10.1016/j.trc.2019.06.012. URL: https://www.sciencedirect.com/science/article/pii/S0968090X18318576.

[25] Alexandra Gavriilidou et al. “Large-Scale Bicycle Flow Experiment: Setup and Implementation”. In: *Transportation Research Record* 2673.5 (2019), pp. 709–719. DOI: 10.1177/0361198119839974. eprint: https://doi.org/10.1177/0361198119839974. URL: https://doi.org/10.1177/0361198119839974.

[26] Christina Garman et al. “Micro-Mobility Vehicle Dynamics and Rider Kinematics during Electric Scooter Riding”. In: Apr. 2020. DOI: 10.4271/2020-01-0935.

[27] Lucas Billstein and Christoffer Svernlöv. “Evaluating the Safety and Performance of Electric Micro-Mobility Vehicles: Comparing E-bike, E-scooter and Segway based on Objective and Subjective Data from a Field Experiment”. In: (2021).

[28] Alessio Violin. “Development of an experimental protocol fortesting new electric personal mobility vehicles”. PhD thesis. Politecnico di Torino, 2020.

[29] Sarosh I Khan and Winai Raksuntorn. “Characteristics of passing and meeting maneuvers on exclusive bicycle paths”. In: *Transportation research record* 1776.1 (2001), pp. 220–228.

[30] Xiaohong Chen, Lishengsa Yue, and Kui Yang. “Safety evaluation of overtaken bicycle on a shared bicycle path”. In: *Tongji Daxue Xuebao* 45.2 (2017), pp. 215–222.

[31] Cheng Wang et al. “Investigating the Factors Affecting Rider’s Decision on Overtaking Behavior: A Naturalistic Riding Research in China”. In: *Sustainability* 14.18 (2022), p. 11495.

[32] Marco Dozza et al. “How do different micro-mobility vehicles affect longitudinal control? Results from a field experiment”. In: *Journal of Safety Research* 84 (2023), pp. 24–32. ISSN: 0022-4375. DOI: https://doi.org/10.1016/j.jsr.2022.10.005. URL: https://www.sciencedirect.com/science/article/pii/S0022437522001591.

[33] Michelangelo-Santo Gulino et al. “Exploring performances of electric micro-mobility vehicles and behavioural patterns of riders for in-depth accident analysis”. In: *Designs* 5.4 (2021), p. 66.

[34] Fluid FreeRide. *Electric Scooter vs Electric Bike*. Accessed January 2022. URL: https://fluidfreeride.com/blogs/news/electric-scooter-vs-electric-bike#:~:text=the%20physical%20element.-,Speed%20%26%20Range,kph)%20than%20e%2Dbikes..

[35] Jay Todd et al. *Behavior of electric scooter operators in naturalistic environments*. Tech. rep. SAE Technical Paper, 2019.

[36] Sergio A Useche et al. “Validation of the Cycling Behavior Questionnaire: a tool for measuring cyclists’ road behaviors”. In: *Transportation research part F: traffic psychology and behaviour* 58 (2018), pp. 1021–1030.

[37] Sonja Haustein and Mette Møller. “E-bike safety: Individual-level factors and incident characteristics”. In: *Journal of Transport & Health* 3.3 (2016), pp. 386–394.

[38] Christos Gioldasis, Zoi Christoforou, and Régine Seidowsky. “Risk-taking behaviors of e-scooter users: A survey in Paris”. In: *Accident Analysis & Prevention* 163 (2021), p. 106427.

[39] Alfredo Garcia et al. “Effect of width and boundary conditions on meeting maneuvers on two-way separated cycle tracks”. In: *Accident Analysis & Prevention* 78 (2015), pp. 127–137.

[40] Dianchao Lin et al. “Phenomena and characteristics of moped-passing-bicycle on shared lanes”. In: *Proceedings of the TRB 93rd Annual Meeting Compendium of Papers*. Transportation Research Board of the National Academies. 2014.

[41] JP Schepers et al. “The safety of electrically assisted bicycles compared to classic bicycles”. In: *Accident Analysis & Prevention* 73 (2014), pp. 174–180.

[42] Jessica B Cicchino, Paige E Kulie, and Melissa L McCarthy. “Severity of e-scooter rider injuries associated with trip characteristics”. In: *Journal of safety research* 76 (2021), pp. 256–261.

[43] A Niska and J Eriksson. *Cycling accident statistics. Background information to the common policy strategy for safe cycling*. 2013.

[44] Hossameldin Mohammed, Alexander Y Bigazzi, and Tarek Sayed. “Characterization of bicycle following and overtaking maneuvers on cycling paths”. In: *Transportation research part C: emerging technologies* 98 (2019), pp. 139–151.

[45] Daniel García-Vallejo, Werner Schiehlen, and Alfonso García-Agúndez. “Dynamics, Control and Stability of Motion of Electric Scooters”. In: *Advances in Dynamics of Vehicles on Roads and Tracks*. Ed. by Matthijs Klomp et al. Cham: Springer International Publishing, 2020, pp. 1199–1209.

[46] Natalia Kovacsova et al. “Riding performance on a conventional bicycle and a pedelec in low speed exercises: Objective and subjective evaluation of middle-aged and older persons”. In: *Transportation research part F: traffic psychology and behaviour* 42 (2016), pp. 28–43.

[47] Yufei Yuan et al. “Investigating cyclist interaction behavior through a controlled laboratory experiment”. In: *Journal of transport and land use* 11.1 (2018), pp. 833–847.

[48] Margherita Pazzini et al. “New Micromobility Means of Transport: An Analysis of E-Scooter Users’ Behaviour in Trondheim”. In: *International Journal of Environmental Research and Public Health* 19.12 (2022). ISSN: 1660-4601. URL: https://www.mdpi.com/1660-4601/19/12/7374.

[49] Thiago Vinícius Louro et al. “Factors Influencing Lateral Distance and Speed of Motorized Vehicles Overtaking Bicycles”. In: *Transportation Research Record* 2677.7 (2023), pp. 51–61. DOI: 10.1177/03611981221150926. eprint: https://doi.org/10.1177/03611981221150926. URL: https://doi.org/10.1177/03611981221150926.

[50] Wikipedia contributors. *Real-time kinematic positioning — Wikipedia, The Free Encyclopedia*. [Online; accessed 17-June-2024]. 2024. URL: https://en.wikipedia.org/wiki/Real-time_kinematic_positioning.

[51] Mark Wagenbuur. *How Wide is a Dutch Cycle Path?* Accessed: 2024-09-15. 2011. URL: https://bicycledutch.wordpress.com/2011/06/30/how-wide-is-a-dutch-cycle-path/.

[52] David S. Moore and George P. McCabe. *Introduction to the Practice of Statistics*. W.H. Freeman, 2003.

[53] Dorine C Duives, Winnie Daamen, and Serge P Hoogendoorn. "State-of-the-art crowd motion simulation models". In: *Transportation research part C: emerging technologies* 37 (2013), pp. 193–209.

[54] P Knoppers, JWC van Lint, and SP Hoogendoorn. "Automatic stabilization of aerial traffic images". English. In: *TRB 2012 Annual Meeting Technical Papers*. Ed. by s.n. 91st Annual Meeting Transportation Research Board, TRB 2012 ; Conference date: 22-01-2012 Through 26-01-2012. Transportation Research Board (TRB), 2012, pp. 1–13. URL: http://www.trb.org/AnnualMeeting2012/AnnualMeeting2012.aspx.

[55] Victor L. Knoop and M.J. Wierbos. *Correction for Positions of Objects Tracked at Height*. Tech. rep. Accessed from personal document. Delft University of Technology, Mar. 2019.

[56] *MPEG transport stream*. https://en.wikipedia.org/wiki/MPEG_transport_stream. Accessed: 2024-09-21.

[57] *MP4 file format*. https://en.wikipedia.org/wiki/MP4_file_format. Accessed: 2024-09-21.

[58] Road Safety Knowledge Centre. *In-Depth Investigation of E-Scooter Performance*. Accessed: 2024-09-22. Road Safety Knowledge Centre, 2023. URL: https://www.roadsafetyknowledgecentre.org.uk/in-depth-investigation-of-e-scooter-performance-report/.

[59] Wikipedia contributors. *Generalized linear model — Wikipedia, The Free Encyclopedia*. [Online; accessed 17-October-2024]. 2024. URL: https://en.wikipedia.org/wiki/Generalized_linear_model.

[60] Wikipedia contributors. *Multivariate analysis of variance — Wikipedia, The Free Encyclopedia*. [Online; accessed 17-October-2024]. 2024. URL: https://en.wikipedia.org/wiki/Multivariate_analysis_of_variance.

[61] Yanzhi Lv and Yuanhao He. "Research on Lane-Changing Decision Making and Planning of Autonomous Vehicles Based on GCN and Multi-Segment Polynomial Curve Optimization". In: *Sensors* 24.5 (2024), p. 1439. DOI: 10.3390/s24051439. URL: https://doi.org/10.3390/s24051439.

[62] Electronics. "Implementation of an Autonomous Overtaking System Based on Time to Lane Crossing Estimation and Model Predictive Control". In: *Electronics* 10.2293 (2021). DOI: 10.3390/electronics10020293. URL: https://doi.org/10.3390/electronics10020293.

[63] World Electr. Veh. J. "Autonomous Vehicle Overtaking: Modeling and an Optimal Trajectory Generation Scheme". In: *World Electric Vehicle Journal* 15.9 (2024), p. 403. DOI: 10.3390/wevj15090403. URL: https://doi.org/10.3390/wevj15090403.

[64] Jens Rasmussen. "Skills, rules, and knowledge; signals, signs, and symbols, and other distinctions in human performance models". In: *IEEE transactions on systems, man, and cybernetics* 3 (1983), pp. 257–266.

[65] HandBrake Project. *HandBrake Features*. 2024. URL: https://handbrake.fr/features.php (visited on 09/21/2024).

[66] LI Yan et al. "Prediction of Bicycle Trajectory Considering Stressful Avoidance Behaviors". In: *Journal of Transportation Systems Engineering and Information Technology* 24.2 (2024), p. 149.

[67] Centre for Research CROW, Contract Standardization in Civil, and Traffic Engineering. *Sign Up for the Bike: Design Manual for a Cycle-Friendly Infrastructure*. Vol. 10. CROW Record. The Hague, Netherlands: Institute for Road Safety Research, 1994.

[68] Bart Veroude, Mark van Gurp, and Otto van Boggelen. *Geactualiseerde aanbevelingen voor de breedte van fietspaden 2022*. With contributions from various experts from government and consultancy agencies. Utrecht, Netherlands, 2022.

[69] Z. Zhang. "A flexible new technique for camera calibration". In: *IEEE Transactions on Pattern Analysis and Machine Intelligence* 22.11 (2000), pp. 1330–1334. DOI: 10.1109/34.888718.

A

Scenario, duration and schedule design

As the primary objective of this study is to examine the influence of two main attributes namely micromobility type and individual factors & experience. The latter has been addressed in the previous section through the participant selection process. For the former, the study design incorporates a range of intra-modal and inter-modal interactions to comprehensively capture the dynamics of overtaking behavior across different micromobility modes. The experimental scenarios include:

1. Two intra-modal interactions:
   (a) E-scooter (ES) vs. E-scooter (ES)
   (b) E-bike (EB) vs. E-bike (EB)
2. Two inter-modal interactions:
   (a) E-scooter (ES) vs. E-bike (EB)
   (b) E-bike (EB) vs. E-scooter (ES)

To broaden the scope of the study and provide a more comprehensive understanding of micromobility interactions, two additional combinations involving conventional bicycles (B) are also considered, which include:

1. Two inter-modal interactions involving conventional bicycles (B):
   (a) E-scooter (ES) vs. Bike (B)
   (b) E-bike (EB) vs. Bike (B)

This inclusion allows for comparative analysis between newer forms of micromobility and traditional cycling. The planned scenario runs and their specific properties are summarized in TableA.1. This table provides a detailed overview of each overtaking combination, the modes involved, and the number of repetitions, offering a clear structure for the experimental design.

Sce No.	**Sce Name**	**Participating mode**			**Exp. duration (min)**
		ES	EB	B	
1	Overtaking-intra1	✓	-	-	12 x 4
2	Overtaking-intra2	-	✓	-	12 x 4
3	Overtaking-inter1	✓	✓	-	12 x 4
4	Overtaking-inter2	✓	✓	-	12 x 4
5	Overtaking-bike1	✓	-	✓	12 x 4
6	Overtaking-bike2	-	✓	✓	12 x 4

Table A.1: Table of Overtaking Scenarios and Experimental Details

The estimation of the duration of each scenario depends on several factors. One is the time it takes to run a lap. The second one is the number of samples(number of laps) that need to be collected for each participant. The final one is the minimum number of experiments necessary for each participant to complete this scenario.

For the time taken to complete a lap, considering that the average speed of the e-bike and e-scooter is around 15km/h and the maximum distance to complete a full lap is roughly 150 meters, it will take around 36 seconds to complete a lap, but taking into account the starting time, the probability of slowing down when turning, etc., a lap of one minute is taken. Each experimental participant needs to run four laps to collect four valid interactive actions. The expected duration for each scenario is presented in TableA.1, the actual duration might be less due to the fact that participant's riding would be scheduled in a consecutive order when conditions allow.

B

Data processing methodology

B.1. Image Correction

Image distortion correction is a vital step in the data processing workflow to ensure accurate spatial analysis of video footage. The primary objective of this correction is to transform the camera's perspective from a side view to a bird's-eye view—perpendicular to the center of the image from above. This transformation allows for precise measurements and analysis of movements within the video frames.

For this purpose, this study employed a tool called ImageTracker developed by Knoppers, van Lint, and Hoogendoorn [54]. The fundamental principle of this tool is to apply geometric transformations—stretching and rotating the image in multiple directions—to convert each frame of the video into a vertically downward view. This process effectively aligns the image plane with the ground plane, minimizing perspective distortion and facilitating accurate trajectory extraction.

Ideally, image distortion correction should also address lens distortions such as barrel distortion, which is common in wide-angle lenses. The chessboard algorithm bt Zhang [69] are typically used for this purpose, requiring images of chessboard patterns at different angles to calculate the correction matrix. However, this study did not incorporate barrel distortion correction due to two primary reasons:

1. Lack of Calibration Images: The data collected did not include the necessary calibration images required for methods like the chessboard algorithm.
2. Focus on Relative Variables: The study concentrates on overtaking behavior, analyzing relative variables such as speed difference and position. Since these variables are less affected by edge distortions, the impact of barrel distortion on the data analysis is minimal.

Despite this, we acknowledge that including barrel distortion correction could enhance the accuracy of the results and remains an area for future improvement.

An essential aspect of the methodology is the conversion of pixel-based trajectories into real-world units (meters). The ImageTracker tool facilitates this by calculating the actual distance represented by each pixel in the image. This involves determining a scale factor based on known measurements within the scene, such as the size of standard floor tiles.

The scale parameter is an average value, which is calculated by manually counting the number of standard-sized floor tiles and determining the total physical length in the X direction, then dividing it by the pixel length in the X direction. The scale factors in the X and Y directions for videos recorded by the same camera should be consistent. In this study, the same scale factor was used for both directions, and the reasonableness of using the same value was proven in the subsequent accuracy verification step.

In addition to the scale parameter, distortion correction involves several other angle parameters. These angles include:

1. Rotation Angle : This is the angle used to rotate the image or the coordinate grid around the center of the image in the plane of the image (2D rotation).
2. WedgeX Angle: This represents a perspective transformation applied along the X-axis (horizontal axis). The wedgeX angle adjusts how the scene appears to tilt toward or away from the viewer along the horizontal direction.
3. WedgeY Angle: This angle is similar to wedgeX, but it applies the transformation along the Y-axis (vertical axis). The wedgeY adjusts the perspective effect as if the scene is tilted up or down

The determination of these parameters is a relatively manual process. Firstly, the Imagetracker is modified to display the comparison between the corrected image and the original image after entering different parameters. Through repeated parameter testing, the best set of parameters was selected for each camera.

B.2. Height Projection

The forth step involves height projection. The reason for performing height projection is that when a camera captures images from an elevated position, objects in the image appear closer to the camera than their actual positions. Correction is necessary to obtain the true positions of the objects. The height projection method employed in this study is based on the approach developed by Knoop and Wierbos [55].

B.2.1. Algorithm

The algorithm processes each point in the trajectory data sequentially:

It first calculates the relative distance R between the object's position and the camera's position in the ground plane using the Pythagorean theorem:

$$R = \sqrt{(x - A)^2 + (y - B)^2} \tag{B.1}$$

Where (X, Y) represents the wrong unprocessed coordinates, and (A, B) represents the camera coordinates.

The algorithm then computes a corrected distance r, which represents the true ground distance that accounts for the height of the object:

$$r = \frac{(H - h) \cdot R}{H} \tag{B.2}$$

This correction is based on the principle of similar triangles, where the ratio of the corrected distance to the observed distance is equal to the ratio of the height difference between the camera and object to the camera height.

Finally, the corrected x and y coordinates (X and Y) are calculated:

$$X = (x - A) \cdot \frac{r}{R} + AY = (y - B) \cdot \frac{r}{R} + B \tag{B.3}$$

These equations adjust the position of the object proportionally based on the ratio of the corrected distance to the observed distance, maintaining the object's relative position with respect to the camera's ground position.

The principle of this method is also illustrated in figureB.1(a) and figureB.1(b).

B.3. Algorithms by the author

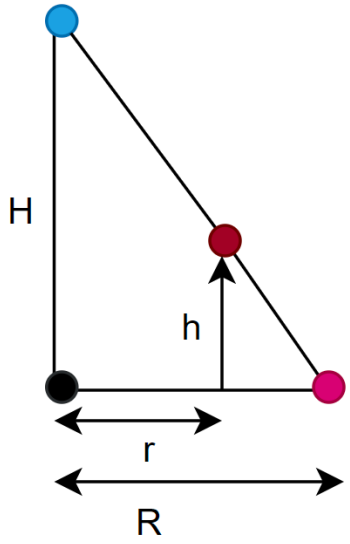

((a)) Side view of camera and observed object

Note: The blue dot represents the camera position in from side view

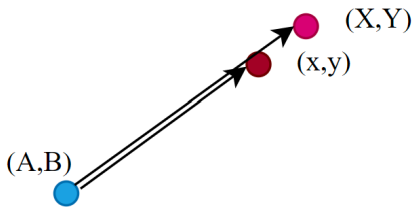

((b)) Top view of camera and observed object

Note: The black dot indicates the camera position in the top view.

Figure B.1: Top and side view of tracked object from study[55]

Algorithm 1 Combine matching trajectories from two videos

Input: Trajectory data from previous video $\mathbf{P}$, Trajectory data from current video $\mathbf{C}$, Distance threshold D, Time threshold T
Output: Merged trajectories $\mathbf{M}$

$\mathbf{M} = \emptyset$
prevIDs $=$ unique$(\mathbf{P}[ID])$
currIDs $=$ unique$(\mathbf{C}[ID])$
for all prevID $\in$ prevIDs **do**
  prevTraj $= \mathbf{P}[\mathbf{P}[ID] ==$ prevID$]$
  prevFrame $=$ lastFrame$($prevTraj$)$
  for all currID $\in$ currIDs **do**
    currTraj $= \mathbf{C}[\mathbf{C}[ID] ==$ currID$]$
    currFrame $=$ firstFrame$($currTraj$)$
    distance $= \sqrt{(\text{currFrame}[x] - \text{prevFrame}[x])^2 + (\text{currFrame}[y] - \text{prevFrame}[y])^2}$
    timeDiff $=$ currFrame$[time]$ $-$ prevFrame$[time]$
    if distance $\leq D$ **and** $0 <$ timeDiff $\leq T$ **then**
      interpFrames $=$ linearInterpolation$($prevFrame, currFrame, timeDiff$)$
      mergedTraj $=$ concatenate$($prevTraj, interpFrames, currTraj$)$
      Add mergedTraj to $\mathbf{M}$
    end if
  end for
end for
if $\mathbf{M} == \emptyset$ **then**
  Output warning: ”No matching trajectories found”
end if
return $\mathbf{M}$

Algorithm 2 Handling split trajectories by shallow Algorithm

Input: Trajectory data $\mathbf{D}$ (containing ID, x, y, time for each point), Spatial threshold S_{th}, Temporal threshold T_{th}
Output: Merged and interpolated trajectory data $\mathbf{D}'$

$\mathbf{D}' = \mathbf{D}$, merged_pairs $= \emptyset$
for all id$_i \in$ unique IDs in $\mathbf{D}$ **do**
  $(x_i, y_i, t_i) =$ the second last point of trajectory id$_i$
  for all id$_j \in$ next two unique IDs after id$_i$ **do**
    $(x_j, y_j, t_j) =$ the second point of trajectory id$_j$
    $\Delta s = \sqrt{(x_j - x_i)^2 + (y_j - y_i)^2}$
    $\Delta t = t_j - t_i$
    if $\Delta s \leq S_{th}$ **and** $0 < \Delta t \leq T_{th}$ **then**
      interpolated_points $=$ linear_interpolation$((x_i, y_i, t_i), (x_j, y_j, t_j))$
      $\mathbf{D}' =$ update_trajectories$(\mathbf{D}', \text{id}_i, \text{id}_j, \text{interpolated_points})$
      merged_pairs $=$ merged_pairs $\cup \{(\text{id}_i, \text{id}_j)\}$
    end if
  end for
end for
$\mathbf{D}' =$ remove_duplicate_timestamps$(\mathbf{D}')$
$\mathbf{D}' =$ reassign_trajectory_ids$(\mathbf{D}')$
return $\mathbf{D}'$

Algorithm 3 Jump Point Detection and Separation

Input:
$D = \{(id_i, x_i, y_i, t_i, traj\_id_i) \mid i = 1, \ldots, n\}$: trajectory data, where i is order of a point on a trajectory with n points
d_{th}: distance threshold
Output:
D': updated trajectory data
Initialize $D' = D$
Let $T = \{traj\_id_i \mid (id_i, x_i, y_i, t_i, traj\_id_i) \in D\}$
$new\_id = \max(T) + 1$
for each $j \in T$ **do**
  Let $P_j = \{(id, x, y, t, traj\_id) \in D' \mid traj\_id = j\}$
  for $k = 1$ to $|P_j| - 1$ **do**
    $d_k = \sqrt{(x_{k+1} - x_k)^2 + (y_{k+1} - y_k)^2}$
    if $d_k > d_{th}$ **then**
      for all $m > k$ **do**
        Update (id_m, x_m, y_m, t_m, j) to $(id_m, x_m, y_m, t_m, new\_id)$ in D'
      end for
      $new\_id = new\_id + 1$
    end if
  end for
end for
return D'

Algorithm 4 Interpolation after jump point split

Input:

$D' = \{(id_i, x_i, y_i, t_i, traj\_id_i) \mid i = 1, \ldots, n\}$: trajectory data from the output of algorithm 4
T_{th}: time threshold
D_{th}: distance threshold
Y_{th}: Y-coordinate threshold

Output:

D'': merged and interpolated trajectory data
Initialize $D'' = \emptyset$
Let $T = \{traj\_id_i \mid (id_i, x_i, y_i, t_i, traj\_id_i) \in D'\}$
for each $j \in T$ **do**
  Let $P_j = \{(id, x, y, t, traj\_id) \in D' \mid traj\_id = j\}$
  $p_{end} = (x_{end}, y_{end}, t_{end})$ where $t_{end} = \max(\{t \mid (id, x, y, t, j) \in P_j\})$
  Find $k \in T \setminus \{j\}$ that minimizes:
    $\sqrt{(x_{start} - x_{end})^2 + (y_{start} - y_{end})^2}$
  subject to:
    $t_{start} - t_{end} \leq T_{th}$
    $\sqrt{(x_{start} - x_{end})^2 + (y_{start} - y_{end})^2} \leq D_{th}$
    $|y_{start} - y_{end}| \leq Y_{th}$
  where $(x_{start}, y_{start}, t_{start})$ is the first point in P_k
  if such k exists **then**
    Interpolate between p_{end} and $(x_{start}, y_{start}, t_{start})$
    $P_{merged} = P_j \cup$ interpolated points $\cup P_k$
    Add P_{merged} to D''
  else
    Add P_j to D''
  end if
end for
for each trajectory P in D'' **do**
  Remove duplicate time points from P
end for
return D''

Algorithm 5 Pairwise Trajectory Matching and Merging (using R1 and R2 as example)

Input:
D_{R1}: trajectory data for Camera R1 (containing X, Y, Time, ID)
D_{R2}: trajectory data for Camera R2 (containing X, Y, Time, ID)
T_{th}: time threshold (maximum allowable time difference for matching)
Output:
D': merged and matched trajectory data
CalculateAvgVelocity($trajectory$**,** $start\_time$**,** end_time**):**
Extract all points in $trajectory$ between $start\_time$ and end_time
Calculate total distance between these points
Calculate time difference ($end\_time - start\_time$)
return average velocity (total distance / time difference)
Load trajectory data D_{R1} and D_{R2}
Extract unique IDs from D_{R1} and D_{R2}
Initialize empty lists: $new\_trajectories$, $matched\_ids$, $match\_details$
for each unique ID i in D_{R1} **do**
  if i not in $matched\_ids$ **then**
    Extract current trajectory data $T_{R1,i}$ from D_{R1}
    $last\_point_R1 =$ last point of $T_{R1,i}$
    $t2 = last\_point_R1.time$
    Step 1: Calculate R1 Velocity (Last 0.5s)
    $t1 = t2 - 0.5$ {Find start time for the last 0.5s in R1}
    $v_{R1,i} =$ **CalculateAvgVelocity**($T_{R1,i}$, $t1$, $t2$)
    $best\_match = NULL$
    $min\_distance_1 = \infty$
    $min\_distance_2 = \infty$
    $min\_speed\_diff = \infty$
    Step 2: Find Best Match in R2
    Find all trajectories in D_{R2} containing $t2'$, the time closest to $t2$
    Initialize list $candidate\_matches$
    for each trajectory $T_{R2,j}$ in D_{R2} containing $t2'$ **do**
      $first\_point_R2 =$ point in $T_{R2,j}$ closest to $t2$
      $spatial\_dist =$ distance between $last\_point_R1$ and $first\_point_R2$
      Step 3: Calculate R2 Velocity (Next 0.5s from Matching Point)
      $t2' = first\_point_R2.time$
      $t3 = t2' + 0.5$ {Find end time for the next 0.5s in R2}
      $v_{R2,j} =$ **CalculateAvgVelocity**($T_{R2,j}$, $t2'$, $t3$)
      $speed\_diff = |v_{R1,i} - v_{R2,j}|$
      Add ($T_{R2,j}$, $spatial\_dist$, $speed\_diff$) to $candidate\_matches$
    end for
    Step 4: Select the Best Match
    Sort $candidate\_matches$ by $spatial\_dist$ and retain the two closest trajectories
    From the two closest, select the trajectory with the smallest $speed\_diff$
    $best\_match =$ selected trajectory $T_{R2,j}$
    if $best\_match$ is not NULL **then**
      Add i and $best\_match$ to $matched\_ids$
      $t2' =$ time in $best\_match$ closest to $t2$
      Step 5: Trajectory Merging
      Remove all points in $T_{R2,j}$ before $t2'$
      Shift remaining points in $T_{R2,j}$ to connect with $T_{R1,i}$
      Merge $T_{R1,i}$ and remaining $T_{R2,j}$
      Add merged trajectory to $new\_trajectories$
    end if
  end if
end for
Combine all trajectories in $new\_trajectories$
return D'

Algorithm 6 Three Camera Trajectory Merge Algorithm

Input:
$data\_r1\_r2$: trajectory data from R1-R2 cameras
$data\_r2\_l1$: trajectory data from R2-L1 cameras
Output:
$merged\_df$: merged trajectory data
Initialize $all\_trajectories = \emptyset$
$final\_id = 1$
for each unique New_ID ($id1$) in $data\_r1\_r2$ **do**
  Extract R1 and R2 data for $id1$ from $data\_r1\_r2$
  if R2 data is empty **then**
    continue
  end if
  $old\_id\_r2 =$ R2 data's Old_ID
  $r1\_end\_time = \max(Time)$ from R1 data
  Find matching R2L1 trajectory in $data\_r2\_l1$ using old_id_r2
  if no matching R2L1 trajectory found **then**
    continue
  end if
  $r2l1\_id =$ matching R2L1 trajectory's New_ID
  Extract R2 and L1 data from $data\_r2\_l1$ for $r2l1\_id$
  Trim R2 data to keep only points after $r1\_end\_time$
  if trimmed R2 data is empty **then**
    continue
  end if
  Add $id1$ to $used\_r1r2\_ids$
  Add $r2l1\_id$ to $used\_r2l1\_ids$
  Calculate spatial offset:
    $r1\_end\_x, r1\_end\_y =$ R1 data coordinates at $r1\_end\_time$
    $data2\_start\_x, data2\_start\_y =$ first point of trimmed R2 data
    $shift\_x = data2\_start\_x - r1\_end\_x$
    $shift\_y = data2\_start\_y - r1\_end\_y$
  Apply spatial offset to trimmed R2 and L1 data
  Remove first point of trimmed R2 data
  Merge R1, trimmed R2, and L1 data
  Assign $final\_id$ to merged trajectory
  Append merged trajectory to $all\_trajectories$
  $final\_id = final\_id + 1$
end for
$merged\_df =$ concatenate $all\_trajectories$
return $merged\_df$

Algorithm 7 Stationary Point Smoothing in Trajectory

Input:
D: Trajectory data with columns [ID, X, Y, Time]
Output:
Updated D with smoothed stationary points
Calculate 'Distance' between consecutive points:
$Distance = \sqrt{(X_2 - X_1)^2 + (Y_2 - Y_1)^2}$
Identify stationary points:
$Stationary = (Distance = 0)$
for each point i in D **do**
  if $Stationary[i]$ is True **then**
    if i is not first or last point **then**
      $X[i] = (X[i-1] + X[i+1])/2$
      $Y[i] = (Y[i-1] + Y[i+1])/2$
    end if
  end if
end for

return Updated D

C

Implementation of experiment design

The contributions of the two Chinese teams were instrumental in the preparation and implementation of the study. Two main teams provided crucial support:

1. The Beijing Team: This group, affiliated with Beijing Jiaotong University, was primarily responsible for the equipment used in data collection for the experiment.
2. The Cangzhou Team: This team was from the university where the experimental site was located. For convenience, we refer to them as the Cangzhou team.

The roles of these teams were distinct and complementary: The Beijing Team's primary responsibility was to assist in acquiring various data collection devices and experimental vehicles. Their expertise in equipment and technical setup was crucial for ensuring the quality and reliability of the data collected.

The Cangzhou Team's contributions were multifaceted: They provided the experimental site Assisted in recruiting participants for the study Offered logistical support throughout the duration of the experiment

This collaborative approach was essential in overcoming the challenges posed by the author's geographical distance from the experimental site. It ensured that the study could be conducted efficiently and effectively, with local expertise complementing the author's research design. The specific contributions of each team at various stages of the experiment will be detailed in the subsequent sections. This breakdown will provide a comprehensive understanding of how the international collaboration facilitated the successful implementation of the research project, highlighting the importance of teamwork in conducting complex field experiments across geographical boundaries.

Of course, in addition to the two Chinese teams, my supervisor, Yufei also fully participated in the execution of the experiment and his contribution at every step was crucial.

C.1. Joint work on experiment location

In regards to the laying of the main track in the test site, it was two days before the start of the experiment. It was done by the author himself and the author's supervisor as well as people from two separate Chinese teams. We tape the ground together.The choice on the color is provided by the supervisor, while the purchase and taping is achieved together.

C.2. Joint work on vehicle selection

The acquisition of vehicles for the experiment involved a collaborative effort. This is done by the author and the two teams, with specific processes for different vehicle types. For e-scooters, the author selected the models, communicated with the Beijing team, who then ordered and shipped them to the experimental site, where the Cangzhou team received and stored them. Prior to the experiment, the author personally assembled, activated, and tested these e-scooters. The e-bikes, on the other hand, were sourced by the Beijing team through renting from students at Beijing Jiaotong University. They were then transported to the experimental site, where the author, along with a member of the Beijing

team, personally received and tested them. This collaborative approach in vehicle acquisition demonstrates the synergy between the author's research requirements and the local teams' resources and logistical capabilities, ensuring that all vehicles met the specific needs of the experiment and maintained consistency and reliability in the equipment used for data collection.

C.3. Joint work on participants recruitment

The recruitment of experimental participants was accomplished with the assistance of the Cangzhou team. The author of this study provided the recruitment requirements to the Cangzhou team based on the experimental design. Subsequently, the Cangzhou team utilized their internal educational network within their campus to recruit participants, adhering as closely as possible to the specified criteria. The Cangzhou team then furnished the author with the information of the recruited participants. Additionally, prior to the commencement of the experiment, they provided a classroom that allowed the author to brief the participants on the experimental procedures, ensuring that all participants were well-informed about their roles and the overall process before the trials began.

And the measure of the sitting or standing heights of each participant is a joint work by the author and the supervisor.

The design of the unique ID system is also jointly designed and achieved by the author and the supervisor.

The identification of trial participants was achieved through a unique combination of a special shape and a Roman numeral, as illustrated in FigureC.1(a) and FigureC.1(b).

This system served to indicate which pattern each trial participant belonged to. Following the assignment of these shape-numeral combinations, participants' names were replaced with these combinations to maintain anonymity. This unique identification is used for two main purposes: it facilitated the author's ability to distinguish participants by mode and vehicle during the experiment, enabled efficient monitoring throughout the trial, and aided in the subsequent attribution of individual characteristics to each trajectory data point during analysis. The specific details for E-bike and E-scooter participants are presented in their respective tables in the appendixF, providing a comprehensive overview of the participant demographics and their assigned identifiers.

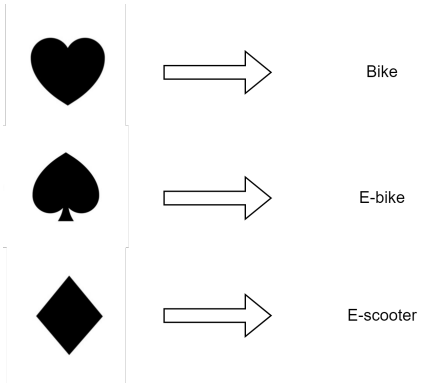

((a)) Special shape

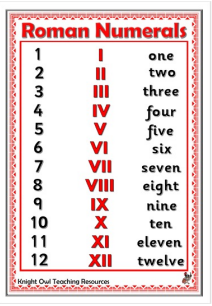

((b)) Roman numeral

Figure C.1: Two different shapes

C.4. Joint work on camera acquisition and setup

The acquisition and transport of the camera was done with the assistance of the Beijing team, with the authors of this paper receiving and testing at the test site. The setup of the cameras involved two main aspects: software configuration and hardware connection. The software configuration was primarily conducted by the author of this study over the three days preceding the experiment, individually setting up each camera. Some aspects of the setup, such as the choice of video recording software and IP address configuration, were based on the supervisor's experience. The adjustment of various camera parameters was guided by the Dahua product manual. The hardware connection phase, which included

assembling the cameras with their supports and mounting them onto the aerial truck, was completed with the assistance of members from the Beijing team.

C.5. Joint work on IMU acquisition

The Inertial Measurement Unit (IMU) devices were provided by the Beijing team. The setup of these IMU devices encompassed both software and hardware aspects. The software setup for the IMU was primarily handled by the Beijing team. This was due to their expertise with the control program, which they had developed based on the original program provided by the device manufacturer. Their extensive experience with the equipment made them the ideal choice for this task. Additionally, the author of this study requested that the IMU unit's time be synchronized with the computer's system time, a requirement that the Beijing team successfully implemented. The hardware setup consisted of two main components: preliminary testing and the actual installation and securing of the devices on the day of the experiment. Both of these tasks were also carried out by the Beijing team.

C.6. Joint work on Experiment Execution

During the entire experiment, the author of this thesis was primarily responsible for monitoring the experimental process, including keeping track of the number of overtaking maneuvers performed by each participant, controlling their entry into the main track, and answering any questions from the participants. The author's supervisor also assisted in the monitoring work, with his main task being to gather the participants for the next round as each round was about to end and to re-explain the experimental procedure to ensure a smooth transition between rounds and minimize waiting time. Throughout the process, two members of the Beijing team were responsible for monitoring the recording status of the two groups of cameras and promptly reporting any issues to the author and the author's supervisor. Two additional members from the Beijing team were mainly in charge of overseeing the data collection work of the IMU units. Furthermore, the Cangzhou team, responsible for the experimental site, provided extensive logistical support. Prior to the start of the experiment, they guided the aerial truck into the experimental site and provided power supply solutions, sun umbrellas, tables, chairs, and assistance with equipment transportation. During the experiment, members of the Cangzhou team helped with charging the electric scooters and provided emergency repairs for one of the electric bicycles that malfunctioned. The logistics team also provided the participants with ample beverages, food, and sun protection tools. Additionally, some of the participants themselves voluntarily helped with some of the site cleanup and equipment transportation tasks after the end of the experiment.

D

Accuracy validation

Table D.1: X Position validation

X Position at A	X Position at A+1s	Calculation Distance	Real Distance	Deviation	Percentage
13.01	10.97	2.04	2.2	0.16	0.072727273
14.02	11.83	2.19	2.4	0.21	0.0875
19.64	15.97	3.67	3.5	0.17	0.048571429
13.42	11.66	1.76	2.0	0.24	0.12
22.01	19.65	2.36	2.4	0.04	0.016666667
19.15	15.75	3.40	3.6	0.20	0.055555556
15.58	11.00	4.58	3.6	0.98	0.272222222
18.67	14.62	4.05	4.2	0.15	0.035714286
14.58	10.00	4.58	4.8	0.22	0.045833333
19.47	16.54	2.93	3.0	0.07	0.023333333
17.68	8.89	8.79	9.0	0.21	0.023333333
14.87	11.70	3.17	3.0	0.17	0.056666667
20.03	13.48	6.55	6.6	0.05	0.007575758
14.03	10.58	3.45	3.6	0.15	0.041666667
19.87	16.96	2.91	2.6	0.31	0.119230769
11.52	7.83	3.69	3.6	0.09	0.025
24.52	21.09	3.43	3.6	0.17	0.047222222
25.05	21.60	3.45	3.6	0.15	0.041666667
11.30	6.04	5.26	5.4	0.14	0.025925926
15.50	11.50	4.00	3.6	0.40	0.111111111
18.39	12.89	5.50	5.4	0.10	0.018518519
15.61	9.92	5.69	6.0	0.31	0.051666667
13.15	8.13	5.02	4.8	0.22	0.045833333
14.58	12.97	1.61	1.8	0.19	0.105555556
8.12	6.80	1.32	1.5	0.18	0.12
11.42	9.13	2.29	2.4	0.11	0.045833333
18.63	16.48	2.15	2.4	0.25	0.104166667
15.90	13.54	2.36	2.4	0.04	0.016666667
22.14	15.59	6.55	6.6	0.05	0.007575758
23.63	18.98	4.65	4.8	0.15	0.03125
Average			0.196		0.060819657

Table D.2: Y Position Data Analysis

X Position at A	X Position at A+1s	Calculation Distance	Real Distance	Deviation	Percentage
11.64	10.18	1.46	1.4	0.06	0.042857143
11.53	10.25	1.28	1.2	0.08	0.066666667
11.49	10.42	1.07	1.2	0.13	0.108333333
11.32	9.74	1.58	1.6	0.02	0.0125
11.22	9.74	1.48	1.4	0.08	0.057142857
11.82	10.66	1.16	1.2	0.04	0.033333333
11.50	10.06	1.44	1.5	0.06	0.04
11.57	10.25	1.32	1.2	0.12	0.1
11.44	10.32	1.12	1.2	0.08	0.066666667
11.70	10.31	1.39	1.2	0.19	0.158333333
13.45	12.14	1.31	1.2	0.11	0.091666667
13.20	12.09	1.11	1.2	0.09	0.075
12.99	11.57	1.42	1.6	0.18	0.1125
13.68	12.20	1.48	1.5	0.02	0.013333333
13.21	11.68	1.53	1.5	0.03	0.02
13.27	12.22	1.05	0.9	0.15	0.166666667
13.41	11.41	2.00	1.8	0.20	0.111111111
13.57	11.97	1.60	1.5	0.10	0.066666667
13.33	12.21	1.12	1.0	0.12	0.12
13.47	12.15	1.32	1.2	0.12	0.1
12.53	10.70	1.83	1.8	0.03	0.016666667
11.49	13.12	1.63	1.6	0.03	0.01875
11.23	12.03	0.80	0.7	0.10	0.142857143
12.51	11.05	1.46	1.5	0.04	0.026666667
12.20	11.22	0.98	0.8	0.18	0.225
11.22	11.40	0.18	0.0	0.18	
11.95	11.43	0.52	0.6	0.08	0.133333333
10.97	11.93	0.96	0.9	0.06	0.066666667
13.90	12.62	1.28	1.2	0.08	0.066666667
11.53	10.90	0.63	0.7	0.07	0.1
Average			0.094333333		0.077961433

E

TMA moving average method verfivation

The FigureE.1 compares the calculation of the four moving average methods when window size=10, and you can see that TMA has the smoothest effect. The FigureE.2 compares the TMA effect of different window sizes, you can see that the change from 10 to 15 is not so obvious, and 10 points is exactly 0.5s, from the choice of value is more reasonable to consider, and finally chose window size=10.

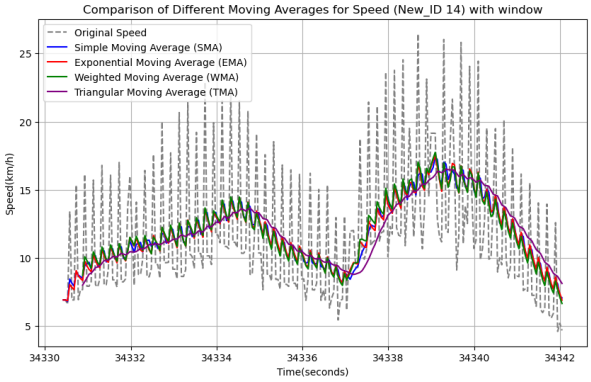

Figure E.1: Moving average methods Comparison

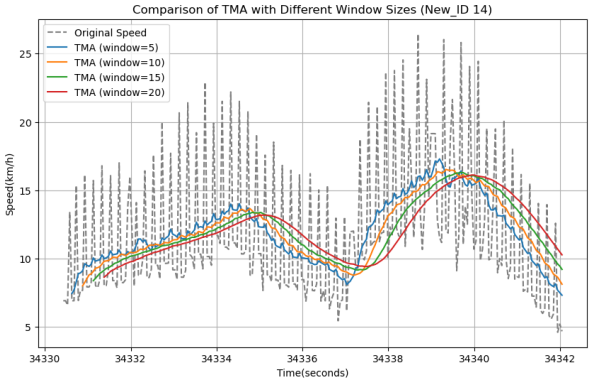

Figure E.2: Comparison of TMA with Different Window Sizes

F

Parameter tables during experiment implementation

Gender	Sitting Height (cm)	Category	Number	Group	Type of e-bike	IMU
Male	173	EB	1	Spade + I	Fat-ebike	
Male	168	EB	1	Spade + II	Fat-ebike	
Male	168	EB	1	Spade + III	Fat-ebike	
Male	168	EB	2	Spade + IV	Regular one	1
Male	168	EB	2	Spade + V	Regular one	1
Male	165	EB	2	Spade + VI	Regular one	1
Male	160	EB	3	Spade + VII	Regular one	
Female	158	EB	3	Spade + VIII	Regular one	
Female	157	EB	3	Spade + IX	Regular one	
Female	155	EB	4	Spade + X	Small wheel one	
Male	155	EB	4	Spade + XI	Small wheel one	
Female	154	EB	4	Spade + XII	Small wheel one	

Table F.1: E-bike riders group information

EB means E-bike; Spade is a shape of playcards; where IMU=1 means that that vehicle is equipped with IMU.

Gender	Standing Height (cm)	Category	Number	Group	IMU
Male	155	ES	1	Diamond I	
Female	165	ES	1	Diamond II	
Female	168	ES	1	Diamond III	
Female	151	ES	1	Diamond IV	
Male	167	ES	2	Diamond V	1
Male	168	ES	2	Diamond VI	1
Male	168	ES	2	Diamond VII	1
Male	174	ES	2	Diamond VIII	1
Male	152	ES	3	Diamond IX	
Male	161	ES	3	Diamond X	
Male	172	ES	3	Diamond XI	
Male	165	ES	3	Diamond XII	

Table F.2: E-scooter riders group information

Es means E-bike; Diamond is a shape of playcards; where IMU=1 means that that vehicle is equipped with IMU.

G

Data processing

Table G.1: RGB values for Red Cap

Parameter	Value
Hats.Color{1}	[230, 42, 69]
Hats.STD{1}	[21, 11, 19]

Table G.2: Detection Areas for Different Cameras

Case Number	Detection Area X Coordinates	Detection Area Y Coordinates
1	[0, 1920, 1920, 0]	[950, 1000, 670, 340]
2	[0, 1920, 1920, 0]	[400, 400, 900, 900]
3	[0, 1600, 1600, 0]	[300, 690, 1060, 850]
4	[0, 1000, 1920, 1920, 940, 0]	[600, 500, 360, 850, 1000, 1000]

Table G.3: R1 Video File Information with exact starting time

Filename	Frame Rate	Time Step	Frame Number	Exact Start Time
2024.05.26 08-40-05.mp4	19.98880383	0.050028006	3	08:40:06.900
2024.05.26 09-00-05.mp4	19.99306198	0.050017351	12	09:00:05.450
2024.05.26 09-23-54.mp4	19.98796236	0.050030112	17	09:23:56.200
2024.05.26 09-33-32.mp4	19.99100909	0.050022487	17	09:33:33.200
2024.05.26 09-53-32.mp4	19.9891001	0.050027265	6	09:53:33.750
2024.05.26 10-13-32.mp4	19.98808299	0.05002981	13	10:13:32.400
2024.05.26 10-33-32.mp4	19.99077759	0.050023067	19	10:33:33.100
2024.05.26 10-53-32.mp4	19.98980182	0.050025508	7	10:53:33.700

where the frame number in The video infromation tables is the number of frame when the time change from second i to i+1.

Table G.4: R2 Video File Information with exact starting time

Filename	Frame Rate	Time Step	Frame Number	Exact Start Time
2024.05.26 08-40-11.mp4	19.97845332	0.050053925	20	08:40:12.049
2024.05.26 08-58-05.mp4	19.99533532	0.050011664	11	08:58:05.500
2024.05.26 09-00-10.mp4	19.94594595	0.050135501	11	09:00:11.499
2024.05.26 09-00-37.mp4	19.96865204	0.050078493	10	09:00:37.549
2024.05.26 09-01-25.mp4	20.00580814	0.049985484	10	09:01:25.550
2024.05.26 09-03-11.mp4	19.98287019	0.050042861	9	09:03:13.600
2024.05.26 09-14-57.mp4	19.99104468	0.050022398	14	09:14:56.350
2024.05.26 09-34-57.mp4	19.98974757	0.050025644	21	09:34:55.999
2024.05.26 09-54-57.mp4	19.99046605	0.050023846	5	09:54:55.800
2024.05.26 10-14-57.mp4	19.98106778	0.050047375	11	10:14:57.500
2024.05.26 10-19-30.mp4	19.98697917	0.050032573	11	10:19:29.500
2024.05.26 11-18-55.mp4	18.70340929	0.053466188	20	11:18:54.984
2024.05.26 11-26-13.mp4	19.98366458	0.050040872	14	11:26:13.349

where the frame number in The video infromation tables is the number of frame when the time change from second i to i+1.

Table G.5: L1 Video File Information with exact starting time

Filename	Frame Rate	Time Step	Frame Number	Exact Start Time
2024.05.26 08-39-57.mp4	17.42634146	0.057384391	11	08:39:40.426
2024.05.26 08-58-33.mp4	19.97583736	0.05006048	10	08:58:32.549
2024.05.26 09-18-33.mp4	19.9741699	0.050064659	15	09:18:33.299
2024.05.26 09-38-34.mp4	19.97916753	0.050052135	2	09:38:33.950
2024.05.26 09-58-34.mp4	19.98250146	0.050043785	12	09:58:32.450
2024.05.26 10-18-34.mp4	19.97833514	0.050054221	3	10:18:32.900
2024.05.26 10-38-34.mp4	19.97666958	0.050058394	10	10:38:33.549
2024.05.26 10-58-34.mp4	18.38596491	0.054389313	15	10:58:33.239
2024.05.26 11-00-19.mp4	19.98444185	0.050038926	14	11:00:19.349
2024.05.26 11-03-03.mp4	19.97833694	0.050054216	2	11:03:02.950
2024.05.26 11-23-03.mp4	19.99025708	0.050024369	11	11:23:03.500

where the frame number in The video infromation tables is the number of frame when the time change from second i to i+1.

Table G.6: L2 Video File Information with exact starting time

Filename	Frame Rate	Time Step	Frame Number	Exact Start Time
2024.05.26 08-59-55.mp4	19.21655334	0.052038468	19	08:59:59.063
2024.05.26 09-19-55.mp4	18.77409664	0.05326488	15	09:19:59.254
2024.05.26 09-39-55.mp4	19.99248842	0.050018786	8	09:39:59.650
2024.05.26 09-59-55.mp4	19.99249937	0.050018759	3	09:59:57.900
2024.05.26 10-19-55.mp4	19.9874974	0.050031276	18	10:19:58.149
2024.05.26 10-39-55.mp4	19.98832798	0.050029197	12	10:39:58.450
2024.05.26 10-59-55.mp4	19.98762267	0.050030962	5	10:59:58.800
2024.05.26 11-09-40.mp4	19.98827961	0.050029318	2	11:09:44.950

where the frame number in The video infromation tables is the number of frame when the time change from second i to i+1.

Table G.7: R1 Camera Coordinates and objective height in height projection

Height	Camera X	Camera Y	Filename
1.8	-3.763855531	6.099179905	Orthorectification_Traj_2024.05.26 08-40-05_new_test.mat
1.68	-3.763855531	6.099179905	Orthorectification_Traj_2024.05.26 09-00-05_new_test.mat
1.74	-3.763855531	6.099179905	Orthorectification_Traj_2024.05.26 09-23-54_new_test.mat
1.74	-3.763855531	6.099179905	Orthorectification_Traj_2024.05.26 09-33-32_new_test.mat
1.6	-3.763855531	6.099179905	Orthorectification_Traj_2024.05.26 09-53-32_new_test.mat
1.65	-3.763855531	6.099179905	Orthorectification_Traj_2024.05.26 10-13-32_new_test.mat
1.73	-3.763855531	6.099179905	Orthorectification_Traj_2024.05.26 10-33-32_new_test.mat
1.8	-3.763855531	6.099179905	Orthorectification_Traj_2024.05.26 10-53-32_new_test.mat

where Orthorectification_Traj_2024.05.26 08-40-05_new_test.mat is the output of image correction

Table G.8: R2 Camera Coordinates and objective height in height projection

Height	Camera X	Camera Y	Filename
1.8	-0.26350166	1.055615153	Orthorectification_Traj_2024.05.26 08-40-11_new_test.mat
1.68	-0.26350166	1.055615153	Orthorectification_Traj_2024.05.26 08-58-05_new_test.mat
1.68	-0.26350166	1.055615153	Orthorectification_Traj_2024.05.26 09-00-10_new_test.mat
1.68	-0.26350166	1.055615153	Orthorectification_Traj_2024.05.26 09-00-37_new_test.mat
1.68	-0.26350166	1.055615153	Orthorectification_Traj_2024.05.26 09-01-25_new_test.mat
1.68	-0.26350166	1.055615153	Orthorectification_Traj_2024.05.26 09-03-11_new_test.mat
1.74	-0.26350166	1.055615153	Orthorectification_Traj_2024.05.26 09-14-57_new_test.mat
1.74	-0.26350166	1.055615153	Orthorectification_Traj_2024.05.26 09-34-57_new_test.mat
1.6	-0.26350166	1.055615153	Orthorectification_Traj_2024.05.26 09-54-57_new_test.mat
1.65	-0.26350166	1.055615153	Orthorectification_Traj_2024.05.26 10-14-57_new_test.mat
1.73	-0.26350166	1.055615153	Orthorectification_Traj_2024.05.26 10-19-30_new_test.mat
1.8	-0.26350166	1.055615153	Orthorectification_Traj_2024.05.26 11-18-55_new_test.mat

where Orthorectification_Traj_2024.05.26 08-40-05_new_test.mat is the output of image correction

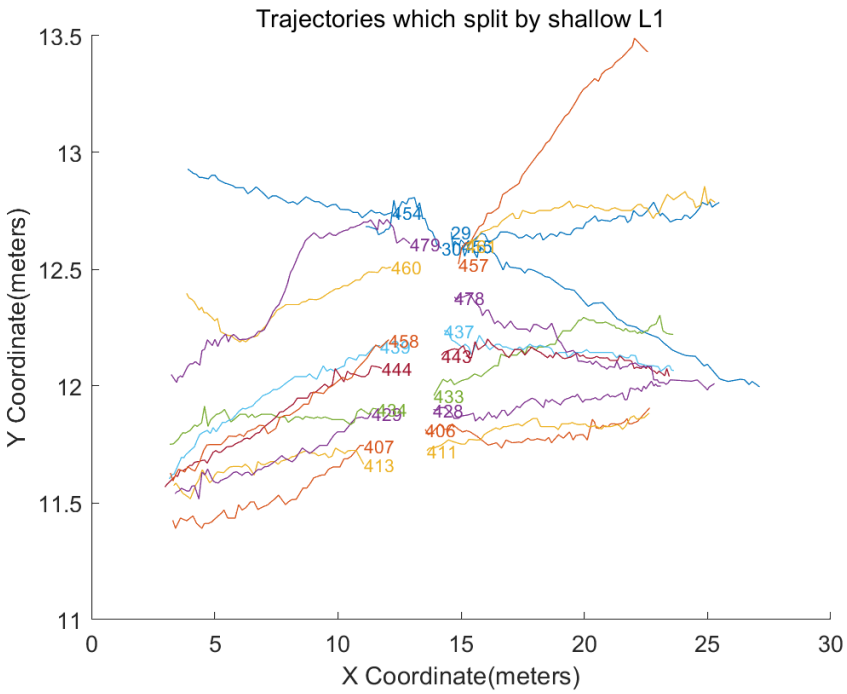

((a)) Trajectories split by shallow L1

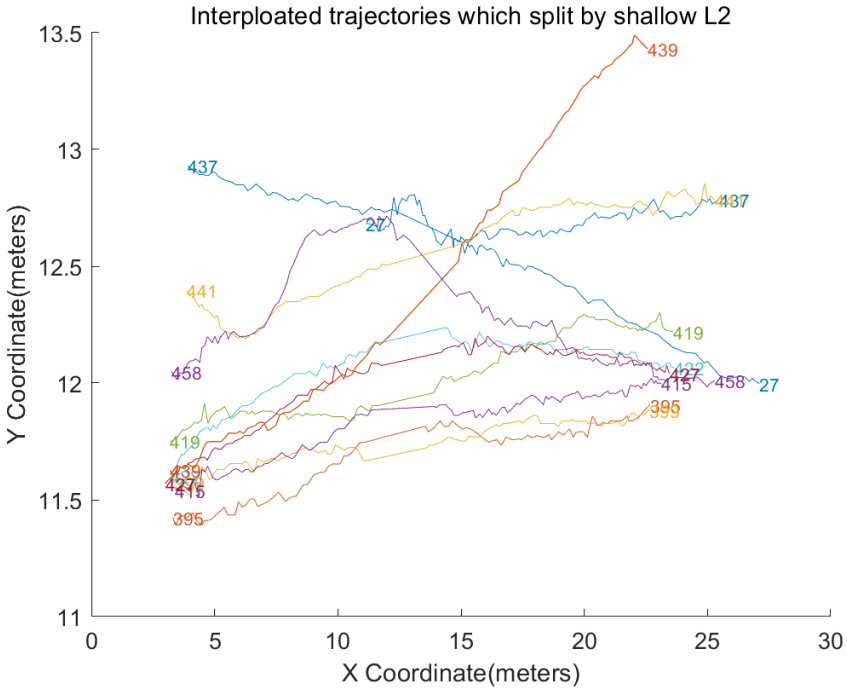

((b)) Interpolated trajectories split by shallow L1

Figure G.1: Handle shallow effect of L1 of camera L1

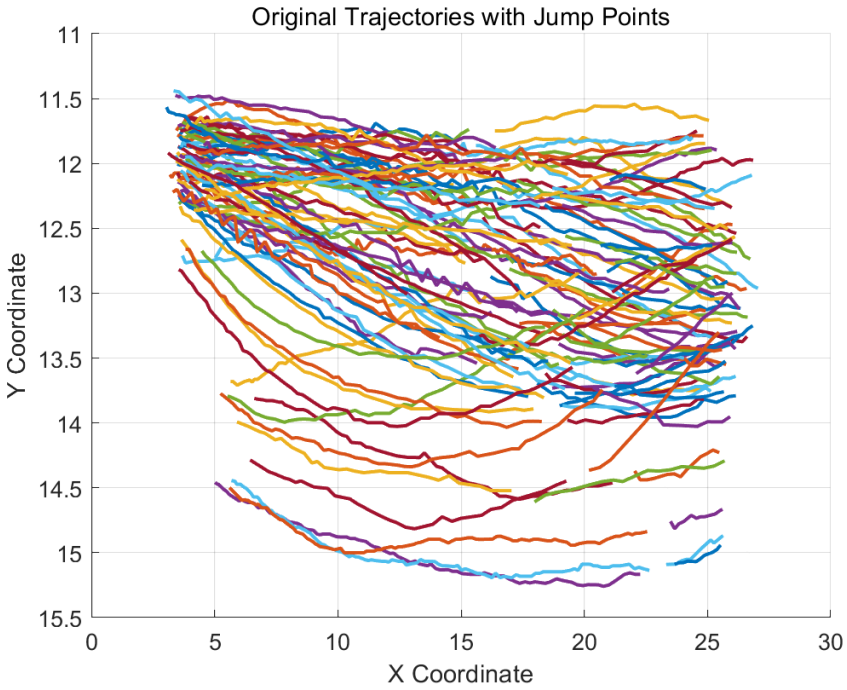

((a)) Original trajectories with jump points of L1

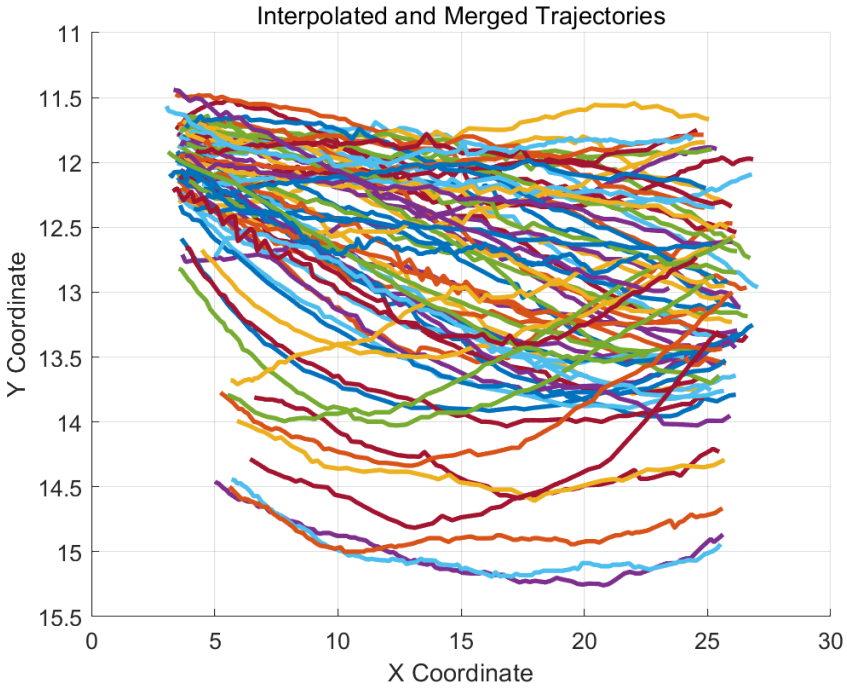

((b)) Interpolated and merged trajectories of L1

Figure G.2: Handle jump point effect of L1 of camera L1

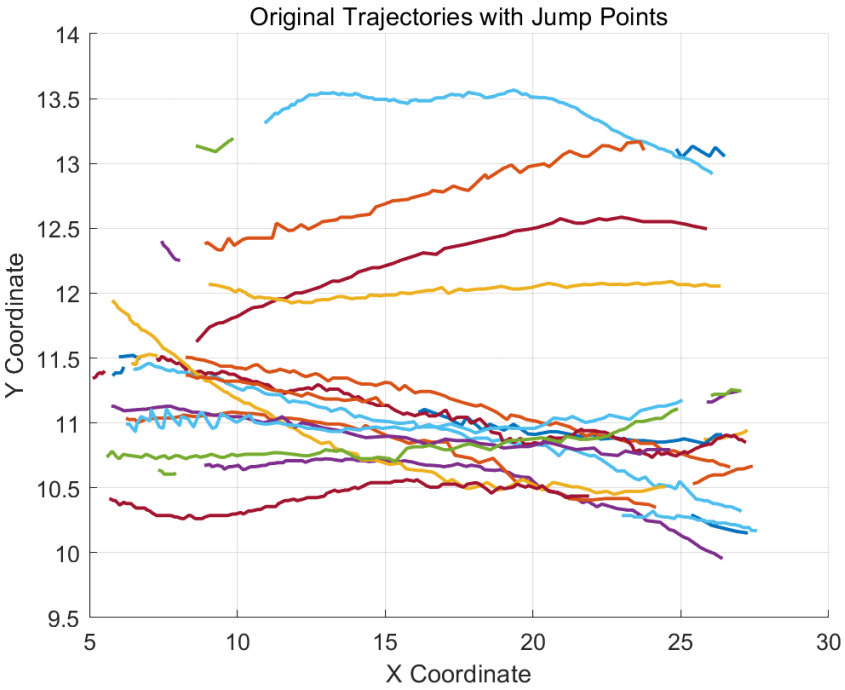

((a)) Original trajectories with jump points of L2

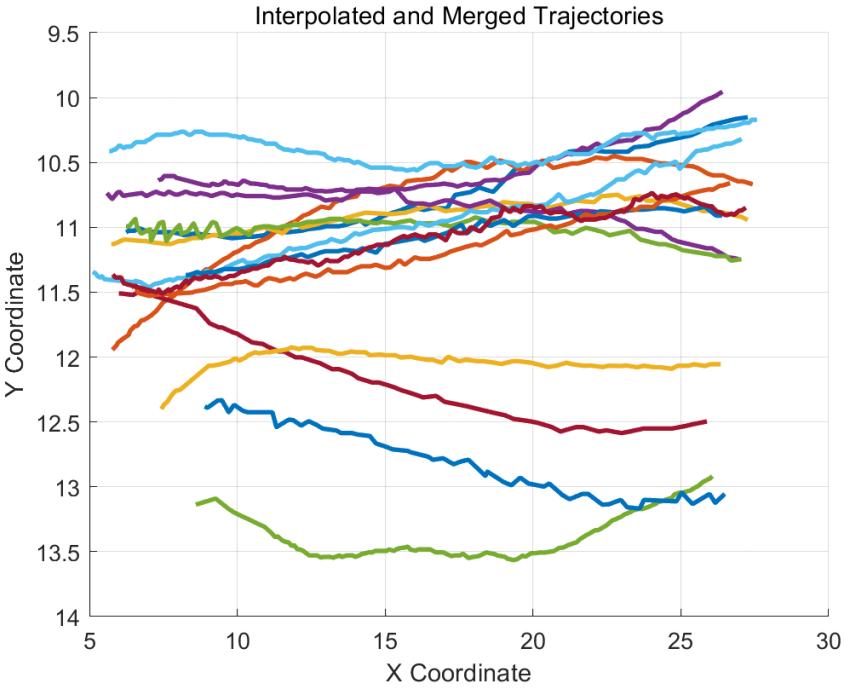

((b)) Interpolated and merged trajectories of L2

Figure G.3: Handle jump point of L2

A study on individual behavior of e-scooter and e-bike users during overtaking

Wenyi Zhang

Abstract

The increasing prevalence of micromobility vehicles in urban environments has raised concerns about safety in shared cycling spaces. This study examines the overtaking behavior of e-scooter and e-bike riders to inform traffic management strategies and infrastructure development. A controlled experiment was conducted using strategically placed cameras to track vehicle trajectories and inertial measurement units (IMUs) to capture roll data. Extensive data processing ensured accuracy and synchronization of trajectory and IMU information. Key findings reveal that e-bikes overtaking e-scooters initiate maneuvers from greater distances but maintain smaller lateral distances compared to e-bikes overtaking e-bikes. Lateral position differences showed a stronger correlation with speed difference than longitudinal position differences. The highest roll rates and angles occurred during the overtaking phase. Pre-overtaking, higher roll rates and angles were observed when e-bikes overtook other e-bikes, indicating greater control adjustments. No significant gender differences were found in overtaking behavior. However, in non-interactive scenarios, male e-scooter riders traveled at higher speeds than females, while no gender differences were observed among e-bike riders. These results provide insights into the complex interactions between different types of micromobility vehicles during overtaking maneuvers. The findings underscore the need for targeted safety interventions and infrastructure improvements to mitigate risks associated with shared cycling spaces, ensuring safer coexistence of micromobility users and conventional cyclists in urban environments.

Keywords: overtaking; micromobility rider; e-bike; e-scooter; video data; roll angle; roll rate

Introduction

The global proliferation of e-scooters and e-bikes has been accompanied by a significant rise in incidents and injury risks, exceeding those associated with traditional bicycles. Despite their distinct dynamics, these vehicles often share the same bike lanes under similar regulations, potentially contributing to an increased number of accidents. Understanding the microscopic behavior of e-bike and e-scooter users interacting with conventional bicycles is essential for enhancing safety on shared paths [1, 2]. E-scooters and e-bikes have surged in popularity in recent years due to decreasing costs, improved motor efficiency, and an emphasis on sustainability [3, 4]. The European Union experienced a significant growth in e-bike sales, reaching 5.3 million units in 2022, up from 854,000 units in 2012, with Germany being the largest market [4]. The rapid expansion of e-scooter services also exemplifies the growing adoption of micromobility, with companies like VOI recording millions of rides by 2020 [5].

However, the increasing prevalence of these vehicles is associated with heightened safety risks. In Germany, injuries among e-bike users rose from 10,505 in 2019 to approximately 22,500 in 2022 [6]. E-bike users face a higher likelihood of thoracic trauma compared to traditional cyclists, due to factors such as their higher speed and increased mass [7, 8]. E-scooters face additional risks, including instability on uneven surfaces due to smaller wheels and stand-up posture, which contributes to elevated ac-

cident rates [9, 10]. Despite these differences, regulatory frameworks often treat e-bikes and e-scooters similarly to conventional bicycles. For example, in many European countries, they are mandated to use bike lanes originally designed for non-motorized bicycles, which can increase safety risks for all users [11, 12]. The safety of these shared paths is largely dependent on understanding the individual behavior of micromobility users, particularly in their interactions with other cyclists. This behavior encompasses both mental decision-making (e.g., path choice) and physical control actions (e.g., steering and body positioning) [8, 13].This study specifically focuses on the overtaking behavior of micromobility users. Overtaking is a critical behavior in mixed traffic flows, especially given the lower visibility and smaller size of e-scooters and e-bikes. It often leads to conflicts that can compromise the safety of bike lanes, making overtaking maneuvers an important focus for improving shared infrastructure [14, 15]. Investigating overtaking behavior aids in determining appropriate bike lane width, informs traffic modeling, and supports safety assessments [10].

The objective of this study is to analyze the overtaking behavior of micromobility users, specifically e-bikes and e-scooters, during interactions with other cyclists. The first step involved a literature review to identify the types of data needed for understanding micromobility overtaking behavior. Subsequently, a comprehensive data collection methodology was developed, focusing on sensor placement, calibration, and minimizing confounding variables during data collection. The conceptual model integrates influencing factors, decision-making processes, and observable control actions. Finally, statistical analysis was used to examine the influence of different combinations of micromobility vehicles and rider characteristics.

Literature review

The literature review summarized current research, identifying individual factors influencing behavior and developing a rough conceptual model for data collection.

Micro-mobility type

Studies have assessed the safety, stability, maneuverability, and comfort of micromobility vehicles. A study revealed that although e-bikes and e-scooters offer superior rider comfort and stability, e-scooters tend to fall short in terms of safety due to inadequate braking performance [16]. Additionally, when compared to bicycles, both e-scooters and other similar micro-mobility devices like Segways also demonstrate inferior braking capabilities, where bicycles are considered to be more stable and safer [17].

Regarding speed, e-bikes and e-scooters generally achieve higher maximum and average speeds than traditional bikes, particularly in conditions that allow the right of way or involve inclines. This capability enhances their overtaking potential but also increases the risks associated with high-speed travel. Studies in different urban settings have shown that while e-scooters often match or slightly exceed the average travel speeds of bicycles, their ability to accelerate more quickly necessitates shorter response times to avoid hazards [18, 19, 20, 21, 22].

Moreover, e-bikes tend to have more conflicts with motorized vehicles than conventional bikes due to their higher speeds and different interaction dynamics with other road users. The design, weight, and acceleration capabilities of e-bikes and e-scooters not only influence their overtaking behavior but also impact how pedestrians and other cyclists perceive and react to these vehicles. For instance, e-bike riders are more likely to undertake overtaking maneuvers, followed by riders of human-powered tricycles and traditional bicycles [23, 24].

Demographic and experience

Various demographic factors, such as gender, age, and riding experience, influence the riding

behavior of cyclists beyond just safety and violations. Gender, for instance, plays a significant role in shaping cyclists' behavior, with male riders exhibiting not only on increased violation rates but also higher speeds, more aggressive maneuvers compared to their female counterparts [18, 25, 24]. Men also tend to overtake more frequently, which impacts interactions with other cyclists and motorized vehicles.

Age is another important factor; younger riders are more likely to overtake frequently and ride at higher speeds. In contrast, older riders, particularly those over 60, tend to be more cautious due to balance issues and reduced physical agility, which is especially evident when handling heavier e-bikes [25, 26]. This age-related caution affects their overtaking frequency and distance maintained during overtaking.

Riding experience also has a notable impact. While one study found that cyclists with longer riding experience exhibit fewer violations [25], another study observed that frequent e-scooter users are more likely to develop risky behaviors [27]. Experienced riders tend to have better control over their vehicles, making them more comfortable in overtaking scenarios, whereas less experienced riders may be more hesitant and conservative in their behavior.

Infrastructure factors

Several studies consistently indicate that lane width affects the likelihood of overtaking maneuvers and meeting clearance. Wider lanes facilitate overtaking, while narrower lanes reduce lateral space and lead to more cautious riding behavior [24, 28].

The influence of obstacles and boundaries on cyclist behavior consistently shows that the presence of obstacles leads to more cautious riding behaviors.For example, obstacles positioned along the lane edges prompt cyclists to maintain lower clearances from these obstacles [10, 28]. Additionally, obstacles at handlebar height specifically have been found to increase braking behaviors, as riders become more cautious to avoid potential balance issues [28]. Thus, while different studies emphasize different cautious behaviors—either reducing clearance or increasing braking—the general trend remains that obstacles cause more cautious maneuvering.

Traffic conditions

Study[29] provided insights into how traffic density affects overtaking dynamics on shared lanes. In scenarios of low traffic density, overtaking maneuvers such as moped-passing-bicycle are observed to be more stable and less likely to encounter disturbances, allowing vehicles to return smoothly to their original lanes post-overtaking. Conversely, in conditions of high traffic density, overtaking becomes more complex and often results in incomplete maneuvers, where vehicles fail to return to their lanes promptly. This variation in traffic dynamics can lead to increased interactions and potential conflicts among road users.

Required data and information

Previous studies on bicycle overtaking behavior have primarily focused on collecting and analyzing trajectory data. Utilizing this fundamental trajectory information, researchers have further calculated more complex measurement indicators such as speed, lateral distance, longitudinal distance and speed difference to gain deeper insights into the behavioral patterns in environments like dedicated bicycle lanes [14, 29, 30, 31].

In addition to trajectory data, some studies employed roll rate and roll angle to compare the stability of different vehicle types in relatively simple task scenarios. The studies compared the absolute mean values of these parameters and the relationship between roll rate and steer rate[16, 32]. Another study [33] utilized these indicators to compare the differences between elderly and young riders. Roll angle refers to the rotational angle of an object along its longitudinal axis, as illustrated in the figure1 taken from [32].

All of the aforementioned indicators are directly relevant to understanding micromobility overtak-

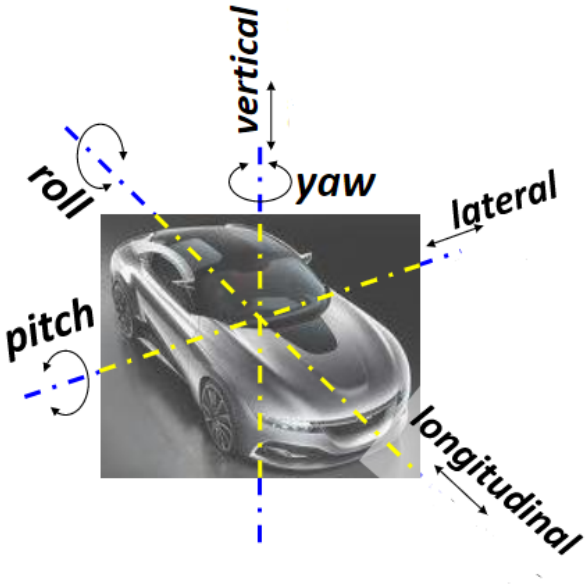

Figure 1: Reference system for the vehicles and directions names

ing behavior, particularly within the context of the decision-making(mental) layer and control action (physical) layer. The decision-making layer involves assessing and determining optimal speed, path selection, and maneuvering strategies to ensure a safe and effective overtaking process. Indicators like speed, speed difference, longitudinal distance, and lateral distance provide critical insights into these mental-level decisions. For instance, overtaking length and longitudinal distance are crucial for understanding path selection, while speed and speed difference reflect the strategies used for adjusting speed—key aspects of decision-making to ensure a safe overtaking maneuver. Lateral distance indicates the rider's avoidance behavior, reflecting safety considerations and decisions regarding adequate clearance from the overtaken vehicle. Roll rate and roll angle are also connected to the mental layer, as they reflect the rider's decisions regarding the extent of body posture adjustments.

Conceptual Model

And since the main research question of this study is to explore the influence of individual factors(gender) and the overtaken vehicle, the conceptual framework is built as shown in Figure2. The core of this conceptual framework in Figure2 revolves around a cyclical interaction between the decision-making(mental) layer and the action (physical) layer. This cycle captures the dynamic nature of the overtaking process for micromobility users.

1. Decision-Making Layer: Riders first make decisions at a mental level, where they assess the need for speed adjustments, path selection, and body action adjustment to ensure a safe overtaking maneuver.

2. Control Actions: These decisions are then executed physically through actions at the physical layer. These include actions like steering adjustments, acceleration, or even posture shifts, which directly affect the micromobility rider's position and movement in space.

3. Micro-Level Variables as Feedback: The result of these control actions is reflected in observable micro-level variables such as speed difference, lateral and longitudinal position differences, roll rate, and roll angle. These variables provide feedback on the success or necessity of further adjustments to the initial decisions.

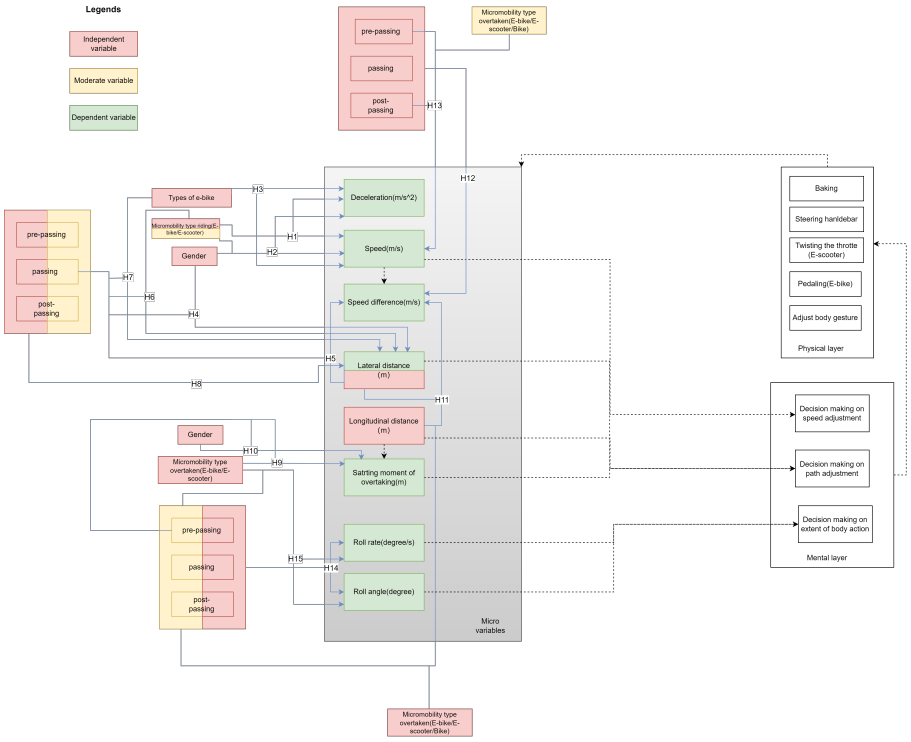

Figure 2: conceptual framework

4. Feedback to Decision-Making: This feedback loop enables the decision-making layer to constantly refine its strategies. The micro-level variables reflect the real-time state of the system, allowing for adjustments to be made, further feeding into control actions in a continuous loop.

In this model, the decision-making process informs actions, which are in turn reflected by micro-variables. These micro-variables provide feedback, creating a continuous cycle that ensures optimal and safe overtaking behavior. This cyclical interaction is fundamental to understanding how micromobility users navigate shared spaces during overtaking maneuvers.

Research methodology

The purpose of this study is to investigate the influence of individual factors and different combinations of micromobility modes on the operational riding behavior during interactive movements. These operational behaviors can be observed through a number of microscopic variables presented in Figure2. First, trajectory data is the necessary data used to study individual behavior. The trajectory data, which captures the position of the vehicle on a two-dimensional plane at specific times, could be used further to derive microscopic variables reflecting the behavior. Key variables include speed, speed difference, and longitudinal and lateral distance differences between vehicles. The accuracy of these variables is heavily dependent on the precision of the trajectory data. For meaningful analysis, the trajectory's precision should ideally be within a 10 cm range[34]. Besides, roll rate and roll angle should be collected to reflect stability. Furthermore, since this study involves different types of micromobility combinations, it is necessary to ensure the controllability of the vehicle combinations and to make sure that the targeted interaction movement takes place.

Data collection approach and equipment

The ability of isolating specific behaviors or conditions of laboratory settings allows for the replication of specific traffic scenarios, including various combinations of overtaking maneuvers between e-bikes, e-scooters, and conventional bicycles. Given the wide range of possible vehicle combinations and interactions, it is challenging to gather comprehensive and valid data through real-world observations. Therefore, a controlled experiment is determined to gather the data on the rider's behavior during overtaking. One of the drawbacks of using a controlled experiment, however, is that as the experiment progresses and the participants become more familiar with the tasks they are performing, as well as possibly with physical and psychological fatigue, the behaviors they exhibit in the experiment may change from what they were at the beginning of the experiment. although physical fatigue is less likely to be an issue for powered vehicles. This disadvantage is referred to as the learning effect. To mitigate the learning effect, it is crucial to minimize riding time, provide adequate rest periods, and ensure that participants engage in a variety of tasks throughout the experiment.

In this study, video extraction technique is used to extract the user's trajectory data. Based on the trajectory data, other measurement variables can be further extrapolated. There are several reasons for choosing cameras to collect data. First, we need to achieve trajectory data with an accuracy of approximately 10 cm. The two most common methods for collecting trajectory data are video extraction and GPS. To achieve this level of accuracy with GPS, high-precision GPS systems, typically classified as Real-Time Kinematic (RTK) GPS, are required. RTK GPS systems enhance the precision of position data using a combination of fixed base stations and mobile receivers[35]. These systems are not only more sophisticated but also significantly more expensive. Secondly, during the research process, there are often multiple vehicles on the track simultaneously, and to accurately capture the trajectory of each vehicle, multiple high-precision GPS devices are needed. In contrast, cameras can provide high-accuracy trajectory data at a lower cost, making them a more economical and practical choice. In this experiment, the Inertial Measurement Unit (IMU) was employed to measure the roll angle and roll rate of e-bikes and e-scooters. Research by [32, 16] used roll angle and roll rate. The roll angle and roll rate were effectively captured using an IMU.

Track design

In designing the track for this experiment, several critical factors were considered to ensure the successful completion of overtaking maneuvers. The track needed to be sufficiently long to accommodate the overtaking process. Assuming the speed of the overtaken mode at a higher bound of 4 m/s and the speed of the overtaking mode at a lower bound of 5 m/s, and considering 5 m safe distance before and after the overtaking process, the minimal track length should be 50 meters, based on the basic physical law (speed × distance / speed difference = 5 × 10/(5 4) m). Consequently, a main track measuring 60 meters in length is designed to provide extra space to accommodate interactions occurring. This track includes two-way bike lanes, each lane being 1.8 meters wide (totaling 3.6 meters), with a buffer distance of ten meters on both the left and right sides. This buffer is intended to accommodate any necessary acceleration or deceleration. The layout is detailed in figure3. The main reference for the 1.8m width of the lanes is based on a study of field measurements of two-way bicycle lanes in the Netherlands[36] of field measurements of two-way bicycle lanes in the Netherlands, which is approximately 370 cm, including the width of the markings in the middle of the road, and therefore selected as 180 cm in this study.

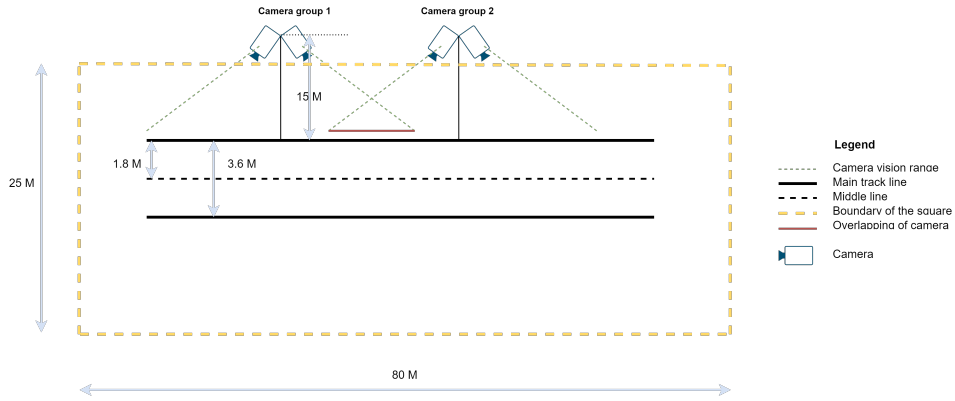

Figure 3: Track design

The order of the camera from right to left is R1-R2-L1-L2

Vehicle and participant selection

The first step of the scenario design is to select the specific models of e-scooter, e-bikes and e-mopeds that to be investigated in this study. In selecting the travel modes, the following three factors are taken into consideration:

- Popularity in the market.
- Easiness of learning to use these e-mode vehicles - the need to avoid vehicles that participants could not learn to ride in a short period of time.
- The maximum speed of the vehicle should be kept below 25 km/h to prevent potential safety issues during the experiment.

To consider the heterogeneity among participants, each scenario should include at least 30 combinations, where one combination involves a rider with the designated mode performing the requested maneuver. The rider should be proficient in operating the specified mode. Ideally, the rider population should encompass a broad range of ages and genders. Considering the trade-off between time, financial budget, and feasibility, 12 combinations were ultimately selected. Consequently, 12 riders can be recruited per mode. And 4 repetitions/runs per combinations of participants (in total 48 runs per scenario) are performed to get statistically significant results.

Scenario, duration and schedule design

This study design incorporates a range of intra-modal and intermodal interactions to comprehensively capture the dynamics of overtaking behavior across different micromobility modes.The planned scenario runs and their specific properties are summarized in Table1. This table provides a detailed overview of each overtaking combination, the modes involved, and the number of repetitions, offering a clear structure for the experimental design.

General instruction and task design

On the straight main track, participants are asked to slow down 5 m before the endpoint (there was a road marker) to facilitate the turning. Prior to conducting the interactive maneuver experiment, it is important to first conduct an unhindered scenario where the rider maintains a normal/desired speed,

Sce No.	Sce Name	Participating mode			Exp. duration (min)
		ES	EB	B	
1	Overtaking-intra1	✓	-	-	12 x 4
2	Overtaking-intra2	-	✓	-	12 x 4
3	Overtaking-inter1	✓	✓	-	12 x 4
4	Overtaking-inter2	✓	✓	-	12 x 4
5	Overtaking-bike1	✓	-	✓	12 x 4
6	Overtaking-bike2	-	✓	✓	12 x 4

Table 1: Table of Overtaking Scenarios and Experimental Details

decelerates to standstill, and then accelerates back to the normal speed without any interruptions. This step is primarily aimed at understanding the rider's speed and acceleration/deceleration capabilities under normal riding conditions, also obtaining the reference values in these key variables. The main tasks for participants are to perform various interactive maneuvers: overtaking, merging, yielding, head-on meeting. The overtaking maneuver, consisted of two types of riders, in which some participants would ride at low speeds on the designed bike lanes as overtaken riders,and the other part of participants would overtake the low-speed vehicles from the left side in a safe manner as overtaking riders. The speedometer dashboard was available for e-scooter, the speed was bounded to be around 10 km/h under the cruise control mode. For the e-bikes or e-mopeds, their speeds were not strictly limited due to the absence of dashboards and cruise control functions. The overtaken riders were asked to ride at a low speed that does not interfere with their control of balance (e.g., requiring additional control maneuvers such as a large wiggle of the steering grip or adjustment of body position). Overtaking riders were merely asked to follow their habits and methods when overtaking low-speed vehicles without colliding. In situations involving yielding to pedestrians at crosswalks or to traffic approaching from the right, riders without the right of way were instructed to behave as they would in reality — continuing to ride, stopping, or yielding — as long as no collision occurred. In cases involving bi-directional encounters, participants must prioritize their riding behavior to prevent head-on collisions or ensure safety

Implementation of experiment

Location selection

The experimental site is a square area located at the Hebei University of Water Resources and Electric Engineering in Cangzhou, China, as shown in the red rectangle part of figure4. The measurements of this square are about 25 meters in width and 80 meters in length. In the actual experiment, the track in figure3 was achieved by means of ground tape, where the boundary line of the road was taped in yellow and black, and the dotted line in the middle of the road was realized by using white ground tape. The area is covered with standard square tiles of size 60 x 60 cm.It is regularly used by pedestrians, bicycles, and motor vehicles within the campus.

Vehicles and Participant usage

For practical reasons, we ended up obtaining three e-scooters on our own, the model being the Ninebot E9, with a top speed of 20 km/h. For the e-bikes, we finally obtained 4 e-bikes. Two of the e-bikes were regular ones; one was foldable, and the other one was a fat e-bike. This implies that the variety within the same e-modes (particularly e-bikes) should be critically considered when analyzing the data.

Regarding rider personal characteristics, combined with the actual recruitment of the experimental participants, a broad coverage in age, and the equal level in gender and riding experience were

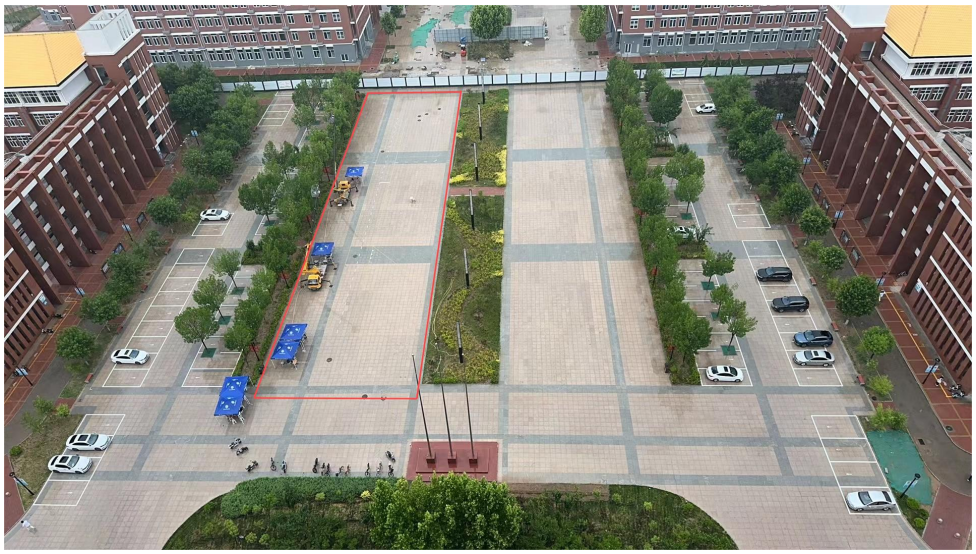

Figure 4: Experiment field

difficult to realize because the participants were mainly university students, with very little difference in age. Most of them had similar experience in using e-scooter and e-bike but varying in familiarity level. In terms of specific arrangements for the participants, two days prior to the experiment, the author explained how they would be asked to ride on the day of the experiment. After the briefing, participants were allowed to voluntarily choose the type of vehicle they wanted to ride. The participants who have more experience in certain modes had the priority of using the corresponding mode in the experiment. Finally, the male/female ratios are 9/3, 8/4, and 9/3 for e-scooter, e-bike, and e-moped, respectively. Although it is not 50/50, the effect of rider gender on micromobility interactions can be accommodated. According to their willingness, the author group the participants. Once the e-scooter and e-bike groups were formed, each participant was assigned a micromobility vehicle based on their height order. This measure was taken because the limited number of e-bikes required three people to share one vehicle, and similar heights ensured that they did not need to adjust the seat height throughout the experiment. After completing the grouping, the participants familiarized themselves with and test drove the vehicles they would use during the experiment. After completing group assignment, participants familiarized themselves with and test drove the vehicles they would use during the experiment, ensuring they were qualified as riders of the assigned modes, despite varying levels of user experience and familiarity. According to[37],riding a bicycle involves a combination of tasks executed based on rules for performing maneuvers and automatic actions for split-second control of the bicycle. We posit that a similar operational process of actions and reactions applies to micromobility traffic. By providing participants with the opportunity and sufficient time to familiarize themselves with riding the vehicles (particularly e-scooters and e-bikes), their riding and interactive maneuvers are expected to reflect their natural behavior under split-second decision-making conditions.

Data Collection equipment setup

The experiment finally used four high resolution cameras (Dahua), which were divided into two sets to cover the whole range of the main track with overlapping area for trajectory stitching purposes. An asymmetric setup of the two cameras will be used, that means one camera would cover most of the interactive area, the other one will cover the central area plus a further area in the riding direction. Before the start of the experiment, the camera was secured to the railing of the aerial platform. The

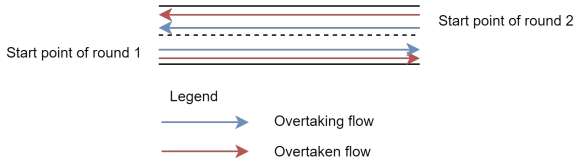

Figure 5: Path of intra mode overtaking

offset angle and focal length of the camera, as well as the position of the aerial work truck and the final operating height, were all adjusted repeatedly according to the output picture of the camera, which was accomplished after achieving the effect of clear video effect and reasonable coverage. The final four cameras all output video in 1920×1080, 20 fps format.

The IMU device was mounted on the e-scooter's steering stem or the e-bike's backseat. Sensor BNO-055 has a built-in Kalman filter algorithm that directly outputs roll angle, yaw angle,and pitch angle. Due to the limitation of the number of IMU devices, only one e-scooter and one e-bike, carried the device throughout the experiment. The devices did not need to dismount or be calibrated again. This allowed consistent and continuous data recording.

Experiment execution

The experiment was conducted on May 26, 2024, at the Hebei University of Water Resources and Electric Engineering. Participants were provided with white T-shirts and red caps, which they wore throughout the experiment to ensure consistent visibility in camera images.

For most design scenarios, participants were instructed to perform their riding tasks in a sequential order, eliminating the need for participants to wait for others to complete a lap before entering the track. This arrangement expedited most overtaking and bypassing scenarios.

To ensure sufficient interactive maneuvers were triggered and captured by cameras in designated areas, multiple vehicles were simultaneously present on both paths, rather than just one vehicle per path. Furthermore, experiment supervisors could slightly control the timing of participants re-entering the designed track after completing a lap, maximizing the likelihood of triggering overtaking maneuvers.

On the day of the experiment, to more effectively capture the overtaking behavior of e-bikes and e-scooters, the experimental path was modified to the form shown in Figure5. Unlike the initially designed complete circular path, the modified experimental path no longer required participants to overtake spontaneously. Instead, experimental monitors were stationed on both sides of the field, responsible for controlling the entry timing of overtaking and overtaken participants in each round of the experiment to ensure the occurrence of overtaking behavior. The main reason for adopting this strategy lies in the relatively small sample size of e-bikes and e-scooters. By controlling the entry timing, the time consumed by experimental participants to complete sufficient overtaking behaviors through meaningless riding can be saved. This meaningless riding may lead to the emergence of the learn effect, which could affect the validity of the experimental results.

By modifying the experimental path and introducing the control of experimental monitors, this study minimizes the influence of the learn effect while ensuring the acquisition of sufficient overtaking behavior samples. This adjustment in the experimental design helps to improve the efficiency of data collection and ensures that the collected data can more accurately reflect the true behavioral characteristics of e-bikes and e-scooters during the overtaking process.

The cameras and IMU units began recording simultaneously after camera parameter adjustments. The researcher then guided participants on the appropriate times to enter the designed track

according to the pre-defined schedule. Once on the track, participants followed their designated paths and performed their assigned tasks.

This design effectively controls for learning effects by introducing variation across scenarios, so while each participant encounters only one session per scenario, the repeated overtakes within each session help capture intra-scenario behavior. The four laps per scenario allow us to observe consistent overtaking patterns and subtle behavioral differences within a single context, thereby balancing the need for representativeness and capturing individual behavior variability.

The object of overtaking is different each time. In addition, the learning effect due to observing the behavior of other experimental participants was also objectively weakened, according to the researchers' observation that the vast majority of experimental participants were playing with their cell phones, etc., in their free time.

Video processing

Video format conversion

The video processing workflow begins with addressing compatibility issues between the original video files and the analysis tools used. Initially, the videos are in HEVC format. This encoding presents challenges for analysis in the researcher's laptops and the workstation of TU Delft. To overcome this limitation, the solution is to convert the video to MPEG-4 format encoded in AVC using a software called Handbrake.

Pixel trajectory extraction

For trajectory extraction, the Moving Object Detection and Tracking (MODT) tool developed by study [38] is employed. The MODT tool has been enhanced to calculate the exact Beijing time for each video frame by determining the millisecond-precise start time using the frame rate and a known end time. Given the end time B (formatted as xx:xx .000) after X frames, starting from A seconds, the start time A is computed as:

$$A = B - \left(\frac{1000 \text{ ms}}{\text{Framerate}} \right) \cdot (X - 1) \tag{1}$$

This setup calculates the precise Beijing time for each frame by adding the known start time to the relative time elapsed since the video began, which ranges from 0 seconds up to the video's total duration. This method ensures accurate synchronization between video frames and real-world time, critical for trajectory merging and IMU data synchronization in research analyses.

Image Correction

Image distortion correction is a vital step in the data processing workflow to ensure accurate spatial analysis of video footage. The primary objective of this correction is to transform the camera's perspective from a side view to a bird's-eye view—perpendicular to the center of the image from above. This transformation allows for precise measurements and analysis of movements within the video frames.For this purpose, this study employed a tool called ImageTracker developed by study[39].

Height Projection

The forth step involves height projection. The reason for performing height projection is that when a camera captures images from an elevated position, objects in the image appear closer to the camera than their actual positions. Correction is necessary to obtain the true positions of the objects. The height projection method employed in this study is based on the approach developed by study [40].

Fixes for trajectory errors

In the initial stage, we removed incorrectly detected trajectories caused by various reasons, such as participant errors and static objects. We used animation playback to spot two main types of errors:

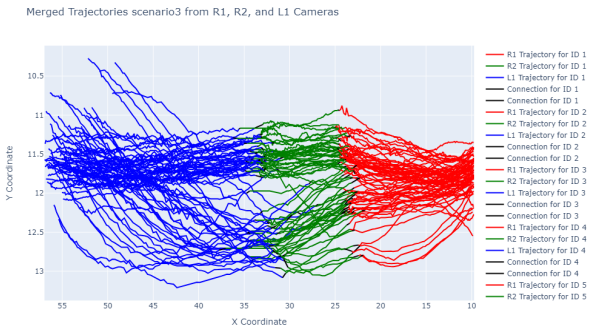

Figure 6: R1R2L1 merged result of scenario3

stationary points and premature exits. For the R1 camera, we adjusted the tool to capture more trajectories, including U-turn behaviors. Unreasonable trajectories were either manually removed or corrected to retain only relevant data.

The next step after removing incorrect trajectories involves addressing trajectories fragmented due to shadow interference. An algorithm was developed to detect and merge adjacent trajectory segments likely belonging to the same vehicle. It examines spatial and temporal continuity between trajectory endpoints and applies predefined thresholds for distance and time gaps. The algorithm then integrates the interpolated points into the existing data and reassigns trajectory IDs for consistency. This approach helps reduce inaccuracies caused by shadows.

The third step involves fixing jump points caused by detection errors, resulting in crossover trajectories. The first step splits trajectories at jump points, while the second step reconstructs complete motion trajectories through interpolation. The algorithm identifies abnormal jumps and separates trajectory segments, then iterates through each unique trajectory ID to find the best matching next trajectory and perform linear interpolation.

Merging of multi-camera trajectories

In this study, camera trajectories are merged in two stages. The first stage merges cameras in pairs, while the second stage uses common data to merge trajectories from more than two cameras. The merging principle involves identifying the closest trajectories and merging them. The detailed pairwise merging algorithm matches trajectories from overlapping cameras. After the matching, the trajectories are merged, and the process retains only the common parts. The next step involves merging trajectories from three or four cameras using overlapping regions. Figure6 shows result of triple camera merging of scenario 3.

Freezing point handle

After merging the trajectories, a freezing point handling process was performed. Some videos showed frame freezing, where consecutive frames had the same position and then jumped. This issue was likely due to computer performance during video conversion. To address this, the study used a repair method to replace coordinates of consecutive identical frames with the average value of the previous and subsequent frames.

Accuracy validation

The primary goal of the accuracy validation process was to confirm that the processed trajectories accurately depict overtaking behaviors in terms of micro-level variables like speed, speed differences, and distances. The absence of a ground-truth system necessitated indirect validation methods based on the 60 cm square tiles at the experimental site:

1. Lateral Accuracy: Lateral distances between vehicles during overtaking were estimated by count-

ing the tile spans and comparing these with the trajectory data, leveraging minimal lateral movement and consistent tile dimensions for accuracy.

2. Longitudinal Accuracy: Longitudinal validation involved estimating the distance riders covered over one-second intervals through tile counts, which was then validated against trajectory lengths to indirectly confirm speed accuracy.

These methods, chosen due to the impracticality of direct speed validation, relied on averaging over time to mitigate fluctuations in speed and acceleration measurements. Further validation for acceleration was conducted by comparing calculated values with existing literature on e-bike and e-scooter accelerations. This approach ensures the reliability of trajectory data for analyzing micromobility overtaking behaviors despite the limitations.

Through multiple comparisons of this nature, we can establish confidence in the accuracy of our trajectory data.For both the X and Y directions, thirty data were selected. For the Y direction, the average error was 0.094 meters. For the X direction, the overall difference was 0.196 meters. In percentage terms, the error/actual value in the X-direction and Y-direction is 6.1% and 7.8%, respectively.

Trajectory labelling

This labeling process is performed manually by watching the video footage and tagging each trajectory accordingly. For example, when a trajectory spans data from multiple cameras (e.g., R1, R2, and L1), it is sufficient to select data from only one of the cameras, such as R2, to label the entire trajectory. Each trajectory is then annotated with various attributes, including the corresponding ID, the participant's gender, the type of vehicle they are riding, and whether they are carrying an IMU device.

Data analysis result

Descriptive statics

Before proceeding to detailed statistical analysis, this section presents some descriptive statistics for the micro variables.

Speed and deceleration

In non-interactive conditions, the average traveling speed for E-bikes was 18.51 km/h (SD = 4.58 km/h), while E-scooters traveled at an average speed of 15.38 km/h (SD = 3.72 km/h). These values, illustrated in Figure7, indicate that E-bikes maintain a higher average speed than E-scooters under non-interactive conditions. Whether it is statistically significant needs further verification, though.

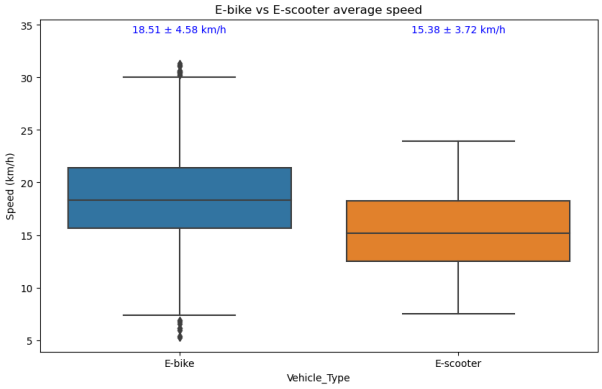

Figure 7: Non-interactive E-bike and e-scooter riding speed

In non-interactive conditions, the average deceleration for E-bikes was 3.83 m/s² (SD = 1.46 m/s²), while E-scooters had an average deceleration of 3.24 m/s² (SD = 0.97 m/s²) as shown in Fig-

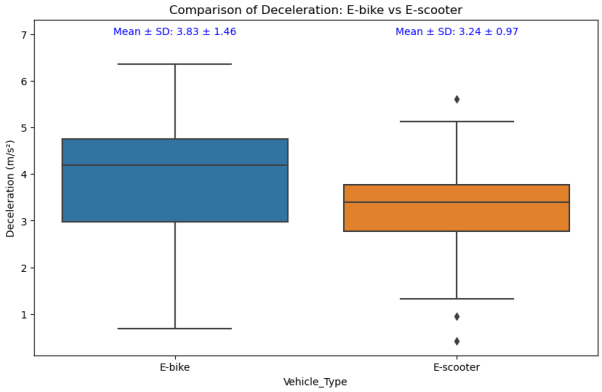

Figure 8: E-bike and E-scooter deceleration

ure8. These findings align with existing research, such as the study by [41], which reported e-scooter deceleration rates between -3.39 m/s² and -3.84 m/s².

Lateral distance

The lateral distance during the passing phase is particularly important in this study, as it reflects the overtaker's lateral avoidance strategy, an essential aspect of path selection. The mean and standard deviation of lateral distances for each overtaking scenario are shown below and in Figure9:

- **E-bike overtaking bike**: 44 samples, Mean ± SD: 1.25 ± 0.26 m
- **E-bike overtaking e-bike**: 50 samples, Mean ± SD: 1.31 ± 0.35 m
- **E-bike overtaking e-scooter**: 46 samples, Mean ± SD: 0.89 ± 0.34 m
- **E-scooter overtaking bike**: 23 samples, Mean ± SD: 1.21 ± 0.35 m
- **E-scooter overtaking e-bike**: 40 samples, Mean ± SD: 1.06 ± 0.31 m
- **E-scooter overtaking e-scooter**: 23 samples, Mean ± SD: 1.08 ± 0.40 m

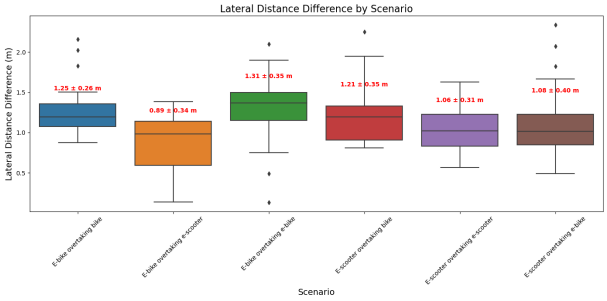

Figure 9: Lateral distance of differenct scenario

Overtaking starting position

The overtaking start moment refers to the longitudinal distance between the overtaker and the overtaken vehicle at the initiation of the overtaking maneuver. Due to missing pre-passing phase data in Scenarios 5, 6, and 7 (E-scooter overtaking bike, E-scooter overtaking e-bike, and E-scooter overtaking e-scooter), this analysis only includes Scenarios 2, 3, and 4. The means and standard deviations for these scenarios are as follows and in Figure10:

- **Scenario 2 (E-bike overtaking bike)**: Mean = 9.75 m, SD = 2.86 m

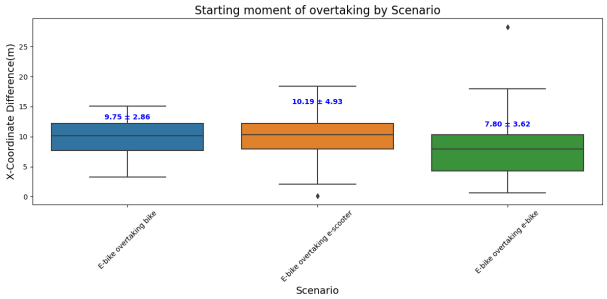

Figure 10: starting position of overtaking

- **Scenario 3 (E-bike overtaking e-scooter)**: Mean = 10.19 m, SD = 3.62 m
- **Scenario 4 (E-bike overtaking e-bike)**: Mean = 7.80 m, SD = 4.93 m

Roll rate and roll angle

This study uses the absolute mean values of roll rate and roll angle, consistent with the methods of [32, 16]. Notably, due to incorrect IMU placement for E-scooters and missing trajectory data for Scenarios 5, 6, and 7, only data from Scenarios 3 and 4 were analyzed. Figure 11 and Figure12 show the variation of roll angle and roll rate across three phases in Scenarios 3 and 4.

Scenario 3:

- **Roll Angle (absolute mean):**
  - Before: Mean = 4.03°, SD = 2.56°
  - During: Mean = 6.66°, SD = 3.71°
  - After: Mean = 4.67°, SD = 2.65°
- **Roll Rate (absolute mean):**
  - Before: Mean = 26.17°/s, SD = 3.64°/s
  - During: Mean = 36.73°/s, SD = 11.57°/s
  - After: Mean = 24.68°/s, SD = 7.56°/s

Scenario 4:

- **Roll Angle (absolute mean):**
  - Before: Mean = 4.48°, SD = 2.87°
  - During: Mean = 7.04°, SD = 4.46°
  - After: Mean = 4.43°, SD = 4.16°
- **Roll Rate (absolute mean):**
  - Before: Mean = 30.41°/s, SD = 6.52°/s
  - During: Mean = 36.21°/s, SD = 25.33°/s
  - After: Mean = 27.49°/s, SD = 12.59°/s

Figure13 shows an example of the change in roll angle and roll rate over time for a trajectory in Scenario 4.

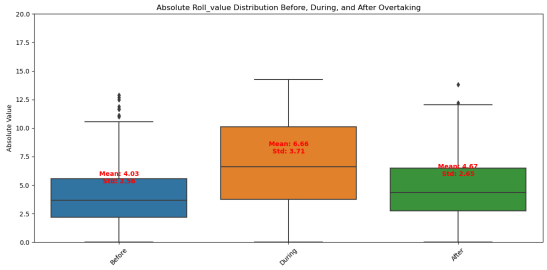

(a) Roll angle across different phases in Scenario 3

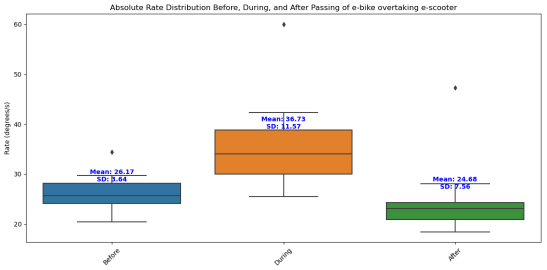

(b) Roll rate across different phases in Scenario 3

Figure 11: Comparison of roll angle and roll rate across different phases in Scenario 3

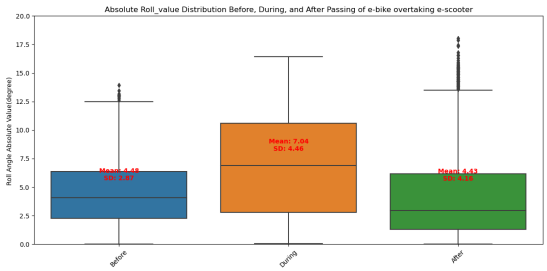

(a) Roll angle across different phases in Scenario 4

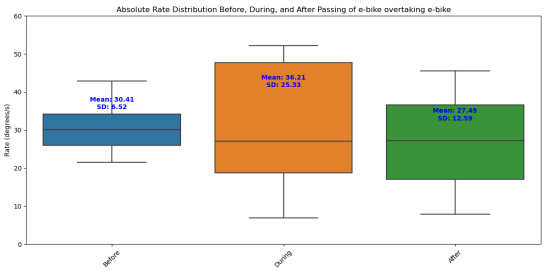

(b) Roll rate across different phases in Scenario 4

Figure 12: Comparison of roll angle and roll rate across different phases in Scenario 4

Statistical analysis

Statistical analysis is performed to verify the relationships represented by the arrows in Figure2.

Lateral distance

The investigation into gender differences in lateral distance during overtaking found no significant differences across scenarios involving e-scooters.

This section also proposed a positive correlation between speed difference and lateral distance during overtaking. Pearson correlation coefficients indicated a moderate to strong positive correlation in scenarios where e-scooters overtook bikes and e-bikes. The detailed regression and grouping analyses further supported these findings, showing that larger speed differences typically correspond to larger lateral distances, indicative of safer overtaking practices.

This section then explored the impact of micromobility types on lateral distance using ANOVA and Tukey's HSD tests. Significant differences were observed between various scenarios, particularly when e-bikes overtook different vehicle types. These differences highlight the influence of vehicle type on overtaking behavior, emphasizing how riders adjust lateral distances based on the perceived size and maneuverability of overtaken vehicles.

Overtaking starting position

The starting position's analysis assessed the impact of micromobility type on overtaking initiation. ANOVA results demonstrated significant differences across scenarios, suggesting that vehicle type affects how and when overtakers initiate maneuvers. The findings indicated that e-bike riders often start overtaking maneuvers later when overtaking other e-bikes, possibly due to familiarity with similar vehicle behaviors.

Regression analysis on speed difference

Multiple regression and phase-wise analyses were conducted to explore the relationships involving speed differences, lateral and longitudinal distances, vehicle types, and overtaking phases. Significant influences were found, with lateral distances showing a stronger impact on speed differences than

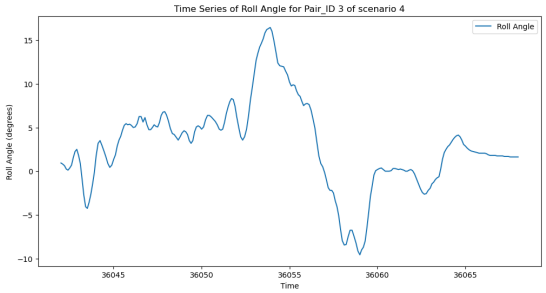

(a) Roll angle over time of Pair 3 in scenario 4

(b) Roll rate over time of Pair 3 in scenario 4

Figure 13: Roll angle and roll rate over time example

longitudinal distances. These insights align with overtaking dynamics, where lateral adjustments during overtaking are crucial for maintaining safety and efficiency.

Roll angle and roll rate

The examination of roll dynamics revealed that roll angles and rates vary significantly across different phases of overtaking and among micromobility types. These variations underscore the physical adjustments riders make during overtaking, particularly in scenarios involving similar types of vehicles, where familiarity and performance expectations influence maneuvering strategies.

Summary

This chapter first compares the normal driving speeds and deceleration capabilities of vehicles in non-interactive scenarios. The results revealed significant speed differences between E-bikes and E-scooters, with E-bikes traveling at notably higher speeds. However, no distinction was observed in their deceleration capabilities. Gender differences in speed were only significant in E-scooter riders, where male riders consistently exhibited higher speeds than females.

To explore the influence of gender factors and the combination of overtaking and overtaken vehicles on overtaking behavior, the study analyzed the lateral position difference. The findings indicate that the maximum lateral distance difference mostly occurs within the passing phase. During this phase, the overtaker's choice of lateral distance is influenced by speed difference; higher speed differences correspond to larger maintained lateral distances. This reflects the riders' adaptation to safety requirements based on speed differentials.

The study then compared the behavioral differences of overtaking vehicles when passing different vehicle types. These differences were less pronounced for E-scooters but more evident for E-bikes, potentially reflecting the overtaking riders' perceptions of their own vehicle's size and that of the overtaken vehicle. Additionally, when comparing different vehicles overtaking the same type, a significant difference emerged only when E-bikes and E-scooters overtook E-bikes, with E-bikes maintaining a larger lateral distance. This increased lateral distance was likely due to that e-scooter riders may perceive themselves as occupying less space and thus more maneuverable compared to e-bike riders, prompting them to feel more comfortable overtaking with a smaller lateral gap. However, it may also be influenced by modifications to the experimental path, which required higher speeds and, consequently, greater spacing to ensure safety.

Using an analysis of the rate of change in lateral position difference, the study detected the initiation points for overtaking maneuvers in E-bikes overtaking E-scooters and E-bikes. Interestingly, E-bikes initiated overtaking of E-scooters at a greater distance compared to overtaking other E-bikes, without significant gender influence.

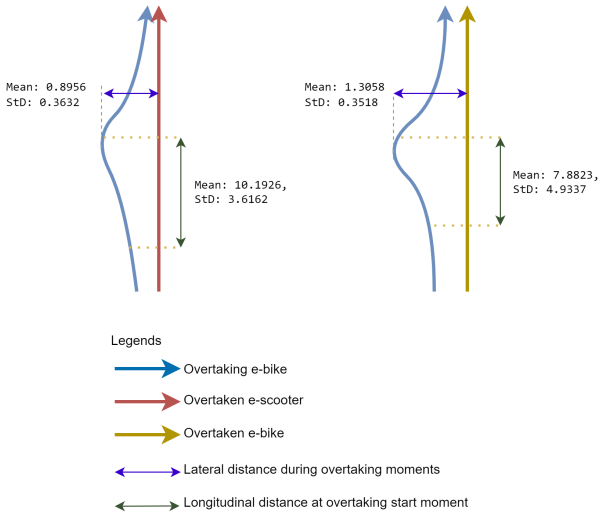

Figure 14: Overtaking pattern of e-bike overtaking e-scooter and e-bike

Combining these findings with the maximum lateral distance difference tests provides an overview of E-bike overtaking patterns for E-scooters and E-bikes, as illustrated in Figure 14. Generally, E-bikes initiate overtaking E-scooters from a greater distance but maintain a smaller maximum lateral distance during the process. Conversely, when overtaking other E-bikes, they initiate the maneuver closer but choose a larger lateral spacing.

This pattern is further corroborated by the phase-wise comparison of roll rates and roll angles' absolute values across different overtaking scenarios. Additionally, this comparison reveals a common motion characteristic: roll rates and roll angles reach their maximum values during the passing phase.

To further understand the differences between pre-passing, overtaking, and post-overtaking phases, the study compared average speeds during these phases for E-bikes overtaking bikes, E-scooters, and E-bikes. These results revealed some experimental design flaws, such as an excess of vehicles on the bike lap leading to continuous deceleration while overtaking two bicycles consecutively(scenario2), and inappropriate timing control during internal overtaking experiments resulting in continuous acceleration during overtaking(scenario4). In Scenario 2, an overtaker may accelerate to a high speed to overtake the first vehicle and then realize that there is a second overtaken vehicle, but instead of accelerating further, he slowly decelerates to overtake the second low-speed vehicle. In scenario 4, since the experimental requirement is to complete the overtaking inside the design track, it may result in the overtaking vehicle that starts later needing to keep accelerating in order to complete the overtaking maneuver before the end of the deisgn track, this phenomenon may also occur in scenario 7, but due to the missing data of 7, it is not possible to test it.

Furthermore, the study examined the behavior of overtaken vehicles during the overtaking process, particularly focusing on speed changes before and after the passing phase, and within the pre-passing phase. When comparing the speed between the pre-passing phase and post-passing phase, E-scooters and E-bikes showed a significantly higher proportion of noticeable speed changes compared to bikes. Due to some E-bike riders' personal preferences, E-bikes as overtaken vehicles demonstrated a markedly higher proportion of acceleration after being overtaken. when comparing within pre-passing phase, e-bike and e-scooter exhibit a slight acceleration at the end of the pre-passing phase, showing that riders alter their speed as a form of defensive or adaptive behavior when interacting with others in close proximity.

The final test results of the relationships in the Conceptual framework are shown below in Figure15 is the conceptual framework that has been tested.

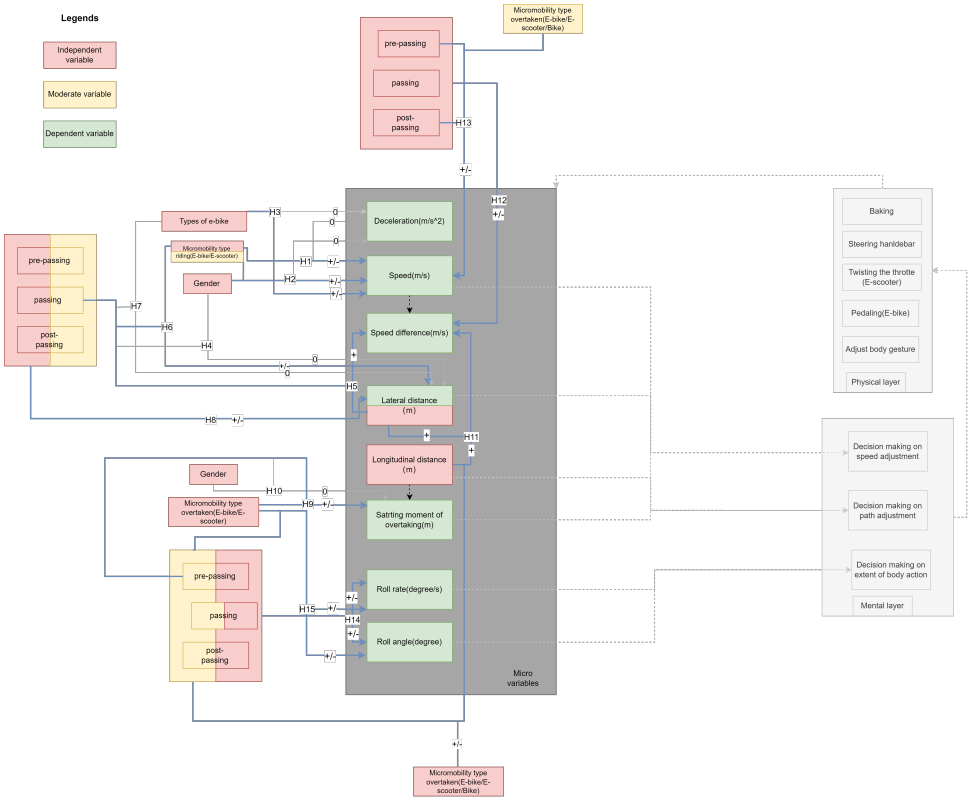

Figure 15: Conceptual framework after test

Where + means there is significant positive relationship, +/- means there is significant relationship but whether it is postive or negative is up to the characteristic, 0 means there is no significant relationship

Conlusion and Discussion

This research aims to investigate the individual behavior of micromobility users, specifically e-bike and e-scooter riders, during their interactions with regular bicycles and with each other. To study and understand rider behavior during overtaking scenarios, this research designed and implemented a controlled experiment to collect trajectory data of e-scooter and e-bike riders through video recording during overtaking maneuvers, along with data on roll angle and roll rate from IMU sensors. After processing the video data, trajectory data of the participants were obtained, which were then synchronized with the IMU data on a common timeline. From these trajectory data, micro-level variables such as lateral position difference, longitudinal position difference, and speed difference were derived. The study then employed statistical methods, including t-tests, ANOVA, Pearson correlation analysis, and regression models, to examine the effects of gender, vehicle type, and other influencing factors on these micro-level variables. Ultimately, the results revealed several behavioral characteristics and patterns during the overtaking process, providing key insights into how different micromobility types and individual characteristics influence rider behavior.

Affect of micro-mobility type combination

In the context of overtaking behavior, micromobility vehicle type had a substantial impact. E-bike riders, when overtaking e-scooters, initiated the overtaking maneuver from a greater distance but maintained a smaller maximum lateral distance throughout the maneuver. Conversely, when overtaking other e-bikes, riders initiated the overtaking maneuver closer to the overtaken vehicle but maintained a larger lateral distance, indicating more caution and space in similar-vehicle interactions.

The vehicle type also influenced the speed difference dynamics during the overtaking process. As the multiple regression analysis, lateral position differences were more strongly correlated with speed difference than longitudinal differences, confirming that riders prioritize lateral safety margins when overtaking. The type of overtaken vehicle also affected the speed, with e-bikes maintaining higher speed diference when overtaking other e-bikes compared to when overtaking e-scooters, demonstrating that vehicle-type familiarity influences rider behavior.

The roll rate and roll angle peaked during the passing phase. Moreover, in the process of E-bike overtaking E-bike, the roll angle and roll rate are significantly larger in the pre-phasing stage when E-bike overtakes E-scooter because more lateral movement has to be accomplished in a shorter period of longitudinal distance.

Gender affect

Gender differences in riding behavior were clearly observed in non-interactive driving, especially for e-scooter riders, where male riders showed significantly higher speeds than female riders. However, no gender-based differences were found for e-bike riders in similar conditions, suggesting that vehicle type plays a role in how gender impacts driving behavior.

Initially, it was hypothesized that gender might influence lateral distance decisions during overtaking, particularly for e-scooter riders. However, subsequent analysis revealed no significant gender-based differences in lateral distances maintained during overtaking maneuvers. This finding suggests that while gender may influence riding speed in non-interactive scenarios, it does not significantly affect spatial decisions during overtaking.

Furthermore, gender had no significant impact on the initiation of overtaking maneuvers. These results collectively indicate that factors such as vehicle type and speed may be more influential than gender in determining both the timing and spatial characteristics of overtaking behaviors.

Societal Contributions

The findings from this research can have several significant applications in guiding infrastructure development, informing traffic regulations, and enhancing the design of traffic simulation models, especially with the growing popularity of micromobility vehicles like e-bikes and e-scooters. The following are some key areas where this research can be applied:

1. Wider and Safer Lanes: Based on the findings that micromobility users, particularly e-bike riders, tend to maintain larger lateral distances when overtaking other vehicles, the study suggests that wider cycling lanes should be considered in urban planning. This would provide adequate space for safe overtaking and reduce the risk of collisions, particularly in areas with high mixed-use traffic involving micromobility vehicles. Wider lanes could ensure safer maneuverability for both overtaking and overtaken riders, especially in congested areas. In the past, the recommended width for two-way bicycle paths in the Netherlands was 2 meters[42], based on the assumption of a minimum lateral spacing of 0.75 meters between two bicycles. This study, however, recommends increasing the minimum width to 2.3 meters, as the observed average maximum lateral spacing in this research was 1.1 meters.

   Coincidentally, in 2022, the CROW Design Manual for Bicycle Traffic updated the recommended width for one-way bicycle paths in the Netherlands from 2 meters to 2.35 meters[43]. However, CROW did not explicitly cite the introduction of e-bikes or e-scooters as a reason for this change; instead, the update was motivated by the potential safety benefits of wider paths. This study's findings further validate the reasoning behind CROW's recommendation, as larger lateral spacing can accommodate various micromobility types and contribute to overall riding safety.

2. Overtaking Distance Guidelines: The analysis of lateral distances and speed differences during overtaking demonstrates the need for clearer guidelines on safe overtaking distances between different types of micromobility vehicles. Transport authorities can use these findings to develop minimum overtaking distance standards for micromobility users. Such guidelines could be integrated into traffic laws, ensuring that riders are aware of the necessary space required to safely overtake other vehicles, ultimately enhancing road safety for all users.

3. Traffic Calming Measures: The differences in speed and acceleration between e-scooters, e-bikes, and traditional bicycles could be used to design more effective traffic calming measures. Implementing speed limits tailored to different types of micromobility vehicles and creating designated overtaking zones could help reduce conflicts between riders and minimize high-risk overtaking behaviors. This approach could also prevent scenarios where slower bicycles are overtaken in unsafe conditions, thus mitigating potential hazards.

4. Micromobility Integration into Traffic Systems: Given the increasing integration of e-bikes and e-scooters into urban transportation, the study's insights into overtaking behavior could inform traffic simulation models that reflect real-world dynamics of mixed micromobility interactions. These models could be used by transportation planners and engineers to simulate and optimize the flow of micromobility vehicles in urban traffic systems, allowing for the development of infrastructure that accommodates the unique behaviors of these vehicles, leading to safer and more efficient traffic networks.

Research contribution

This study presents a comprehensive experimental design process that can serve as a reference for future researchers undertaking similar investigations in the field of micromobility behavior. The methodology developed here offers a systematic approach to studying complex interactions between different types of micromobility vehicles and users.

Moreover, this research has resulted in the development of a robust video data processing pipeline. This pipeline is characterized by its adaptability to datasets of varying quality, making it particularly suitable for studies where data collection conditions may not be ideal. The process is designed with a focus on reproducibility, allowing other researchers to apply and build upon this methodology in their own work.

The video processing workflow developed in this study addresses common challenges in micromobility research, such as multi-camera trajectory merging, time synchronization across different data sources, and trajectory smoothing. By providing solutions to these technical hurdles, this research contributes to the standardization of data processing methods in micromobility studies. Furthermore, the approach taken in this study to define and analyze overtaking phases offers a nuanced framework for examining micromobility interactions. This framework can be adapted and refined by future researchers to explore various aspects of micromobility behavior beyond overtaking.

In summary, the methodological contributions of this study - including the experimental design, data processing pipeline, and analytical framework - provide a solid foundation for future research in micromobility behavior. These tools and approaches can enhance the rigor and comparability of studies in this rapidly evolving field.

Limitations and recommendation for future research

This study provides valuable insights into micromobility overtaking behavior. However, several limitations should be recognized and addressed in future research. Each limitation highlights areas for improvement and suggests potential avenues for further investigation:

1. **Cultural and Market Context:** This study was conducted within the unique micromobility landscape of China, where e-mopeds dominate and e-bikes are less common, with e-scooters primarily used in specific areas such as university campuses. While participants were given time to adjust to the vehicles, their behavior may not fully reflect that of experienced riders in regions like Europe, where e-bikes are more prevalent and used in diverse settings. These contextual factors may have influenced overtaking behaviors specific to the Chinese market. Future research should consider cross-cultural comparisons in regions with established e-bike ecosystems to examine if local factors and cultural norms shape rider behavior, ultimately determining if findings are generalizable or if region-specific safety guidelines are necessary.

2. **Experimental Design Constraints:** The simultaneous presence of multiple slow-moving vehicles in the study may have impacted participant behavior, particularly when e-bikes overtook bicycles. This multi-target environment might have inadvertently altered overtaking decisions, introducing confounding variables. To address this, future studies should control for individual overtaking events by isolating specific scenarios. For example, carefully staged setups or virtual simulations could allow researchers to capture single overtaking actions without additional distractions, thereby providing a clearer understanding of specific overtaking initiation behaviors across micromobility types.

3. **Data Collection Challenges:** Several technical issues impacted data quality and analysis:

- **Camera Positioning:** Non-vertical camera placements, combined with the absence of calibration images, led to edge distortions that compromised visual data accuracy. Future research should prioritize comprehensive camera calibration, possibly using pre-calibration with a chessboard or software that automatically corrects distortions. Advanced video processing tools, such as motion-capture software, could further enhance data fidelity.
- **Equipment Setup:** Extended multi-camera recordings highlighted the need for more robust data capture systems. To address issues such as data loss during transfer and the need for frequent camera synchronization, future studies could use high-performance setups, including Power over Ethernet (PoE) collect station and backup systems to preserve data integrity. Real-time monitoring of data collection could further ensure recording reliability.
- **IMU Data Collection:** Incorrect sensor placement on the e-scooter's stems led to incorrect roll rate and angle measurements, as the data did not reflect the travel direction. Future research should focus on calibrating and securing IMU devices in a way that aligns the sensor measurements with the vehicle's travel direction, ensuring that the roll rate and angle data are consistent with the e-scooter's actual movement. Testing and validating sensor orientation and placement prior to data collection can help improve the accuracy of dynamic measurements for micromobility vehicles.

4. **Data Processing and Analysis:** Although this study developed a novel video data processing pipeline, further refinements could improve robustness. Future research should enhance this pipeline, specifically targeting improvements in distortion correction and multi-camera trajectory merging. Applying machine learning algorithms for trajectory tracking and pattern recognition could yield deeper insights. Additionally, automated data alignment solutions could simplify the data processing workflow, supporting the scalability of future studies on micromobility interactions.

To build on these findings, future research should focus on:

1. Conducting cross-cultural studies in various micromobility markets to understand behavioral differences.
2. Designing experiments that isolate individual overtaking maneuvers to minimize external influences.
3. Enhancing data collection methodologies, with attention to camera calibration, sensor placement, and real-time equipment monitoring.
4. Developing sophisticated data processing techniques, such as machine learning-based trajectory analysis.
5. Exploring long-term studies on how rider behaviors evolve with increased exposure to different micromobility vehicles.

By addressing these limitations and implementing the recommended improvements, future research can contribute to a more comprehensive understanding of micromobility overtaking behaviors and inform the development of safety guidelines tailored to diverse rider groups and regions.

References

[1] Zoi Christoforou et al. “Who is using e-scooters and how? Evidence from Paris”. In: *Transportation research part D: transport and environment* 92 (2021), p. 102708.

[2] Michelangelo-Santo Gulino et al. “Exploring Performances of Electric Micro-Mobility Vehicles and Behavioural Patterns of Riders for In-Depth Accident Analysis”. In: *Designs* 5.4 (2021). ISSN: 2411-9660. URL: https://www.mdpi.com/2411-9660/5/4/66.

[3] Rijwiel en Automobiel Industrie Vereniging. *Number of electric bicycles sold in the European Union (EU-28) from 2006 to 2022 (in 1,000 units)*. Statista. Retrieved March 31, 2024, from https://www.statista.com/statistics/397765/electric-bicycle-sales-in-the-european-union-eu/. 2023.

[4] ZIV. *E-bike sales volume in Germany from 2011 to 2022*. Statista. Retrieved March 10, 2024. 2023. URL: https://www.statista.com/statistics/1265760/e-bikes-sold-number-germany/.

[5] Giulia Oeschger, Páraic Carroll, and Brian Caulfield. “Micromobility and public transport integration: The current state of knowledge”. In: *Transportation Research Part D: Transport and Environment* 89 (2020), p. 102628. ISSN: 1361-9209. DOI: https://doi.org/10.1016/j.trd.2020.102628. URL: https://www.sciencedirect.com/science/article/pii/S1361920920308130.

[6] Statistisches Bundesamt. *Number of pedestrian, cycling and e-scooter traffic crash injuries in Germany from 2019 to 2022, by mode*. Statista. Retrieved March 09, 2024. 2023. URL: https://www.statista.com/statistics/1399153/active-and-micro-mobility-traffic-crash-injuries-germany-by-mode/.

[7] E. M. J. Verstappen et al. “Bicycle-related injuries in the emergency department: a comparison between E-bikes and conventional bicycles: a prospective observational study”. In: *European Journal of Trauma and Emergency Surgery* 47.6 (2021), pp. 1853–1860. DOI: 10.1007/s00068-020-01366-5.

[8] Lu Han. “Perceived Risk of Interaction with E-Bikes”. Master’s thesis. Delft: Delft University of Technology, Oct. 2023. URL: http://resolver.tudelft.nl/uuid:8c9c976a-2ed6-45a6-b2bd-85e1dfb4ae60.

[9] Qingyu Ma et al. “E-Scooter safety: The riding risk analysis based on mobile sensing data”. In: *Accident Analysis & Prevention* 151 (2021), p. 105954.

[10] Alejandra Sofía Fonseca-Cabrera et al. “Micromobility Users’ Behaviour and Perceived Risk during Meeting Manoeuvres”. In: *International Journal of Environmental Research and Public Health* 18.23 (2021). ISSN: 1660-4601. URL: https://www.mdpi.com/1660-4601/18/23/12465.

[11] Rijksoverheid. *Welke regels gelden voor mijn elektrische fiets (e-bike)?* 2023. URL: https://www.rijksoverheid.nl/onderwerpen/fiets/vraag-en-antwoord/welke-regels-gelden-voor-mijn-elektrische-fiets-e-bike (visited on 03/12/2024).

[12] Euronews. *Electric scooters: What are the rules across Europe and where are injuries highest?* Sept. 2023. URL: https://www.euronews.com/next/2023/09/01/electric-scooters-what-are-the-rules-across-europe-and-where-are-injuries-highest (visited on 03/12/2024).

[13] Christina Garman et al. “Micro-Mobility Vehicle Dynamics and Rider Kinematics during Electric Scooter Riding”. In: Apr. 2020. DOI: 10.4271/2020-01-0935.

[14] Sarosh I Khan and Winai Raksuntorn. “Characteristics of passing and meeting maneuvers on exclusive bicycle paths”. In: *Transportation research record* 1776.1 (2001), pp. 220–228.

[15] Xiaohong Chen, Lishengsa Yue, and Kui Yang. “Safety evaluation of overtaken bicycle on a shared bicycle path”. In: *Tongji Daxue Xuebao* 45.2 (2017), pp. 215–222.

[16] Lucas Billstein and Christoffer Svernlöv. “Evaluating the Safety and Performance of Electric Micro-Mobility Vehicles: Comparing E-bike, E-scooter and Segway based on Objective and Subjective Data from a Field Experiment”. In: (2021).

[17] Marco Dozza et al. “How do different micro-mobility vehicles affect longitudinal control? Results from a field experiment”. In: *Journal of Safety Research* 84 (2023), pp. 24–32. ISSN: 0022-4375. DOI: https://doi.org/10.1016/j.jsr.2022.10.005. URL: https://www.sciencedirect.com/science/article/pii/S0022437522001591.

[18] Michelangelo-Santo Gulino et al. “Exploring performances of electric micro-mobility vehicles and behavioural patterns of riders for in-depth accident analysis”. In: *Designs* 5.4 (2021), p. 66.

[19] Katja Schleinitz et al. “The German Naturalistic Cycling Study–Comparing cycling speed of riders of different e-bikes and conventional bicycles”. In: *Safety science* 92 (2017), pp. 290–297.

[20] Mohammed Hamad Almannaa et al. “A comparative analysis of e-scooter and e-bike usage patterns: Findings from the City of Austin, TX”. In: *International Journal of Sustainable Transportation* 15.7 (2021), pp. 571–579.

[21] Fluid FreeRide. *Electric Scooter vs Electric Bike*. Accessed January 2022. URL: https://fluidfreeride.com/blogs/news/electric-scooter-vs-electric-bike#:~:text=the%20physical%20element.-,Speed%20%26%20Range,kph)%20than%20e%2Dbikes..

[22] Jay Todd et al. *Behavior of electric scooter operators in naturalistic environments*. Tech. rep. SAE Technical Paper, 2019.

[23] Marco Dozza, Giulio Francesco Bianchi Piccinini, and Julia Werneke. “Using naturalistic data to assess e-cyclist behavior”. In: *Transportation research part F: traffic psychology and behaviour* 41 (2016), pp. 217–226.

[24] Cheng Wang et al. “Investigating the Factors Affecting Rider’s Decision on Overtaking Behavior: A Naturalistic Riding Research in China”. In: *Sustainability* 14.18 (2022), p. 11495.

[25] Sergio A Useche et al. “Validation of the Cycling Behavior Questionnaire: a tool for measuring cyclists’ road behaviors”. In: *Transportation research part F: traffic psychology and behaviour* 58 (2018), pp. 1021–1030.

[26] Sonja Haustein and Mette Møller. “E-bike safety: Individual-level factors and incident characteristics”. In: *Journal of Transport & Health* 3.3 (2016), pp. 386–394.

[27] Christos Gioldasis, Zoi Christoforou, and Régine Seidowsky. “Risk-taking behaviors of e-scooter users: A survey in Paris”. In: *Accident Analysis & Prevention* 163 (2021), p. 106427.

[28] Alfredo Garcia et al. “Effect of width and boundary conditions on meeting maneuvers on two-way separated cycle tracks”. In: *Accident Analysis & Prevention* 78 (2015), pp. 127–137.

[29] Dianchao Lin et al. “Phenomena and characteristics of moped-passing-bicycle on shared lanes”. In: *Proceedings of the TRB 93rd Annual Meeting Compendium of Papers*. Transportation Research Board of the National Academies. 2014.

[30] Hossameldin Mohammed, Alexander Y Bigazzi, and Tarek Sayed. “Characterization of bicycle following and overtaking maneuvers on cycling paths”. In: *Transportation research part C: emerging technologies* 98 (2019), pp. 139–151.

[31] Daniel García-Vallejo, Werner Schiehlen, and Alfonso García-Agúndez. “Dynamics, Control and Stability of Motion of Electric Scooters”. In: *Advances in Dynamics of Vehicles on Roads and Tracks*. Ed. by Matthijs Klomp et al. Cham: Springer International Publishing, 2020, pp. 1199–1209.

[32] Alessio Violin. “Development of an experimental protocol fortesting new electric personal mobility vehicles”. PhD thesis. Politecnico di Torino, 2020.

[33] Natalia Kovacsova et al. “Riding performance on a conventional bicycle and a pedelec in low speed exercises: Objective and subjective evaluation of middle-aged and older persons”. In: *Transportation research part F: traffic psychology and behaviour* 42 (2016), pp. 28–43.

[34] Alexandra Gavriilidou et al. “Large-Scale Bicycle Flow Experiment: Setup and Implementation”. In: *Transportation Research Record* 2673.5 (2019), pp. 709–719. DOI: 10.1177/0361198119839974. eprint: https://doi.org/10.1177/0361198119839974. URL: https://doi.org/10.1177/0361198119839974.

[35] Wikipedia contributors. *Real-time kinematic positioning — Wikipedia, The Free Encyclopedia*. [Online; accessed 17-June-2024]. 2024. URL: https://en.wikipedia.org/wiki/Real-time_kinematic_positioning.

[36] Mark Wagenbuur. *How Wide is a Dutch Cycle Path?* Accessed: 2024-09-15. 2011. URL: https://bicycledutch.wordpress.com/2011/06/30/how-wide-is-a-dutch-cycle-path/.

[37] Jens Rasmussen. “Skills, rules, and knowledge; signals, signs, and symbols, and other distinctions in human performance models”. In: *IEEE transactions on systems, man, and cybernetics* 3 (1983), pp. 257–266.

[38] Dorine C Duives, Winnie Daamen, and Serge P Hoogendoorn. “State-of-the-art crowd motion simulation models”. In: *Transportation research part C: emerging technologies* 37 (2013), pp. 193–209.

[39] P Knoppers, JWC van Lint, and SP Hoogendoorn. “Automatic stabilization of aerial traffic images”. English. In: *TRB 2012 Annual Meeting Technical Papers*. Ed. by s.n. 91st Annual Meeting Transportation Research Board, TRB 2012 ; Conference date: 22-01-2012 Through 26-01-2012. Transportation Research Board (TRB), 2012, pp. 1–13. URL: http://www.trb.org/AnnualMeeting2012/AnnualMeeting2012.aspx.

[40] Victor L. Knoop and M.J. Wierbos. *Correction for Positions of Objects Tracked at Height*. Tech. rep. Accessed from personal document. Delft University of Technology, Mar. 2019.

[41] Road Safety Knowledge Centre. *In-Depth Investigation of E-Scooter Performance*. Accessed: 2024-09-22. Road Safety Knowledge Centre, 2023. URL: https://www.roadsafetyknowledgecentre.org.uk/in-depth-investigation-of-e-scooter-performance-report/.

[42] Centre for Research CROW, Contract Standardization in Civil, and Traffic Engineering. *Sign Up for the Bike: Design Manual for a Cycle-Friendly Infrastructure*. Vol. 10. CROW Record. The Hague, Netherlands: Institute for Road Safety Research, 1994.

[43] Bart Veroude, Mark van Gurp, and Otto van Boggelen. *Geactualiseerde aanbevelingen voor de breedte van fietspaden 2022*. With contributions from various experts from government and consultancy agencies. Utrecht, Netherlands, 2022.